Caenorhabditis elegans as an animal host to study oomycete infection: Discovery of the *chitinase-like* gene family, resistance genes that are transcriptionally controlled by the antagonistic paralogs *pals-22* and *pals-25*

Guled Ali Osman

Department of Life Sciences

Imperial College London

Thesis submitted for the degree of Doctor of Philosophy

Declaration of Originality

I declare that the work presented herein this thesis is appropriately referenced and a product of my own work.

Copyright Declaration

Acknowledgements

Even after spending over 17 hours in the lab, extracting RNA that would later help us to discover a new class of *C. elegans* resistance genes, travelling for 3 hours and mostly on foot to get home due to a city-wide underground tube strike and coming back early, I still felt excited and eager to get back to my experiments. It was these and many other moments of commitment that I realised I enjoyed performing research, it didn't feel like a chore nor did I ever need to find motivation to perform my experiments. To be part of a field that allows you to utilise your creativity, learn, contribute towards expanding human knowledge and potentially be a benefit to the world is a great privilege.

Now for the thanks, I will keep this short, otherwise it would be a chapter in and of itself. I have learnt a lot in the Barkoulas lab and from Imperial College London. I would like to thank all those who have helped me, supported me and given me authentic advice. I would like to acknowledge that without Dr Marie-Anne Felix's interest in the natural ecology of *C. elegans* and isolating the mysterious Lisbon pathogen, this PhD most likely would not have existed. I would also like to acknowledge the many researchers that have collaborated with us during the course of my studies, including but not limited to Dr Emily Troemel.

Lastly, I would like to thank the most important people in my life, my family and friends, not everyone is as fortunate to have such caring and supportive people.

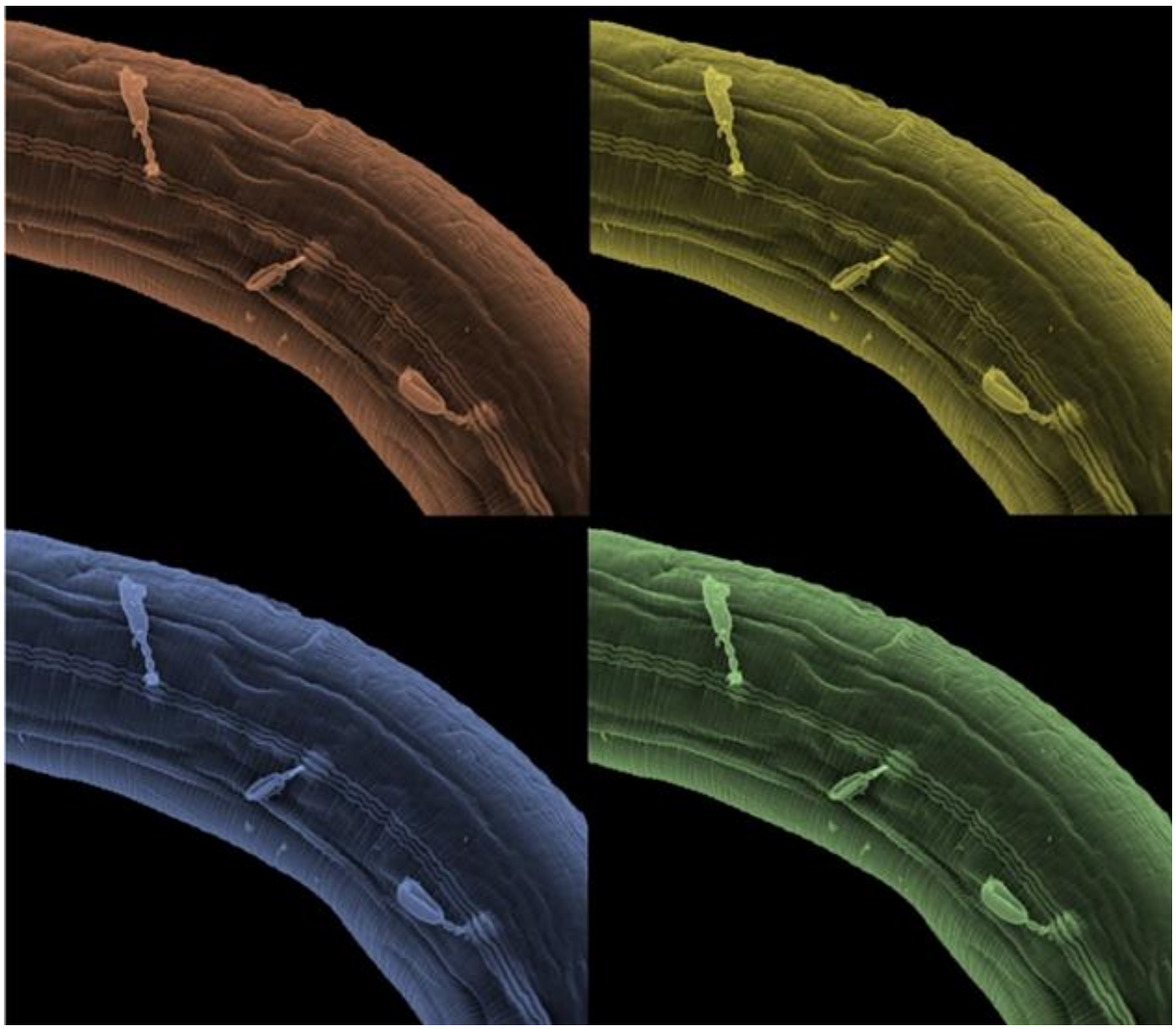

Abstract

The nematode *Caenorhabditis elegans* is used as a model system to study eukaryotic molecular responses to pathogens. These investigations have contributed to revealing key *C. elegans* innate immune defense mechanisms, such as the expression of inducible pathogen specific resistance genes. In general, researchers have mainly utilised pathogens not shown to naturally interact with *C. elegans*, or natural pathogens largely restricted to species of fungi and microsporidia. Towards the goal of expanding this field, we have identified the oomycete *Myzocytiopsis humicola*, as a new natural pathogen of *C. elegans*. Due in part to the absence of robust and genetically tractable experimental systems, animal pathogenic oomycetes encompass a diverse range of under-studied organisms. Thus, our discovery has provided us the opportunity to establish a novel and experimentally tractable pathosystem to examine animal oomycete infections. In this thesis, we will present this new experimental system, the pathogen infection strategy and how *C. elegans* responds transcriptionally to an oomycete infection. Additionally, we will describe the discovery of the *chitinase-like* (*chil*) genes, a novel family of uncharacterised *C. elegans* resistance genes, and discuss their functional role to antagonise *M. humicola* infection. Intriguingly, we show, *chil* gene expression is induced in response to pathogen detection, an ability previously not attributed to *C. elegans*. Finally, we will also describe our efforts to find transcriptional regulators of *chil* gene expression, and the discovery of the *pals-22*/*pals-25* genes, *C. elegans* specific antagonistic paralogs involved in a novel mechanism that balances development against immunity. In summary, the work presented here, expands our knowledge of natural pathogens of *C. elegans*, introduces a new genetically tractable pathosystem to examine how animals respond to an oomycete infection, reveals a novel family of *C. elegans* pathogen resistance genes and a new *C. elegans* specific mechanism that regulates development and immunity.

Contents

List of figures

List of tables

Chapter 1. General introduction

1. Introduction.

1.1. The model organism *Caenorhabditis elegans*.

Caenorhabditis elegans (*C. elegans*) is a microscopic transparent nematode, and while anatomically simple (Figure 1.1), it exhibits many of the same differentiated tissue and cell types observed to exist in more complex multicellular eukaryotes (Strange, 2006). Due in part to this characteristic, *C. elegans* has been successfully used as a model organism to discover important biological mechanisms that have also been shown to be evolutionarily conserved in higher eukaryotes. These include, but are not limited to programmed cell death (Hengartner et al., 1992) and RNA interference (Fire et al., 1998), a post-transcriptional gene silencing mechanism that has been exploited by researchers to perform targeted gene loss-of-function studies (Silva et al., 2004). Other advantageous traits also include a short life cycle (Figure 1.2), which allows for quick experimentation, stereotypical development, genetic amenability and a wealth of molecular tools available to study gene function (Chalfie et al., 1994; Sulston and Horvitz, 1977; Sulston et al., 1983).

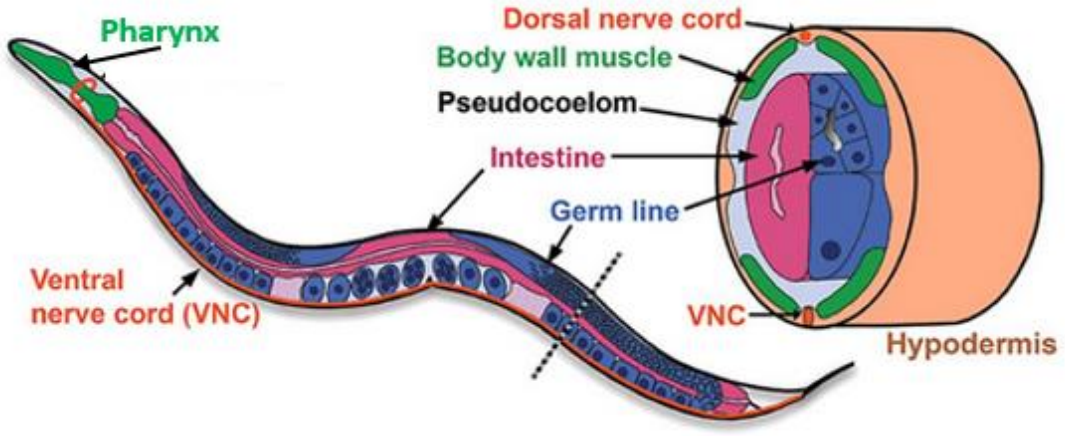

Figure 1.1: A Cartoon depicting a simplified transverse ventral section of an adult *C. elegans* hermaphrodite. Anatomically, the adult hermaphrodite *C. elegans* is comprised of an unsegmented tubular body, which encases two concentric cylinders (an inner and outer tube) separated by a pseudocoelom, a fluid filled cavity that provides internal hydrostatic pressure to maintain the nematode's structure. The outer tube contains the hypodermis (*C. elegans* epithelium), muscles and neurons (both ventral and dorsal nerve cords). The inner tube envelops the pharynx and intestine, both are components of the *C. elegans* alimentary system, as well as the gonads which contain the germ line. The image is adapted from (Strange, 2006).

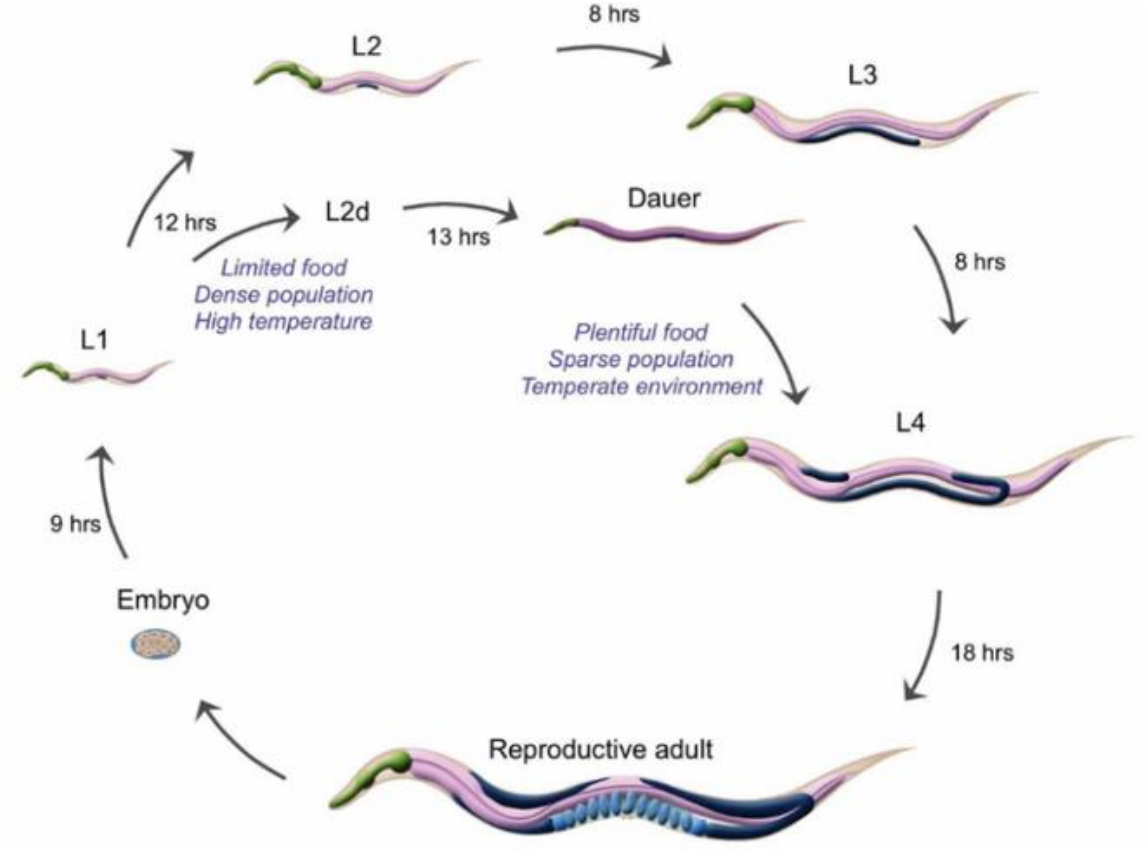

Figure 1.2: A schematic depiction of the hermaphrodite *C. elegans* life cycle. Under optimum conditions such as low crowding and sufficient food, the *C. elegans* hermaphrodite completes its life cycle in three days at 20ºC. The life cycle of *C. elegans* is comprised of an embryonic period, and post-embryonic stages consisting of four larvae phases (L1, L2, L3, and L4) before a fertile adult stage. In the event the environment is not conducive for development, e.g. limited food, dense population, or high temperatures, the L2 larvae can arrest/delay development and enter the dauer (enduring) stage, an effective method that extends *C. elegans* lifespan by many weeks, and permits the nematode to survive longer against hostile environments. Upon exposure to improved conditions, such as the availability of food, the dauer exits this specialized resilient stage and develop into the reproductive adult (Corsi, 2006; Strange, 2006). The image is taken from WormAtlas.

1.2. *C. elegans* as a model organism to study infection.

Whilst *C. elegans* has been extensively used in such fields of study as developmental biology since its inception as a model organism in 1974 (Brenner, 1974), *C. elegans* has only been relatively recently utilised in the discipline of infection studies (Tan et al., 1999). Tan and colleagues proof-of-principle study (Tan et al., 1999), reported that the pathogen *Pseudomonas aeruginosa* (*P. aeruginosa*), previously not shown to naturally interact with nematodes could efficiently infect *C. elegans*. Intriguingly, this study also showed that the PA14 mutants displaying reduced pathogenicity to mammals and plants, similarly exhibited a diminished lethality against the invertebrate *C. elegans*. These findings highlighted that pathogens such as *P. aeruginosa* employ universal mechanisms of virulence to infect phylogenetically divergent eukaryotes, and also presented a strong case to use *C. elegans* as a host to study medically relevant pathogens. *C. elegans* has since been successfully adopted to investigate the virulence mechanisms employed by bacteria *Enterococcus faecalis*, *Yersinia pestis*, *Salmonella typhimurium* (Aballay et al., 2000; Darby et al., 2002; Garsin et al., 2002), and the yeast *Candida albicans* (Kabir and Hussain, 2009).

Through the use of the above stated microbes and pathogens shown to naturally interact with *C. elegans* (natural pathogens) (Figure 1.3), including the fungal pathogen *Drechmeria coniospora* (*D. coniospora*) (Jansson, 1994), microsporidia such as *Nematocida parisii* (*N. parisii*) (Troemel et al., 2008), gram negative *Microbacterium nematophilum* (*M. nematophilum*) (Hodgkin et al., 2000) and the Orsay virus that is distantly related to known noda viruses (Félix et al., 2011), components of the *C. elegans* immune system have been discovered.

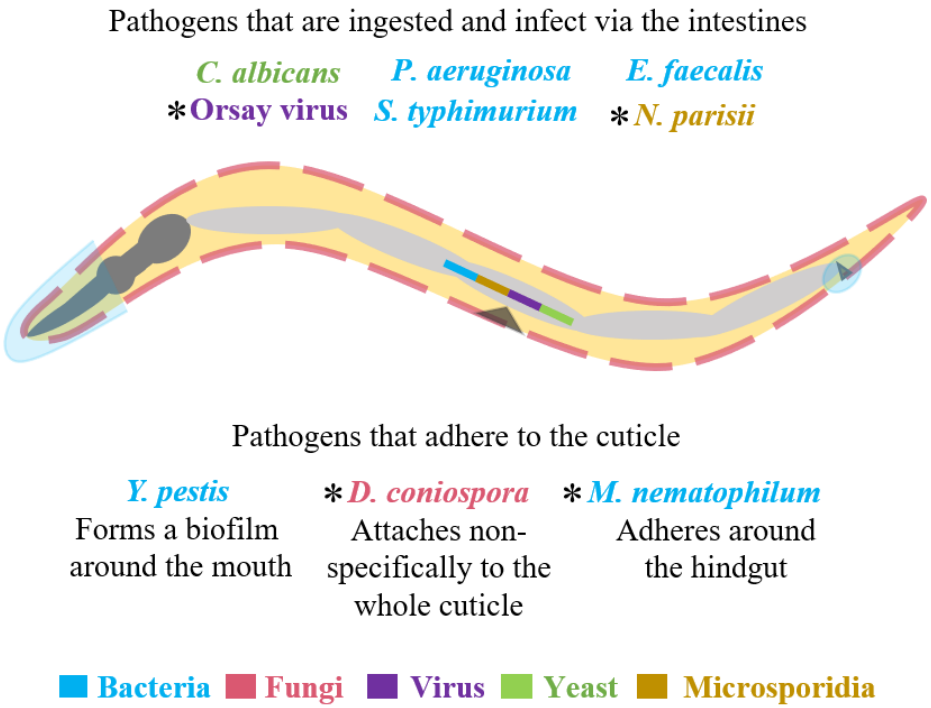

Figure 1.3: A cartoon depicting pathogens that are used to infect *C. elegans* and their routes of infection. *C. elegans* has been used to study a range of pathogens. These organisms can infect *C. elegans* by adhering to the nematode's integument as in the case of *D. coniospora*, *M. nematophilum* and *Y. pestis*. They can also be unwittingly ingested to later colonise and infect nematodes via the intestines, such as in the case of *P. aeruginosa*, *S. typhimurium*, *E. faecalis*, *C. albicans*, Orsay virus and *N. parisii*. The pathogens that have been shown to interact with *C. elegans* in its natural habitat (natural pathogens) are highlighted with an Asterix.

1.3. *C. elegans* pathogen defense mechanisms.

C. elegans relies entirely on an innate immune system, which involves biochemical, genetic mechanisms and physical barriers. *C. elegans* physical barriers protect against both biotic and abiotic threats and is comprised of both an external and an internal component. The external barrier, the exoskeleton, defined as the cuticle, forms a protective, highly impervious layer between the nematodes internal organs and its environment. The cuticle is an extracellular matrix, which is predominantly composed of collagen-like proteins (Chisholm and Hsiao, 2012; Johnstone, 1994). The internal barrier, a "grinder" located in a neuromuscular tube called the pharynx, prevents intact and potentially pathogenic organisms from reaching and infecting via the intestine (Gravato-Nobre and Hodgkin, 2005).

In the event a biotic threat circumvents the physical barriers used by *C. elegans* to prevent infection, both constitutively expressed and inducible processes of the innate immune system are recruited to antagonise infection. The constitutive component serves as a continuous physiological barrier, and is in part comprised of various antimicrobial peptides (AMP), including saposin-like protein-1 that is constitutively expressed in the intestine (Alper et al., 2007; Zhang and Kato, 2003). The second component, which was first described by Mallo and colleagues (Mallo et al., 2002), modulates the induction and or expression of resistance genes used to both antagonise and prevent infections (Pujol et al., 2008; Zugasti and Ewbank, 2009). This inducible response is partly regulated by signalling cascades also termed innate immunity pathways (Millet and Ewbank, 2004). The p38 mitogen-activated protein kinase (MAPK) is one such pathway (Kim et al., 2002). Intriguingly, this pathway has also been shown to regulate the tissue specific expression of resistance genes in a pathogen specific manner (Alegado and Tan, 2008; Pujol et al., 2008). The p38 MAPK pathway is a kinase signalling cascade, a cassette comprised of the upstream Toll/IL-1 resistance (TIR) domain containing protein TIR-1 and three protein kinases NSY-1, SEK-1 and PMK-1 (Figure 1.4); TIR-1 activates NSY-1,NSY-1

then phosphorylates SEK-1, which in turn phosphorylates and activates PMK-1, this results in downstream regulators of the pathway being activated such as the transcription factor SKN-1. Ultimately, the activation of the pathway results in the induced expression of immunity related genes to increase host survival (Andrusiak and Jin, 2016; Inoue et al., 2005; Kim et al., 2002; Liberati et al., 2004; Papp et al., 2012).

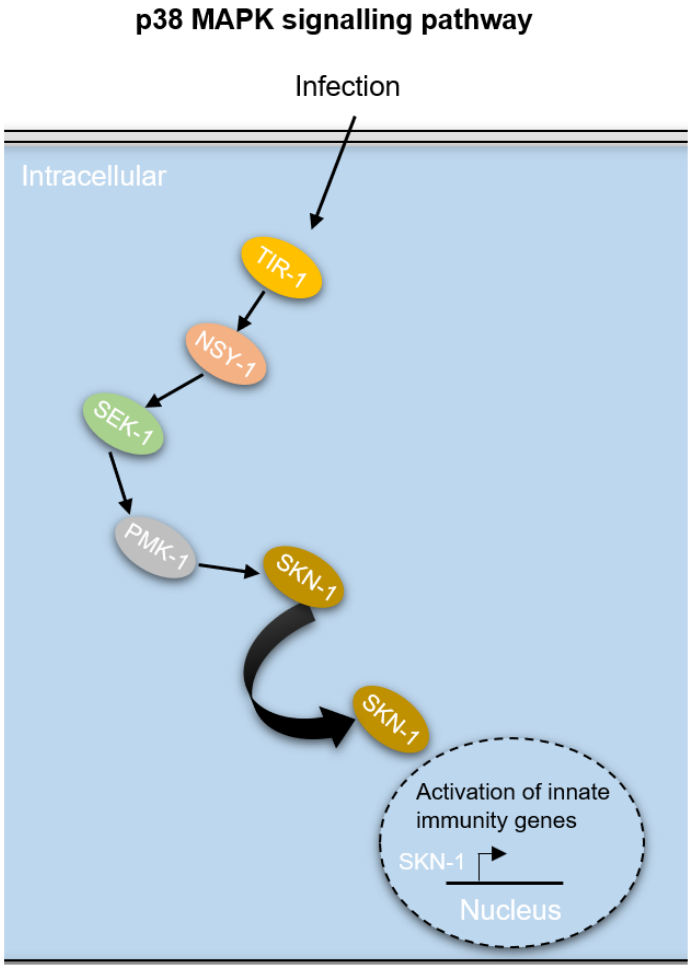

Figure 1.4: A cartoon depicting the *C. elegans* p38 MAPK innate immunity pathway. In the event of an infection, the p38 MAPK pathway is activated to induce the expression of immunity genes to increase host survival. This pathway is principally comprised of a kinase signalling cascade activated by TIR-1; TIR-1→ NSY-1→ SEK-1 → PMK-1. Following a series of phosphorylation and activation events, downstream regulators of the p38 MAPK pathway such as the transcription factor SKN-1 are activated. Once active, SKN-1 translocates to the nucleus to induce the expression of immunity related genes. The figure was constructed using data from (Andrusiak and Jin, 2016; Inoue et al., 2005; Kim et al., 2002; Liberati et al., 2004; Papp et al., 2012).

1.4. *C. elegans* pathogen detection mechanisms.

Recently, through the use of transcriptional profiling techniques, *C. elegans* has been shown to initiate pathogen specific immune responses, as indicated by the unique sets of genes induced by infection with a divergent range of pathogens. Interestingly, this has even been the case when comparing gene sets generated by pathogens with superficially similar means of infection (Bakowski et al., 2014; Engelmann et al., 2011; Feinbaum et al., 2012; Irazoqui et al., 2010a; Wong et al., 2007). Taken together, these results suggest the existence of processes that allow *C. elegans* to distinguish between differing biotic threats and mount an appropriate microbe-specific immune response. Conceivably, this may involve mechanisms to detect conserved pathogen associated molecular patterns (PAMPs), comparable to that of other organisms, such as those employed by *Drosophila melanogaster*, however, there is no evidence that *C. elegans* can detect PAMPs. Intriguingly, *C. elegans* lacks most of the toll-like receptor signalling pathway components attributed to perform this function in other organisms (Irazoqui et al., 2010b). Of note, the single homolog of this signalling pathway TOL-1, does not appear to act canonically. This perhaps implies, the presence of a more archaic and potentially divergent mechanism of pathogen detection.

Whilst mechanisms for direct pathogen detection have not be reported, there have been discoveries of "surveillance" type systems that are employed by *C. elegans* to perform indirect pathogen detection. This can involve the detection of abrupt pathogen induced perturbations to physiological processes such as translation (Chou et al., 2013; Dunbar et al., 2012; McEwan et al., 2012; Pellegrino et al., 2014), or damage associated molecular pattern/receptor interactions to detect structural damage that is associated with infection and abiotic stresses (Zugasti et al., 2014).

1.5. *C. elegans* natural ecology.

Despite its extensive use as a pathosystem, little is known about the natural biotic interactions and ecology of this metazoan (Kiontke, 2006). Recently, researchers have begun to recognise without these indispensable facets of information, our ability to understand and investigate *C. elegans* evolution, genome and responses to infections would be quite restricted. With this appreciation, efforts have been made to actively isolate wild-caught *C. elegans* strains and document their natural habitat and biotic interactions. These investigations have not only led to the re-classification of *C. elegans* from a soil dwelling nematode to a coloniser of microbe rich environments in nature (Barrière and Félix, 2005; Félix and Braendle, 2010), but they have also started to reveal pathogens that interact with *C. elegans* in its natural habitat. This information will undoubtedly help to both contextualise, and understand genes of unknown function, including seemingly redundant genes that are otherwise essential for *C. elegans* survival in its natural environment.

To expand our knowledge of *C. elegans* transcriptional responses to stresses faced in its native ecology and establish a novel pathosystem, we have used *Myzocytiopsis humicola*, an oomycete newly discovered to be a pathogen that naturally interacts with *C elegans*.

1.6. Pathogenic oomycetes.

Oomycetes encompass a diverse group of eukaryotic organisms that were once classified as fungi due to superficially similar traits. Oomycetes are in fact divergent microorganisms with greater taxonomic affinity to brown algae and diatoms (Cavalier-Smith and Chao, 2006; Dick, 1969; Kamoun, 2003). Pathogenic oomycetes infect a range of plant and animal hosts (Figure 1.5). The most extensively studied member of these heterotrophs is *Phytophthora infestans*, the pathogen responsible for the 'great Irish famine' of the 1850s (Yoshida et al., 2013).

In contrast to plant pathogenic oomycetes, research on animal pathogenic oomycetes has been limited due in part to a paucity of tractable experimental hosts. In fact, previous attempts in establishing experimental systems to study animal pathogenic oomycetes, have largely been hindered by either the observation of inconsistent disease phenotypes, or a scarcity of biological tools to study infection at the molecular level in less well developed model systems, see table 1.1 (Belmonte et al., 2014; Phillips et al., 2008; Trolezi et al., 2017; Yadav et al., 2016; Zanette et al., 2013). This is unfortunate when considering the invasive treatments required for patients suffering from pythiosis, a rare disease caused by the mammalian infecting oomycete *Pythium insidiosum*. Most patients often require surgical removal of infected sites due to the absence of effective treatments. However, there has been some limited success with a modified *P. insidiosum* antigen formulation as a form of immunotherapy, although early administration is required for an efficacious outcome (Gaastra et al., 2010; Keoprasom et al., 2013; Mendoza and Vilela, 2013; Phillips et al., 2008). In addition, the oomycete *Saprolegnia parasitica*, which is a pathogen of fresh water fish, has a devastating effect on aquaculture farming (Earle and Hintz, 2014). Therefore, as can be appreciated, the isolation of *Myzocytiopsis humicola*, a pathogenic oomycete that naturally interacts with the genetically

tractable model organism *C. elegans*, has provided us the opportunity to establish a new animal-oomycete pathosystem.

Table 1.1. A review of previous attempts to establish an animal-oomycete pathosystem.

Model organism	Oomycete species	Limitations/Ref
Labeo rohita, *Cyprinus carpio*	*Aphanomyces invadans*	Limited molecular tools, inconsistencies in scoring. [1]
Salmo salar	*S. parasitica*	Limited molecular tools, inconsistencies in scoring, inconsistent disease phenotype. [2]
Oryctolagus cuniculus	*P. insidiosum*	Does not represent the disease phenotype of naturally acquired pythiosis. [3]
Drosophila melanogaster	*P. insidiosum*	Inconsistencies in scoring, the disease phenotype is minimal. [4]

[1] Yadav et al., 2014, 2016; [2] Belmonte et al., 2014; [3] Trolezi et al., 2017; [4] Zanette et al., 2013.

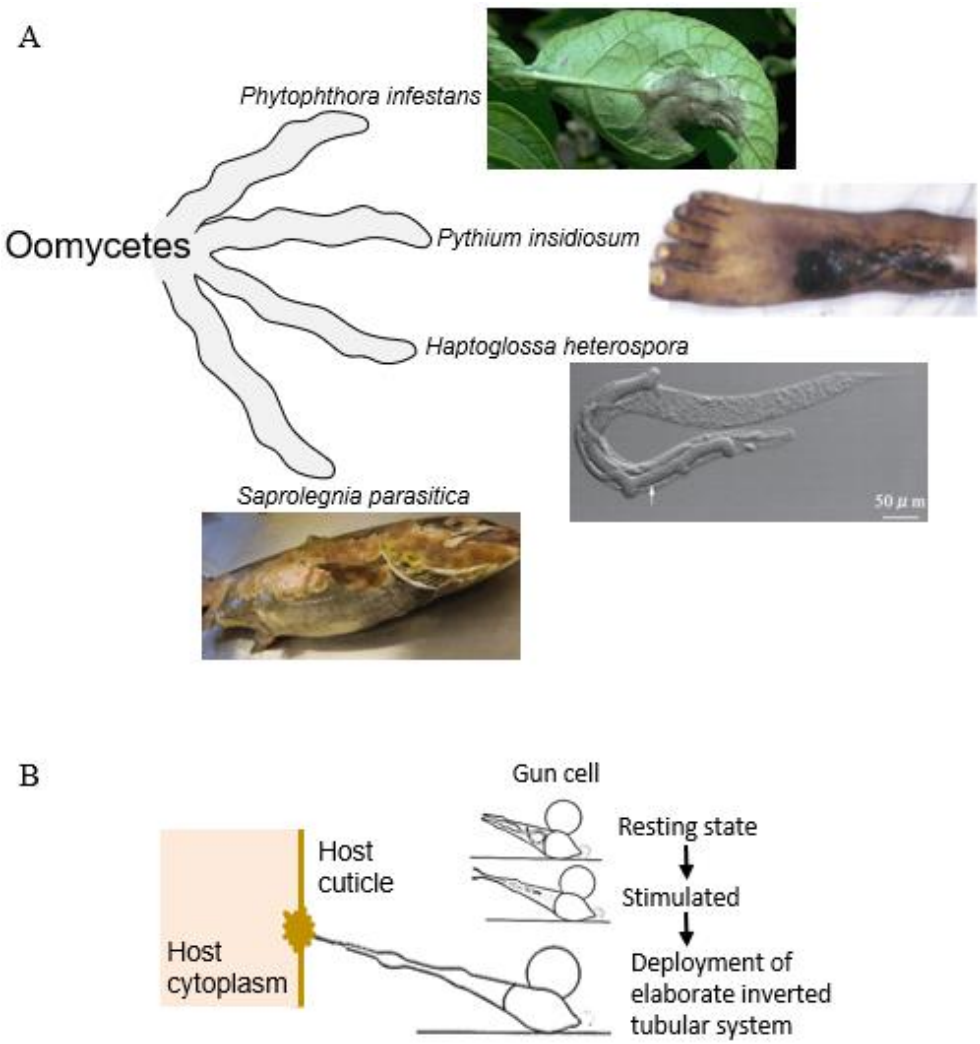

Figure 1.5: Pathogenic oomycetes. (A) An illustration depicting a range of pathogenic oomycetes. Pathogenic oomycetes have evolved to infect an array of hosts including plants: *Phytophthora infestans*, fish: *Saprolegnia parasitica*, mammals including humans: *Pythium insidiosum*, and microscopic animals such as nematodes: *Haptoglossa heterospora*. **(B)** A cartoon depicting the mechanism deployed by *H. heterospora* to infect rotifers, tardigrades and nematodes. These pathogenic organisms have evolved unique and complex methods to infect their target hosts via gun cells that act as retracted hypodermic needles. These cells when stimulated to fire, deploy an elaborate inverted tubular system to rupture the host's cuticle and inject the sporidium, the infectious cellular unit directly into the host's cytoplasm. The figures are adapted from (Barron, 1987; Glockling and Beakes, 2008; Hakariya et al., 2002; Robb and Barron, 1982; Sarowar et al., 2014).

1.7. *Myzocytiopsis humicola*.

Myzocytiopsis humicola (*M. humicola*) is a nematophagous, holocarpic, obligate oomycete that has been shown to infect a range of *Rhabditids* nematodes and rotifers (Glockling and Beakes, 2000). Although previous studies have provided morphological characterisation of some nematophagous oomycetes, including members of the *Myzocytiopsis* genus, such as *M. humicola* (Glockling and Beakes, 2008), how the host responds to an oomycete infection at the molecular level had not been examined, nor had there been prior evidence showing that *C. elegans* could be infected by an oomycete. Members of the *Myzocytiopsis* genus are historically taxonomically classified, and are based entirely on species-specific stages of infection, namely differences in morphology i.e. spores morphology and spore release methods (Figure 1.6). *M. humicola* infections are initiated by the successful attachment of spores termed cytospores to the integument of passing nematodes. Upon successful attachment and penetration, thalli growth is initiated. Subsequently, while killing the animal in the process, the thali colonise the host and partition into sporangia. Finally, the sporangia mature within the host and cytospores are released through protrusions called exiting tubes, this is done in an attempt to propagate *M. humicola* and infect additional hosts. For species such as *M. humicola* (Figure 1.6A) zoospores mature within the sporangium before being directly released via an evacuation tube, where subsequently, the biflagellated spores encyst and develop adhesive 'bud'-like extensions to attach onto nematode integuments. In contrast, species such as *M. vermicola* (Figure 1.6B) and *M. lenticularis* (Figure 1.6C), the sporangium release their zoospores via a papilla, a fine transparent vesicle where the zoospores mature before being released. Later, the spores encyst and either directly attach onto a favourable host, or develop adhesive extensions similar to *M. humicola*. In species such as *M. subuliformis* (Figure 1.6D), elongated, tapered aplanospores are released directly from the

sporangium, which later develop adhesive tips to attach onto hosts (Glockling and Beakes, 2000, 2008).

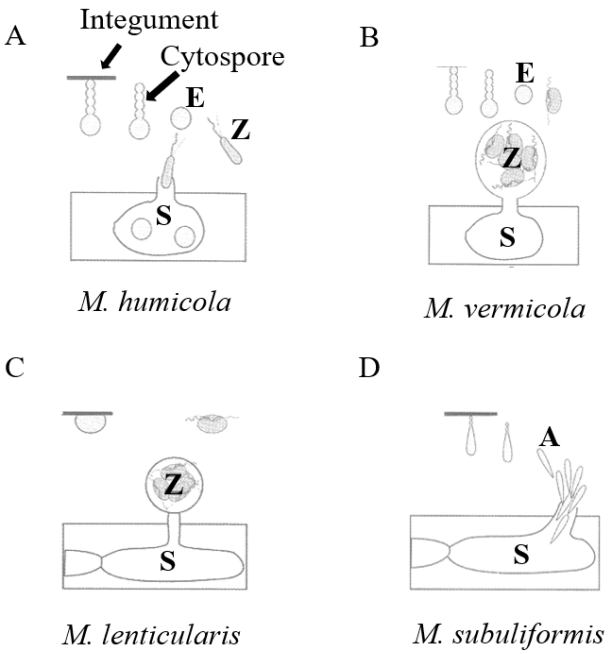

Figure 1.6: Illustrations summarising the key morphological variations between isolates of the *Myzocytiopsis* genus. Members of the *Myzocytiopsis* genius display distinct differences in the morphology of mature sporangia and infectious spores, as well as spore release methods. Species such as *M. humicola* **(A)** produce biflagellated zoospores that are released directly from mature sporangia through an exiting tube. Subsequently, the spores encyst and develop extensions to attach onto the nematode cuticle. In addition, the zoospores mature within the sporangium before being released. For species such as *M. vermicola* **(B)** and *M. lenticularis* **(C)**, zoospores are separated from sporangium and released via vesicles called papilla, also, the zoospores develop within these vesicles before being released into the environment. Later, the infectious zoospores encyst and either develop adhesive extensions comparable to *M. humicola*, or directly attach onto a favourable host. In contrast, species such as *M. subuliformis* produce morphologically distinct tapered, elongated spores termed aplanospores **(D)**. Comparable to *M. humicola*, *M. subuliformis* aplanospores are released directly from mature sporangium and develop adhesive extensions outside of the host. S = sporangia; Z = motile zoospores; E= encysted spore; A = aplanospores. The images are adapted from (Glockling and Beakes, 2000).

1.8. Aims of this project.

Animal pathogenic oomycetes encompass a diverse group of under-studied parasites that pose a threat both economically and medically, this has been in part due to a paucity of genetically amenable host systems. As a consequence, currently, we have a poor understanding of how animals respond to pathogenic oomycetes at the molecular level. Overall, this project has attempted to redress this limitation by establishing, characterising and validating a novel oomycete-*C. elegans* pathosystem, followed by the dissection and the characterisation of *C. elegans* innate immune responses to the oomycete.

Chapter 3 describes phylogenetic and morphological studies that identify the oomycete *M. humicola* as a new natural pathogen of *C. elegans*, a genetically tractable model host. This chapter also includes efforts to design an infection assay. We also demonstrate that the *C. elegans* p38 MAPK innate immunity pathway, contributes to confer *C. elegans* resistance against the nematophagous oomycete.

In chapter 4, to delineate *C. elegans* innate immune responses to the oomycete, we analysed *C. elegans* transcriptional response post exposure to *M. humicola*. In addition, we show how this led to the discovery of a novel family of inducible resistance genes, the *chitinase-like* (*chil*) genes. Chapter 4 also describes our investigations that reveal the *chil* genes hinder the initiation of infection by antagonising *M. humicola* attachment.

Considering this project entails the first recorded efforts to study the *chil* genes, in chapter 5, we sought to further characterise these genes, by examining if previously reported transcriptional regulators of inducible *C. elegans* resistance genes, such as the p38 MAPK pathway and the GATA transcription factor ELT-3, could play a role in regulating the expression of *chil-27*. In this chapter, we also reveal that the *chil* genes are induced as a

consequence of pathogen detection rather than infection, and we demonstrate that the process requires normal amphid morphology.

In light of the unique functional and phenotypic characteristics demonstrated by the *chil* genes, in chapter 6, we performed forward genetic mutagenesis screens to find key transcriptional regulators of the *chil* genes. In this chapter, we also describe the discovery of the antagonistic paralogs *pals-22* and *pals-25*, novel genes that transcriptionally regulate *chil-27* expression. In addition, we also present investigations that reveal the phenotypic consequences mutations in *pals-22* and *pals-25* have on *C. elegans* development, and its capacity to resist *M. humicola*-mediated killing.

Chapter 2. Materials and methods

2.1. Key materials used and generated.

Table 2.1.1. Experimental model organisms: oomycete and nematode strains.

Experimental Organism	Strain	Allele	Description	Source/Ref
M. humicola	JUo1	Not applicable	A Lisbon isolated nematophagous oomycete.	This study
C. elegans	JU2519	Not applicable	Lisbon wild-caught *C. elegans* strain co-isolated with *M. humicola*.	This study
C. elegans	N2	Not applicable	Lab wild-type reference strain.	*Caenorhabditis* Genetics Center (CGC)
C. elegans	KU4	*sek-1*(*km4*) *X*	2084 bp deletion within the *sek-1* gene.	CGC
C. elegans	KU25	*pmk-1*(*km25*) *IV*	375 bp deletion within the *pmk-1* gene.	CGC
C. elegans	CB1377	*daf-6*(*e1377*) *X*	Missense mutation.	CGC
C. elegans	EG1000	*dpy-5*(*e61*) *I; rol-6*(*e187*) *II; lon-1*(*e1820*) *III*	Mapping strain containing mutations located on chromosomes I, II and III.	CGC
C. elegans	EG1020	*bli-6*(*sc16*) *IV; dpy-11*(*e224*) *V; lon-2*(*e678*) *X*	Mapping strain containing mutations located on chromosomes IV, V and VI.	CGC
C. elegans	MBA281	*icbIs4*[*chil-27p*::GFP, *col-12p*::mCherry-pest] *II*	Stable *chil-27* transcriptional reporter line. Transgene integrated into chromosome II.	This study
C. elegans	MBA282	*icbIs5*[*chil-27p*::GFP, *col-12p*::mCherry-pest] *II*	Stable *chil-27* transcriptional reporter line. Transgene integrated into chromosomes I & IV.	This study
C. elegans	MBA280	*icbIs6*[*chil-28p*::GFP, *col-12p*::mCherry-pest] *V*	Stable *chil-28* transcriptional reporter line. Transgene integrated into chromosome V.	This study
C. elegans	MBA397	*elt-3(gk121) X; icbIs4*[*chil-27p*::GFP, *col-12p*::mCherry-pest] *II*	The *chil-27p*::GFP transcriptional reporter transferred into mutant backgrounds.	This study
C. elegans	MBA400	*sek-1(km4) X; icbIs4*		This study
C. elegans	MBA504	*daf-6(e1377) X; icbIs4*		This study
C. elegans	MBA311	*icbEx79*[WRM065aH01, *myo-2p*::GFP]	N2 Transgenic animals harbouring supernumerary copies of genes *chil-1* to *chil-9*.	This study

C. elegans	MBA314	*icbEx82*[WRM0619bB10, *myo-2p*::GFP]	N2 Transgenic animals harbouring supernumerary copies of genes *chil-18* to *chil-27*.	This study
C. elegans	MBA631	*icbEx161*[WRM0627dG07, *myo-2p*::dsRed]	Control for fosmid infection assay, animals harbour supernumerary copies of gene *lin-22* and partial *ndnf-1*.	This study
C. elegans	MBA381	*chil-4*(*icb48*) *II*	CRSPR mutant with hygromycin resistance gene inserted into *chil-4*.	This study
C. elegans	MBA383	*chil-9*(*icb53*) *II*	CRSPR mutant with hygromycin resistance gene inserted into *chil-9*.	This study
C. elegans	MBA474	*chil-18*(*icb57*) *II*	CRSPR mutant with hygromycin resistance gene inserted into *chil-18*.	This study
C. elegans	MBA477	*chil-27*(*icb60*) *II*	CRSPR mutant with hygromycin resistance gene inserted into *chil-27*.	This study
C. elegans	MBA657	*icbEx169*[*rps-0p*::HYGB::*unc54*, *myo-2p*::GFP]	CRISPR infection assay control, animals harbour supernumerary copies of the hygromycin resistance gene.	This study
C. elegans	MBA954	[*chil-27p*::CHIL-27::GFP, *col-12p*::mCherry-pest]	Animals harbour the CHIL-27 translational reporter.	This study
C. elegans	MBA352	*icbIs4*[*chil-27p*::GFP, c*ol-12p*::mCherry-pest] II; *pals-22*(*icb88*) *III*	EMS generated *pals-22* loss-of-function mutant. W110STOP.	This study
C. elegans	MBA480	*icbIs5*[*chil-27p*::GFP, *col-12p*::mCherry-pest] II; *pals-22*(*icb89*) *III*	EMS generated *pals-22* loss-of-function mutant. 200 bp deletion spanning exons 1 and 2.	This study
C. elegans	MBA457	*icbIs4*[*chil-27p*::GFP, *col-12p*::mCherry-pest] II; *pals-22*(*icb90*) *III*	EMS generated *pals-22* loss-of-function mutant. W96STOP.	This study
C. elegans	MBA791	*icbIs4*[*chil-27p*::GFP, *col-12p*::mCherry-pest] II; *pals-22*(*icb90*) *pals-25*(*icb91*) *III*	EMS generated *pals-25* loss-of-function mutant using strain MBA457 (*pals-22*(*icb90*)). A116V.	This study
C. elegans	MBA792	*icbIs4*[*chil-27p*::GFP, *col-12p*::mCherry-pest] II; *pals-*	EMS generated *pals-25* loss-of-function mutant using strain MBA457 (*pals-22*(*icb90*)). G40D.	This study

		22(*icb90*) *pals-25*(*icb92*) *III*		
C. elegans	MBA299	*icbIs4*[*chil-27p*::GFP, *col-12p*::mCherry-pest] II; *pals-25*(*icb98*) *III*	EMS generated *pals-25* gain-of-function mutant. Q293STOP in *pals-25*.	This study

Table 2.1.2. Recombinant DNA: plasmids, fosmids.

Recombinant DNA	Identifier/construct	Description	Source/Ref
Plasmid	L3135. Addgene #1531	Vector used to generate the transcriptional reporters.	Barkoulas lab
Plasmid	pGO4 [*chil-27p*::*pes-10*::GFP::*unc54*]; backbone L3135	*chil-27* GFP transcriptional reporter.	This Study
Plasmid	pGO7 [*chil-28p*::*pes-10*::GFP::*unc54*]; backbone L3135	*chil-28* GFP transcriptional reporter.	This Study
Plasmid	pCHMH1195 [*col-12p*::mCherry-pest]	*col-12* mCherry transcriptional reporter.	(Perales et al., 2014)
Plasmid	*myo-2p*::GFP; backbone L3790. Addgene #1596	*myo-2* GFP transcriptional reporter.	Gift from the Marie-Anne Felix lab
Fosmid	WRM065aH01	Fosmid containing a 34,592 bp fragment of the N2 genome spanning chromosome II, position 9842328..9876919. Encompassing genes *chil-1* to *chil-9*.	Source bioscience
Fosmid	WRM0619bB10	Fosmid containing a 35,769bp fragment of the N2 genome spanning chromosome II, position 9444160..9479928. Encompassing genes *chil-18* to *chil-27*.	Source bioscience
Plasmid	pDNRhyg [*rps-0p*::HYGB::*unc54* 3'UTR]	Template used to amplify the hygromycin resistance gene.	Gift from the Marie-Anne Felix lab
Plasmid	pGO16 [pU6::*chil-4*_sgRNA]	*chil-4* guide sgRNA.	This Study
Plasmid	pGO22; backbone BJ97	*chil-4* repair template.	This Study
Plasmid	pGO17 [pU6::*chil-9*_sgRNA]	*chil-9* guide sgRNA.	This Study
Plasmid	pGO23; backbone BJ97	*chil-9* repair template.	This Study
Plasmid	pGO20 [pU6::*chil-18*_sgRNA]	*chil-18* guide sgRNA.	This Study
Plasmid	pEC1; backbone BJ97	*chil-18* repair template.	This Study

Plasmid	pGO22 [pU6::*chil-27*_sgRNA]	*chil-27* guide sgRNA.	This Study
Plasmid	pEC2; backbone BJ97	*chil-27* repair template.	This Study
Plasmid	[*eft-3p*::*cas9*-SV40_NLS::*tbb-2* 3'UTR]. Addgene #46168	Cas-9.	(Friedland et al., 2013)
Plasmid	pMA122 [*hsp-16.41p*::*peel-1*::*tbb-2* 3' UTR]. Addgene #34873	Heat shock toxin.	(Frøkjær-Jensen et al., 2012)
Plasmid	pGO24[*arf-3p*::CHIL-27::GFP::*unc-54* 3' UTR] ; backbone pUC57	CHIL-27 translational reporter under the control of the *arf-3* promoter.	This study
Plasmid	pGO25 [*chil-27p::*pes-10::GFP::CHIL-27::*unc-54* 3' UTR]; backbone pUC57	CHIL-27 translational reporter under the control of its native promoter.	This study
Plasmid	*myo2-p::*dsRed	*myo-2* dsRed transcriptional reporter.	Gift from the Marie-Anne Felix lab
Plasmid	pIR5 [*arf-3p*::*pes-10*::*unc54* 3'UTR]; backbone pUC57	Used to generate the CHIL-27 translational reporter.	Barkoulas lab

Table 2.1.3. List of oligonucleotides used in this study.

Identifier	Sequence (5'→3')	Source/Ref
UN-up18S43	CGTAACAAGGTT TCCGTAGGTGAAC	(Lévesque and De Cock, 2004)
UN-1o28S22	GTTTCTTTTCCTCCG CTTATTGATATG	(Lévesque and De Cock, 2004)
Myzo18S	ATAGTCTACTCGATAGTACC	This study
Myzo18AS	TATGGTTAAGACTACGATGG	This study
Cox2F	GGCAAATGGGTTTTCAAGATCC	(Spies et al., 2016)
Cox2R	CCATGATTAATACCACAAATTTCAC TAC	(Spies et al., 2016)
Chil-27F	CGATAAGCTTtcaagtgttggattcgaatgga	This study
Chil-27R	TATCTCTAGAatgaagtgaggaaatgggcg	This study
Chil-28F	CGATAAGCTTtctctgatctgaactccgatttt	This study
Chil-28R	TATCTCTAGAtgggatggagtaggcatgac	This study
chil4_CRISP1F	ATTTAGGTGACACTATAGAATATCA AACTCAACAAGTGTCCCTCTTTTA	This study
chil4_CRISP1R	GCGCACAACCATCAAGAC CCTATACTGATCATTACTTTC	This study
chil4_CRISP2F	Ggaatttttcaatcaagtgaaagtt tCGGACAATCAAATTCTCGTTC	This study
chil4_CRISPR2R	TCGATAAGCTTGGATCCTCTAGCTT ACTAGCTTTTCATCTCCGGTGCATA	This study
chil9_CRISRP1F	ATTTAGGTGACACTATAGAATATC AATTCGAACTCAACAAGCGTCC	This study
chil9_CRISP1R	GCGCACAACCATCAAG ACCCTATGCTGATCATTACTTTC	This study
chil9_CRISP2F	Ggaatttttcaatcaagtgaaagt	This study

	ttCGGACAGTACAACTCTGGTG	
chil9_CRISP2R	TCGATAAGCTTGGATCCTCTAGCTT ACTAGGATCTCATTCCTCCTATCTC	This study
chil18_CRISP1F	ATTTAGGTGACACTATAGAATA TCAtgatgcaaactactctgaggaa	This study
chil18_CRISP1R	CAATGCGCACAACCATCAAG ACcaattgaaatcataactttagtgtcag	This study
chil18_CRISP2F	Ggaatttttcaatcaagtgaaagtttgc ggagatcacaacagtgaag	This study
chil18_CRISP2R	TCGATAAGCTTGGATCCTCTAG CTTACTAGcttgtacgagcgagtttcatca	This study
chil27_CRISP1F	ATTTAGGTGACACTATAGA ATATCAatccgtcagccctaaacgaa	This study
chil27_CRISP1R	CAATGCGCACAACCATCAA GACcacttgaatattgagaggtgac	This study
chil27_CRISP2F	Ggaatttttcaatcaagtgaaagtt tgaggactgcaacaccggtagg	This study
chil27_CRISP2R	TCGATAAGCTTGGATCCTCTA GCTTACTAGgtggtggccgtacaactttc	This study
hygro-gR	ACTCTCGCACGGAAGAGAC	This study
hygro-gF	ACGGCAATTTCGATGATGCA	This study
chil-4HygF	gcactggagatgagaagaatacg	This study
chil-4HygR	tcatgaaaacaaagttgctcga	This study
chil-9hygR	tgattctacagccacccattt	This study
chil-9_HygR	catgtccaaaatatatcgactcca	This study
chil-18hyginsF	tcgtagtagtgtcgcaatttga	This study
chil-18fullR	gaaaatctctgcgtccaatagc	This study
newchil-27R	ttagcccatcatccctatcg	This study
hygro-F	gtcttgatggttgtgcgcattg	This study
hygro-R	aaactttcacttgattgaaaaattcc	This study
Chil-27PrF	CGATGAATTCttaatatcataaaacatttatg	This study
Chil-27PrR	TATCAGGCCTttttatataattcttcggcgta	This study
GFP-CAAX-pIR5F	TTGCTTGGAGGGTACCGAGTTTAAA CATTTATGAGTAAAGGAGAAGAAC	This study
cl27_NfusR_piR5	GTAATTGGACTTAGAAGTCAGAGGC AATTTTTACAATGAGAATCCTAGTG GTG	This study
mchy_Nfus_cl27	GGATCTGCTGGATCTGCTGCTGGAT CTGGAGAATTTATGTCTACGCCGAA GAATTAT	This study
mchy_NfsF_Pir5	TTGCTTGGAGGGTACCGAGTTTAAA CATTTATGGTCTCAAAGGGTGAAGA	This study
FISH 18S-1	cgaagctgcattggtttcaa	This study
FISH 18S-2	cgcacagttattatgactca	This study
FISH 18S-3	attgttctcattccaattgc	This study
FISH 18S-4	gacgttcaaaccagaaatcc	This study
FISH 18S-5	cacttccaaaggaagcggac	This study
FISH 18S-6	atggctcaaacatccttagt	This study
FISH 18S-8	gcaaacgcctgctttaaaca	This study
FISH 18S-9	aatagaccaccaaggtcgta	This study
FISH 18S-10	ttaatcattaccctggtgtg	This study
FISH L30-1	gtcttcttagaggcaaccat	This study
FISH L30-2	ggtggagtgttggaagcaat	This study

FISH L30-4	agatcgttattagtgccaga	This study
FISH L30-5	ggaagtatttaccacaggcg	This study
FISH L30-6	aggatgcacatgcaggatac	This study
FISH L30-7	gaatatcagaatcaccggca	This study
FISH L30-8	aattatcggatcccatagca	This study
smFISH chil-27-1	taattcttcggcgtagacat	This study
smFISH chil-27-2	cctgtcatttttctcatcta	This study
smFISH chil-27-3	ttcatttgcagtgacgttgt	This study
smFISH chil-27-4	cccatggcattatttgcaaa	This study
smFISH chil-27-5	catcattttcttttgcagga	This study
smFISH chil-27-6	tctattggtggaatttctga	This study
smFISH chil-27-7	gggtagttgaagctatatca	This study
smFISH chil-27-8	agcctgatgaatccgttaat	This study
smFISH chil-27-9	actttgtcaggtggtttttc	This study
smFISH chil-27-10	atcagctgcgaagaggacaa	This study
smFISH chil-27-11	ctctacgcttccatcaaatc	This study
smFISH chil-27-12	atgtgcgcgatgaatgatcc	This study
smFISH chil-27-13	tgtgagctctctattttcga	This study
smFISH chil-27-14	tattggatcgtccaccaatt	This study
smFISH chil-27-15	gatccgcaataacaagtggc	This study
smFISH chil-27-16	tccatctagttgatattcct	This study
smFISH chil-27-17	gcccacttccaaagtaaatc	This study
smFISH chil-27-18	ccgagaacatttctttgtgt	This study
smFISH chil-27-19	agcttttgtttcaattcaca	This study
smFISH chil-27-20	catcaggcagaatttgcaca	This study
smFISH chil-27-21	gaacagctcccaactcgatg	This study
smFISH chil-27-22	gagaggtgacccatttgcag	This study
smFISH chil-27-23	tgcagtcctccacttgaata	This study
smFISH chil-27-24	cacgacttctgtatctggtc	This study
smFISH chil-27-25	tagattccagttctgagtca	This study
smFISH chil-27-26	gtcgacggtaagtttctttg	This study
smFISH chil-27-27	tgaagatttccatccgatgt	This study
smFISH chil-27-28	ttcatagcaatctcatcctc	This study
smFISH chil-27-29	agcttgctcctttaacttta	This study
smFISH chil-27-30	gtgcgcccatcaattttaaa	This study
smFISH chil-27-31	tcttttcttatcatgagcca	This study
smFISH chil-27-32	ccaagccgatattcttttag	This study
smFISH chil-27-33	tttccaaattaagtccgagt	This study
smFISH chil-27-34	tctactctgaaggaactcct	This study
smFISH chil-27-35	tctttctttctttaatctct	This study
smFISH chil-27-36	ggccgtacaactttcgataa	This study
C29f9.1 F2	AATTCAGATGATGTTCCTGAGCA	This study
C29f9.1 R2	CCGCCCATCCCTAATTCTGA	This study
pals-25FullF	ATGGTTTTACACTTTGATTTC	This study
pals-25FullR	TGATTGTTTTGAATAAAGT	This study
Elt-3genoF	tttctccagtgccatcttcc	This study
Elt-3genoR1	cggttaagaccgaaggtcag	This study
Elt-3genoR2	AGGACGTCGGTTTCTCTTCA	This study
Sek-1(km4)F	gagacgacacactgattgcc	This study
Sek-1(km4)Rmut	tcgcaaatctagcatagcact	This study
Sek-1(km4)Wt	AATTTCCGCGTCACAGACTG	This study

Table 2.1.4. Bacterial strains used for *C. elegans* maintenance and RNAi.

Experimental Organism	Strain	Gene targeted	Description	Source/Ref
E. coli	OP50	Not applicable	Standard bacteria used to culture *C. elegans*.	CGC
E. coli	HTT15	*unc-22*	Control to test the potency of the RNAi plates.	Gift from Dr Richard Poole & Dr Arantza Barrios/(Reboul et al., 2003)
E. coli	HTT15	No gene targeted	Control for RNAi experiments, empty vector.	Gift from Dr Richard Poole & Dr Arantza Barrios/(Reboul et al., 2003)
E. coli	HTT15	*pals-22*	Used for the RNAi knockdown of *pal-22*.	Gift from Dr Richard Poole & Dr Arantza Barrios/(Reboul et al., 2003)
E. coli	HTT15	*pals-25*	Used for the RNAi knockdown of *pal-25*.	Gift from Dr Emily Troemel/(Reddy et al., 2019)

2.2. Methods used.

2.2.1. General nematode maintenance.

Strains discussed herein this study, were cultured on petri dishes containing 1.7% agar nematode growth media (NGM) seeded with a lawn of *Escherichia coli* OP50 as the food source (Brenner, 1974; Wood ed., 1988). NGM media was composed of 0.25% bactopeptone, 0.3% NaCl and 1.7% agar, 5µg/ml cholesterol, 1mM $MgSO_4$, 25mM KPO_4 and 1mM $CaCl_2$. Unless otherwise indicated, N2, the *C. elegans* Bristol isolate was used as the lab wild-type reference strain. Additionally, all strains were maintained at 20ºC under standard conditions. The list of nematode strains used and generated in the completion of this study can be found in table 2.1.1.

To obtain developmentally synchronised and or relatively sterile populations, we 'bleached' gravid hermaphrodites with a sodium hypochlorite solution (0.3% commercial bleach v/v in 1N NaoH) and washed the released embryos twice with M9 buffer (0.3% KH2PO4, 0.6% Na2HPO4, 0.5% NaCl and 1mM MgSO4). The harvested embryos were then seeded onto NGM plates and cultured until the desired developmental stage for experiments was reached.

2.2.2. Pathogen maintenance and oomycete molecular characterisation.

The isolated nematophagous oomycete strain JUo1 discussed herein this study, thus far, is described as an obligate pathogen requiring a host to complete its life cycle and has not been successfully grown independent of a host. Therefore, we maintained the pathogen on OP50 seeded NGM plates containing N2. The maintenance plates were incubated at 25ºC and were 'chunked' every two or three days.

To molecularly characterise the Lisbon isolated organism, we amplified sections of the pathogen's genome. To amplify the internal transcribed spacer 1 (ITS), we used universal eukaryotic primers UN-up18S43/UN-1o28S22 (Lévesque and De Cock, 2004). To amplify 18S ribosomal and cytochrome c oxidase subunit 2 rDNA, we used primers Myzo18S/Myzo18AS and Cox2F/Cox-2R (Spies et al., 2016) respectively. To analyse the isolated amplicons, we used sanger sequencing followed by BLASTn searches (NCBI GenBank database) and phylogenetic analysis of the rDNA amplicons. In all instances, crude pathogen genomic DNA from lysed infected animals was used. The phylogenetic analysis was performed using the maximum likelihood method based on the Tamura-Nei model. The phylogenetic trees were constructed using Geneious version 10.2.2. The primers used can be found in table 2.1.3.

2.2.3. Scanning electron microscopy (SEM).

For SEM experiments, mixed populations of pathogen treated nematodes were collected into 1.5ml Eppendorf tubes using sterile water, and then washed twice with M9 buffer. The animals were then fixed at room temperature using a 3% glutaraldehyde in M9 solution for 3hrs. During the duration of the fixation period, the samples were placed on a horizontal Eppendorf rotator set to 15 rpm. Following the fixation, the samples were then washed twice in M9, and gradually dehydrated with a series of increasing ethanol concentration washes (30%, 50%, 60%, 70%, 80%, 90%, 100%). Next, the samples underwent supercritical drying with the assistance of a critical point dryer (K850, ProScitech). Finally, the samples were then sputter coated twice at 90 second durations with gold/palladium using a SC7620 Mini Sputter Coater/Glow Discharge System (Quorum technologies). SEM samples were imaged with a JSM-6390 (JEOL) scanning electron microscope using a 5 to 25kVolt acceleration voltage.

2.2.4. *M. humicola* infection assays.

All infection assays were carried out at 25ºC on 1.7% NGM plates seeded with 50µl lawns of OP50. In addition, unless otherwise stated, developmentally synchronized L4 animals were used at the start of each assay. Infection assays were carried out in triplicates and consisted of 50 nematodes being transferred onto NGM plates containing 3 *M. humicola* infected animals full of sporangia, or onto control plates devoid of the pathogen. The nematodes were only exposed to the pathogen for the first 48hrs, afterwards, for the remainder of the assay, the oomycete exposed animals were transferred onto new NGM plates without the pathogen. In both conditions, the surviving animals were transferred onto new plates every 24hrs. The plates were scored every 24hrs for the number of infected (visible sporangia), dead (unresponsive to touch yet displaying no visible sporangia), and missing animals over a period of 7 days. Assays were experimentally reproduced at least twice with three technical replicates per assay. GraphPad Prism 7 (GraphPad Software Inc.) was used to plot and compare survival curves, each survival curve represents pooling of the technical replicates (N=150). The log-rank (Kaplan–Meier) test was used to assess statistical significance, and a P value of <0.05 was considered statistically significant.

2.2.5. RNA preparation and transcriptomics analysis.

Populations of N2 hermaphrodites exposed to desired conditions, treatments and at relevant time-points were collected and placed into 50µl of TRIzol reagent, and total RNA was extracted and prepared using a Direct-zol RNA miniprep kit (Zymo Research) as per the manufacturer's instructions. The Illumina TruSeq RNA library preparation kit was used to produce the library preparation. The quality and quantity of RNA was determined using the RNA ScreenType System on a 2100 Bioanalyzer (Agilent). For the RNA extracted to analyse *C. elegans* gene changes post exposure to *M. humicola*, we performed infection assays in

triplicates as previously described, and at the relevant times points RNA was extracted from 50 animals per infection or control plate.

The sequencing data was processed and aligned to the *C. elegans* reference genome using Bowtie2 (Langmead and Salzberg, 2012). Counts were generated by converting alignments using BEDtools (Quinlan and Hall, 2010), counts then underwent normalisation using DESeq2 (Love et al., 2014) in R (R Development Core Team, 2011). The differences in gene expression were calculated with the DESeq2 package using the negative binomial test with Benjamini-Hochberg multiple test. The raw data from the RNA-seq experiment has been deposited to NCBI GEO under the accession GSE101647. For the comparative transcriptomics analysis, we compared the percentage similarity of our data set to the gene sets compiled by (Bakowski et al., 2014) after *N. parisii* infection, which was supplemented with data generated from *C. elegans* infections with pathogens *P. luminescens*, *E. faecalis* and *S. marcescens*, *D. coniospora* and *Harposporium. spp* from (Engelmann et al., 2011), Orsay-like virus from (Sarkies et al., 2013), *S. aureus* from (Irazoqui et al., 2010a), *P. aeruginosa* from (Troemel et al., 2006) and *B. thuringiensis* generated data set imported from WormExp (Yang et al., 2016).

2.2.6. Generation of the transcriptional reporters and their genome integration.

To produce the *chil-27* transcriptional reporter, we amplified with primers Chil-27F/Chil-27R, a 1.6kb genomic fragment containing sequences upstream of the *chil-27* start codon. The primers also introduced a HindIII and XbaI restriction enzyme sites into the 5' and 3' regions of the amplicon respectively. Subsequently, the amplicon was digested with both HindIII and XbaI and cloned into the vector L3135 (Addgene #1531), generating the transgene *chil-27p*::*pes-10*::GFP::*unc-54 3'UTR* (plasmid pGO4). The *chil-28* transcriptional reporter construct was produced using the same method as pGO4 and entailed amplifying a 0.4kb

fragment with primers Chil-28F/Chil-28R, followed by cloning into vector L3135 in the same manner as pGO4 to generate construct pGO7 [*chil-28p*::*pes-10*::GFP::*unc-54 3'UTR*]. Both constructs were verified with sanger sequencing. These transcriptional reporter constructs were injected into N2 at a concentration of 30ng/µl together with 20ng/µl of plasmid pCMH1195 (Perales et al., 2014) [*col-12p*::mCherry-pest] as a co-injection marker.

To obtain genome integration and stable transgenic nematodes, extrachromosomal lines harbouring reporters of interest, along with their respective co-injection marker, were subjected to gamma irradiation. Successful chromosomal integrations were mapped using the triply-marked strains EG1000 (*dpy-5*(*e61*) *I; rol-6*(*e187*) *II; lon-1*(*e1820*) *III*) and EG1020 (*bli-6*(*sc16*) *IV; dpy-11*(*e224*) *V; lon-2*(*e678*) *X*). Using this method, we generated and mapped two independent *chil-27p*::GFP harbouring lines; *icbIs4* (transgene was integrated into chromosome II) and *icbIs5* (transgene was integrated into chromosome I & IV) and one line containing the *chil-28p*::GFP transgene (integration was mapped to chromosome V). In all instances, we back-crossed the integrated lines x10 with N2.

2.2.7. Generation of the *chil* gene overexpressing lines.

To produce the *chil-1* to *chil-9* or *chil-18* to *chil-27* overexpression lines, we injected fosmid clones WRM065aH01 or WRM0619bB10 (Source Bioscience) respectively into N2. The fosmids contained N2 chromosome II genomic regions encompassing positions 9842328-9876919 or 9444160-9479928, which contained either *chil-1* to *chil-9* in a 34,592 bp fragment or *chil-18* to *chil-27* in a 35,769bp fragment. Fosmid clones were injected at a concentration of 20ng/µl with 5ng/µl of *myo-2p*::GFP as the co-injection marker. In each instance, three independent lines were obtained and used for the analysis. Both fosmids were verified by Sanger sequencing.

2.2.8. Generation of the CRISPR genome edited mutants.

To generate the *chil-4, 9, 18* and *27* CRISPR-mediated mutants, we inserted the Hygromycin (HYGB) resistance cassette [*rps-0p*::HYGB::*unc54 3'UTR*] within our target *chil* genes by using the technique developed by (Chen et al., 2013). Towards this goal, we produced constructs containing sgRNAs targeting genes *chil-4*; GAAAGTAATGATCAGTATAGG(CGG), *chil-9;* ATCTGCACCGTTGTATGG(AGG), *chil-18*; ATCTGCACCGTTGTATGG(AGG) and *chil-27*; ACCTCTCAATATTCAAGTGG(AGG). The pam motifs are indicated with brackets. These constructs were generated as previously described by (Friedland et al., 2013). The repair templates for the homologous recombination HYGB knock-in, were constructed in a two-step method. Initially, we PCR amplified a 0.8kb to 1kb fragment of genomic region upstream (*chil*-(n)_CRISP1F/1R oligos) and downstream (*chil*-(n)_CRISPR2F/2R oligos) of the PAM motif and the 2.0kb HYGB cassette (hygro-F/R). The resulting amplicons with complementary sequences were then used in a multi-fragment Gibson assembly reaction and cloned into plasmid BJ97 using restriction enzyme SpeI. To perform the CRISPR genome editing, we injected N2 day-1 adult hermaphrodites with a mixture containing 50ng/µl of *eft-3p*::*cas9*, 25ng/µl of the sgRNA guide (*pU6*::[respective *chil* gene sgRNA]), 10ng/µl of the heat shock inducible toxin plasmid pMA122 [*hsp-16.41p*::PEEL-1::*tbb-2 3'UTR*], 30ng/µl of the respective *chil* gene repair template plasmid and 5ng/µl of *myo2p*::dsRed as the co-injection marker. Successful genome editing was validated by detecting the homozygous insertion of the HYGB resistance cassette with PCRs. For this, we used chromosomal primers that annealed outside of the repair template (chil-4HygF/chil-4HygR, chil-9hygF/chil-9hygR, chil-18hyginsF/chil-18fullR and chil-27F/newchil-27R). In addition, we also used HYGB specific primers (hygro-gR/ hygro-gF). All primers used towards the generation and genotyping of the CRISPR-mediated mutants can be found in table 2.1.3.

2.2.9. Generation of the CHIL-27 translational reporter.

To study the sub-cellular localisation of CHIL-27, we generated an N-terminal GFP fusion construct under the control of the native *chil-27* promoter. Towards this goal, we initially produced an intermediary construct. This entailed amplifying the entire open reading frame of the N2 *chil-27* gene including its stop codon, with primers mchy_Nfus_cl27/cl27_NfusR_PiR5 and a GFP coding cassette with primers GFP-CAAX-pIR5F/mchy_NfsF_Pir5. For the amplification of the *chil-27* gene, worm lysate was used as the template, whilst for the GFP cassette, we used plasmid pGO4 [*chil-27p*::*pes-10*::GFP::*unc-54 3'UTR*]. The two fragments carried sequence complementarity, with overlaps introduced at the 3' end of the GFP amplicon, and 5' end of the *chil-27* amplicon, consisting of a 36bp flexible linker sequence to provide protein stability. Subsequently, these two fragments underwent PCR fusion (Hobert, 2002) to produce the N-terminally tagged product GFP::CHIL-27. The fused products which carried sequence similarities to the destination plasmid pIR5 [*arf-3p*::*pes-10*::GFP::*unc54 3'UTR*] were both digested with SwaI and cloned using Gibson assembly to generate plasmid pGO24 [*arf-3p*::*pes-10*::GFP::CHIL-27::*unc-54 3'UTR*]. Next, we amplified the promoter region of *chil-27* using primers Chil-27PrF/Chil-27PrR from plasmid pGO4 [*chil-27p*::*pes-10::unc-54 3'UTR*]. The primers also introduced an EcoRI and StuI restriction enzyme sites into the 5' and 3' regions of the amplicon respectively. Afterwards, both the amplified *chil-27* promoter which carried sequence similarities to the destination plasmid pGO24 were both digested with EcoRI and StuI, followed by cloning using Gibson assembly to generate the construct pGO25 [*chil-27p*::*pes-10*::GFP::CHIL-27*::unc-54 3'UTR*]. To study CHIL-27 expression, we injected N2 with 20ng/µl of the translational reporter and 5ng/µl of *col-12p*::mCherry-pest as a co-injection marker.

2.2.10. smFISH and FISH.

For the smFISH and FISH experiments, mixed or age synchronized populations of nematodes under the desired conditions and treatments were fixed as previously described by (Raj et al., 2008). For both instances when examining either *chil-27* transcription or staining the oomycete *M. humicola*, we hybridized the fixed animals overnight at 37ºC with 20nM of relevant oligo probes. Images were taken using a cooled DU-934 CCD-17291 camera (Andor) acquiring 0.5-1.0µm step z-stacks and a motorized, inverted epifluorescence Ti-eclipse microscope (Nikon). For the pathogen quantification experiments, we used the Zeiss Axio zoom V16 (Zeiss) microscope. A complete list of the *chil-27* smFISH and the *M. humicola* 18S/L30 FISH Quasar 670 tagged (Biosearch technologies) oligo probes are presented in table 2.1.3.

2.2.11. Abiotic stress assays.

All *chil-27p*::GFP reporter abiotic stress assays were conducted using the integrated strain *icbls4* and were monitored using a Zeiss Axio Zoom V16 scope (Zeiss). To assess whether heat shock could induce the reporter, the transgenic nematodes were placed at 33ºC for 4hrs and 37ºC for 1hr, animals were then observed over a 48hr period for GFP expression. To examine if chemically induced endoplasmic stress could activate the *chil-27p*::GFP reporter, we examined transgenic animals treated with 0.5µg/ml Tunicamycin (Sigma-aldrich) for 48hrs. To investigate whether starvation could induce expression of the transcriptional reporter, transgenic animals were maintained on non-seeded NGM plates supplemented with ampicillin (25µg/ml) for 48hrs at 20ºC. To assess if mechanical damage could activate *chil-27p*::GFP, animals were immobilised with Halocarbon oil (Sigma-aldrich) and pierced three times with a microinjection needle along the midbody. Once pricked, the nematodes were recovered using M9 and examined for GFP fluorescence during a 48hr period. The

hyperosmotic stress assays were performed as previously described by (Pujol et al., 2008). In all instances age synchronized L4 animals were used at the start of the assays.

2.2.12. Mutant crosses.

We utilised conventional genetic crosses to transfer the *chil-27* transcriptional reporter into N2 mutant backgrounds using integrated strain *icbls4*. With this method, we transferred the transgene into mutants *elt-3*(*gk121*), *sek-1*(*km4*) and *daf-6*(*e1377*). Strains *elt-3(gk121)* and *sek-1*(*km4*) were genotyped by PCR and agarose gel electrophoresis with primers Elt-3F/Elt-3R1/Elt-3R2 and Sek-1(km4)F/Sek-1(km4)Rmut/Sek-1(km4)Wt respectively. Strain *daf-6*(*e1377*) was phenotyped; the presence and or absence of dauers was observed under set conditions (Halaschek-Wiener et al., 2005; Riddle et al., 1997). All strains were homozygous for both the *chil-27p*::GFP and the *col-12p*::mCherry transgenes. List of all the strains generated can be found in table 2.1.1.

2.2.13. *chil-27* induction assays and the preparation of heat killed pathogen.

Induction assays were carried out in duplicates and consisted of exposing 50 transgenic animals harbouring the *chil-27p*::GFP reporter to *M. humicola*. After 48hrs or when a desired time had passed, the transgenic animals were anaesthetised with sodium azide (10mM), and the number of GFP positive and GFP negative animals were counted. As a positive control, strains *icbls4* or *icbls5* was used. As a negative control, the same population of transgenic animals were also cultured under the same conditions but were not exposed to the pathogen. All induction assays were carried out at 25^{o}C on 1.7% NGM plates seeded with lawns of OP50. In addition, unless otherwise stated, induction assays were carried out using developmentally synchronized L4 animals. Experiments were reproduced at least twice and GraphPad Prism 7

(GraphPad Software Inc.) was used to plot results. The Fischer's exact test was used to assess statistical significance, a *P* value of <0.05 was considered statistically significant.

The oomycete extract used in some instances of induction assays was prepared by washing off both pathogen, and infected animals from *M. humicola* maintenance plates with sterile water, followed by passing the mixture through a filter prior to autoclaving. For the heat killed pathogen induction assay, infected animals were picked and placed into 1.5ml Eppendorf tubes, autoclaved for 20 minutes at 121ºC and allowed to cool prior to their use in induction assays.

2.2.14. General, fluorescence and atomic force microscopy.

Reporter induction assays were conducted with a Zeiss Axio zoom V16 (Zeiss) using 800ms exposure time and an Axio 506 mono camera (Zeiss). For standard fluorescence microscopy either a Nikon Ti-eclipse or a Leica SP5 Inverted Confocal Microscope (HCXPL APO 63x 1.40-0.6 oil objective) was used. DIC imaging was performed using either an upright Axio A1 Scope (Zeiss) or an inverted Leica DMIRBE microscope. In all instances, unless otherwise stated, the animals were mounted onto 3% agar pads containing M9 and nematodes were anaesthetised using sodium azide (10mM). Atomic force microscopy was performed as previously described by (Essmann et al., 2017).

2.2.15. Forward genetic screens.

To obtain the *pals-22* (alleles *icb88*, *icb89* and *icb90*) and *pals-25* (*icb98*) mutants, we performed standard ethyl-methanesulfonate (EMS, Sigma-aldrich) mutagenesis as previously described by (Kutscher and Shaham, 2014) on the stable transgenic strains *icbIs4* (transgene integration mapped to chromosome II) or *icbIs5* (transgene integration mapped to chromosome

I & IV) respectively. The strains harboured the fluorescent reporters *chil-27p*::GFP and *col-12p*::mCherry. In both instances, L4 (P0) transgenic animals were incubated in 24mM EMS for 4 hours at 20ºC. Subsequently, the F2 generations on the same plate were screened and GFP+ animals were manually collected using an Axio Zoomv16 (Zeiss) dissecting microscope. In all instances, EMS mutants were backcrossed at least x4 using N2, *icbIs4* or *icbIs5*. Complementation experiments were performed by generating heterozygous animals for the *pals-22* alleles *icb88* and *icb90* and examining for GFP expression.

The *pals-22* alleles *icb88* and *icb90* were identified by performing Hawaiian SNP mapping, and whole genome sequencing (WGS) of F2 recombinant animals generated by crossing the mutants to CB4856, a polymorphic isolate (Doitsidou et al., 2008). The *pals-22*(*icb89*) allele was identified by PCR using primers C29f9.1 F2 and C29f9.1 R2 spanning exons 1 and 2 of the *pals-22* gene and sanger sequencing. For the WGS analysis of mutants, genomic DNA was prepared using a Puregene Core kit (Qiagen). For the WGS analysis, the Galaxy-Cloud map pipeline (Minevich et al., 2012) was used to analyse SNPs and identify causative mutations for the *pals-22* alleles (*icb88* and *icb90 III*) and the *pals-25* (*icb98*) allele.

For the *pals-22*(*icb90*) suppressor screen, strain *icb90* was incubated as described above but with 17mM of EMS, and animals displaying no GFP expression were manually selected. The two *pals-25* alleles (*pals-22*(*icb90*)*pals-25*(*icb91*) *III* and *pals-22*(*icb90*)*pals-25*(*icb92*) *III*) were identified by direct whole genome sequencing of mutant strains.

2.2.16. RNAi gene knockdown.

For the RNAi knockdown of target genes, developmentally synchronised embryos, obtained from the 'bleaching' of gravid hermaphrodites, were subjected continuously to RNAi by feeding for one generation on RNAi compatible NGM plates. To produce the RNAi plates,

NGM media prior to pouring, but subsequent to autoclaving and cooling, were supplemented with 1mM isopropyl B-D-1-thiogalactopyranoside (IPTG), 6.25μg/ml tetracycline and 25μg/ml ampicillin. For the RNAi knockdown of desired genes, the plates were then seeded with IPTG inducible dsRNA expressing *E. coli* strain HT115 harbouring gDNA (Ahringer library), or cDNA fragments (Vidal library) cloned into the L4440 vector (Addgene plasmid #1648). The bacteria containing the desired clones were grown overnight at 37ºC, 250rpm in LB containing ampicillin (25μg/ml). The RNAi plates were then seeded with 100μl of the bacteria culture and used only after a minimum of 2 days following seeding. Empty vector without any insert was used as the control treatment. In addition, to test the potency of the RNAi plates, nematodes were subjected to *unc-22* RNAi. The *unc-22* RNAi is regularly used to confirm the quality of RNAi plates, because silencing results in a distinctive phenotype characterised by the loss of co-ordination, decreased movement and "twitching" pattern along the body-wall musculature (Moerman et al., 1979). All the RNAi clones used in this study were verified with Sanger sequencing.

Chapter 3. The characterisation and development of a new *C. elegans* pathosystem

3.1. Introduction.

In the lab, N2, the wild-type reference *C. elegans* strain, is grown on sterile agar plates. An environment that is conceivably quite divergent to the natural ecology of *C. elegans*. Despite its extensive use as a pathosystem, little is known about the natural biotic interactions and ecology of this metazoan (Kiontke, 2006). Studying an animal's habitat, and particularly its interactions with natural pathogens, can provide indispensable facets of information that are required to obtain a comprehensive understanding of an organism's genome evolution, and can also aide in the discovery of novel responses to both biotic and abiotic threats. With these appreciations, over the last years, researchers have begun to actively isolate wild-caught *C. elegans* strains and document their natural habitat. These investigations have not only led to the re-classification of *C. elegans* from a soil dwelling nematode, to a coloniser of microbe rich environments in nature (Barrière and Félix, 2005; Félix and Braendle, 2010), but they have also started to reveal natural pathogens of *C. elegans*. Pathogens that exhibit specific means of gaining entry and infecting *C. elegans*, including the fungal pathogen *Drechmeria coniospora*, which can attach non-specifically to the whole cuticle (Jansson, 1994), microsporidia such as *Nematocida parisii*, an intestinal intracelular pathogen that gains entry through ingestion (Troemel et al., 2008), the gram positive *Microbacterium nematophilum* that adheres to the posterior region of the cuticle and hindgut (Hodgkin et al., 2000), and the Orsay virus which is distantly related to known noda-viruses that also enters by way of ingestion (Félix et al., 2011).

To further our knowledge on the plethora of as yet identified microbes *C. elegans* encounters in its habitat, we collected wild-caught *C. elegans*, with the aim of co-isolating natural pathogens. Here, we report, the isolation of a new eukaryotic pathogen of *C. elegans*, an oomycete. Pathogenic oomycetes encompass eukaryotes that were once classified as fungi, partly because they exhibited superficially similar morphology to true fungi, such as growing filamentous branching mycelia. Oomycetes are known today to be divergent microorganisms,

with greater taxonomic affinity to diatoms and brown algae (Cavalier-Smith and Chao, 2006; Kamoun, 2003).

Pathogenic oomycetes infect a range of animal and plant hosts (Phillips et al., 2008). In contrast to plant pathogenic oomycetes, research on animal pathogenic oomycetes has been limited, in part, due to a paucity of genetically tractable hosts. Additionally, previous attempts to establish experimental systems to study animal pathogenic oomycetes, have also been hindered by the observation of inconsistent disease phenotypes, the under development of the model systems, or due to a scarcity of biological tools (Phillips et al., 2008; Zanette et al., 2013). These are unfortunate limitations, when considering the invasive treatments required for patients suffering from pythiosis, a rare disease caused by the mammalian infecting oomycete *Pythium insidiosum* (Mendoza and Vilela, 2013). Also, the oomycete *Saprolegnia parasitica*, a pathogen of fresh water fish, has a devastating economic impact on aquaculture farming (Phillips et al., 2008). Therefore, as can be appreciated, our identification of an oomycete that naturally infects *C. elegans*, a genetically tractable and well-established model organism, has provided us the opportunity to introduce a robust and novel pathosystem.

In this chapter, we show that the pathogen is a newly isolated strain of *Myzocytiopsis humicola*, a holocarpic obligate nematophagous oomycete that has previously been shown to infect other *Rhabditids* nematodes (Glockling and Beakes, 2000). In addition, we will present a detailed morphological characterisation of the pathogen's life cycle, as well as the design of an infection assay, a robust method to measure the rate of *M. humicola* infection in a controlled manner. Through the employment of our infection assay and stable genetic mutants, we will also demonstrate that the p38 MAPK innate immunity pathway antagonises *M. humicola* infection. In summary, we present the discovery and characterisation of a new class of natural pathogen that infects *C. elegans*, and the establishment of a novel pathosystem that can be used to study animal immune responses to an oomycete infection.

3.2. Results.

3.2.1. The identification of an oomycete that naturally infects *C. elegans*.

While sampling for nematodes from rotting vegetation in the botanical garden of the university of Lisbon, Portugal (Figures 3.1A and B), Dr Marie-Anne Felix found some non-responsive animals that harboured small, 'sphere'-like shaped objects within their bodies (Figures 3.1C and D). These abnormal animals were among the population of a wild-caught *C. elegans* isolate (JU2519). This irregular phenotype was observed to be distinctly absent from healthy animals (Figures 3.1C and E). Furthermore, we found that the addition of dead nematodes displaying this pronounced symptom, to NGM plates containing N2 animals, the lab wild-type *C. elegans* reference strain, resulted in the horizontal transmission of this phenotype to the population. In contrast, we did not detect the symptom could be spread vertically, as progeny isolated either by bleaching gravid hermaphrodites, or by mechanically separating eggs once laid but before hatching, resulted in the development of healthy adults. Based on these findings, and the presence of nuclei within these foreign spheres, we conjectured that the observed phenotype was the sign of a putative infection, caused by a eukaryotic nematophagous pathogen.

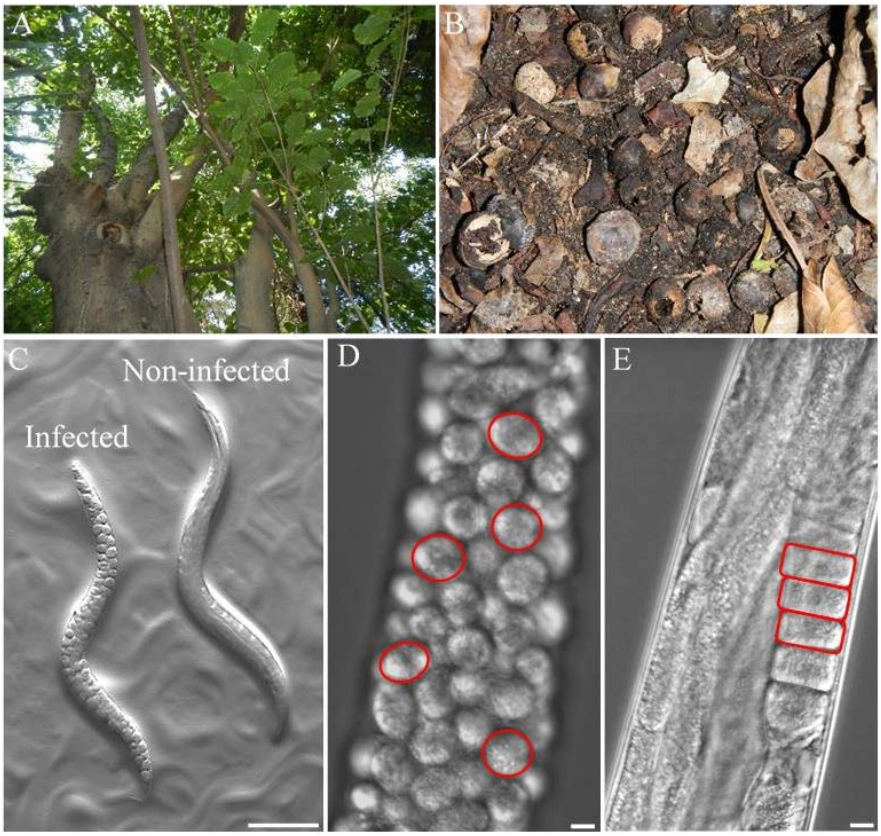

Figure 3.1: The identification of a new natural pathogen of *C. elegans*. (A-B) The pathogen was co-isolated with wild-caught *C. elegans* sampled from beneath a *Ficus isophlebia* tree (A) rotting vegetation (B). **(C)** A single infected and non-infected *C. elegans* hermaphrodites on an agar plate. An animal infected with the Lisbon pathogen exhibiting 'sphere'-like structures from the tip of the mouth to the tail (Left), a pronounced phenotype that is absent in non-infected animals (Right). **(D)** A close-up of an infected animal displaying the foreign 'sphere'-like objects underneath the cuticle (marked by red circles). **(E)** A close-up of a non-infected animal showing no such objects and instead containing stacked oocytes (marked by red rectangles). The animals presented are day-1 adults. Scale bars represent 100µm. The photographs A and B were taken by Dr Marie-Anne Felix.

To determine the identity of the isolated pathogen, we initially amplified the 18S rDNA sequence from infected animals with universal eukaryotic 18S primers. Following sequencing, and a blast search in the GenBank database, the organism was shown to be most closely related to the oomycetes, and specifically to members of the *Myzocytiopsis* genus, a diverse group of eukaryotic organisms that have previously been shown to infect a range of nematodes and rotifers (Glockling and Beakes, 2000). For ease of discussion, we will only mention the top 5 results below. Through the use of pairwise comparisons, we found that the Lisbon isolate sequence, was over 99% similar to the 18S rDNA GenBank sequences of *Myzocytiopsis* species *M. glutinospora* (99.9%), *M. humicola* (99.9%) and *M. subuliformis* (99.5%), and displayed over 98% similarity to *M. vermicola* (98.6%) and *M. venatrix* (98.7%) (see Table 3.1). Additionally, by constructing a phylogenetic tree based on comparisons of the 18S rDNA sequences, we discovered that the Lisbon isolated oomycete formed a clade, clustering into a polytomy with *M. glutinospora*, *M. humicola* and *M. subuliformis* (Figure 3.2A). These findings implied that either the Lisbon oomycete was a new species, a sister taxon most closely related to *M. glutinospora*, *M. humicola* and *M. subuliformis*, or more likely that the 18S rDNA-based analysis lacked the resolving power needed, to classify the newly isolated oomycete past the genus level, as these sequences were very similar.

To identify further the pathogen, we performed additional phylogenetic analysis with amplified mitochondrial encoded cytochrome c oxidase subunit 2 (COX-2), and the ribosomal internal transcribed spacer (ITS) rDNA sequences, the two most common regions of DNA employed for the molecular identification of oomycetes to the species level (Lévesque and De Cock, 2004; Robideau et al., 2011). In contrast to the 18S rDNA, we found that both the COX-2 (Figure 3.2B) and ITS (Figure 3.2C) based analysis gave greater resolution. In fact, the Lisbon isolated oomycete branched into a dichotomy, distinctly bifurcating into a single clade with *M. humicola* in both instances. Additionally, we found that the genetic distance between

the Lisbon isolate and *M. humicola* was smaller in comparison to other *Myzocytiopsis* species. For example, 93.6% for COX-2 between the Lisbon isolate and *M. humicola*, as opposed to 91.7% between the Lisbon isolate and *M. glutinospora*, or 88.3% for ITS between the Lisbon isolate and *M. humicola*, as opposed to 85.7% between the Lisbon isolate and *M. glutinospora* (see Table 3.1). Taken together, these results suggest that the pathogen we identified was likely to either be a new isolate of *M. humicola*, or a very close relative of the species. To distinguish between these two possibilities, we reasoned that morphological characterisation would be required to definitively identify the Lisbon isolated nematophagous oomycete as *M. humicola*, or a genetically similar sister species.

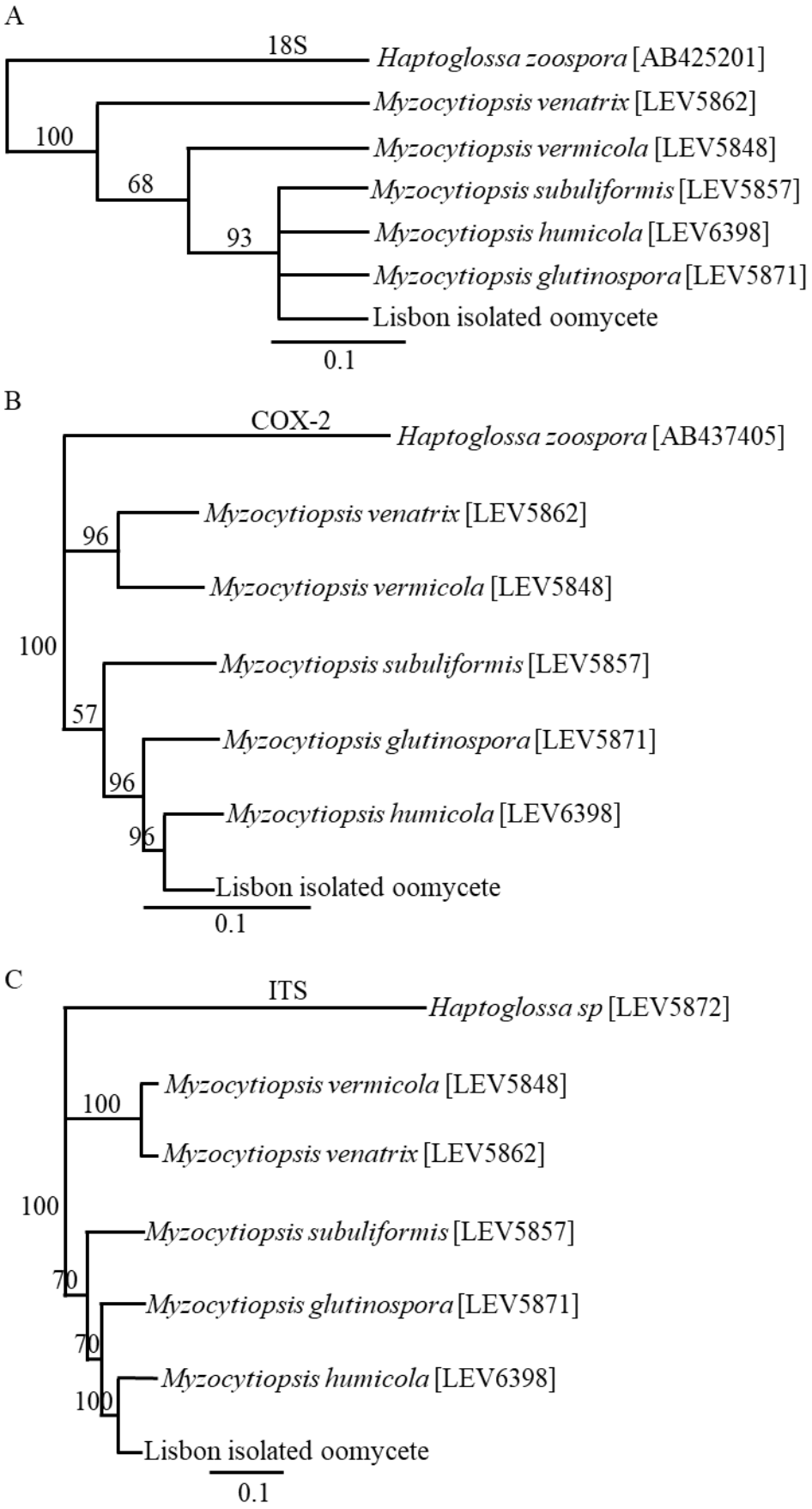
A
18S
Haptoglossa zoospora [AB425201]
Myzocytiopsis venatrix [LEV5862]
Myzocytiopsis vermicola [LEV5848]
Myzocytiopsis subuliformis [LEV5857]
Myzocytiopsis humicola [LEV6398]
Myzocytiopsis glutinospora [LEV5871]
Lisbon isolated oomycete
100
68
93
0.1
B
COX-2
Haptoglossa zoospora [AB437405]
Myzocytiopsis venatrix [LEV5862]
Myzocytiopsis vermicola [LEV5848]
Myzocytiopsis subuliformis [LEV5857]
Myzocytiopsis glutinospora [LEV5871]
Myzocytiopsis humicola [LEV6398]
Lisbon isolated oomycete
96
100
57
96
96
0.1
C
ITS
Haptoglossa sp [LEV5872]
Myzocytiopsis vermicola [LEV5848]
Myzocytiopsis venatrix [LEV5862]
Myzocytiopsis subuliformis [LEV5857]
Myzocytiopsis glutinospora [LEV5871]
Myzocytiopsis humicola [LEV6398]
Lisbon isolated oomycete
100
100
70
70
100
0.1

Figure 3.2: The Lisbon isolated pathogen is an oomycete closely related to *M. humicola*. Phylogenetic analysis indicates that the Lisbon isolated pathogen is an oomycete most closely related to *M. humicola*. The phylogenetic trees are based on alignments of the Lisbon isolated oomycete 18S **(A)**, COX-2 **(B)** and ITS **(C)** rDNA sequences, to that of available *Myzocytiopsis* species. The 18S phylogenetic based analysis clustered the Lisbon isolated oomycete into a polytomy with *M. glutinospora*, *M. humicola* and *M. subuliformis*. In contrast, both the COX-2 and ITS phylograms placed the Lisbon pathogen into a dichotomy with *M. humicola*. A basal oomycete (*Haptoglossa*) was used as an outgroup in each instance. The evolutionary history was inferred with the maximum likelihood method based on the Tamura-Nei model. The numbers at the branch nodes indicate bootstrap values based on 100 replicates, and the branches supported by bootstrap value of >50% are shown. Scale bars represent changes per site. The branch lengths indicate the amount of character change. The trees were created using Geneious version 10.2.2. The NCBI accession numbers for reference sequences are presented within brackets.

Table 3.1. The percentage genetic similarity between the Lisbon isolated oomycete and other *Myzocytiopsis* species. Pairwise comparisons between the Lisbon isolate 18S, COX-2 and ITS rDNA sequences to that of other *Myzocytiopsis* species.

		***Myzocytiopsis* species**				
rDNA sequences		*M. humicola*	*M. vermicola*	*M. subuliformis*	*M. glutinospora*	*M. venatrix*
Lisbon isolate	18S	99.9%	98.6%	99.5%	99.9%	98.7%
	COX-2	93.6%	87.5%	85.1%	91.7%	87.1%
	ITS	88.3%	76.2%	79.7%	85.7%	75.7%

3.2.2. The morphological characterisation of the oomycete's life cycle in *C. elegans*.

Because species of the *Myzocytiopsis* genus have been morphologically characterised, and display distinct spore morphology and spore release methods (Glockling and Beakes, 2000), we next sought to identify the oomycete by morphologically characterising its life cycle. As this is an obligate pathogen of *C. elegans*, it is not possible to culture the oomycete independently of the host. Therefore, we performed all morphological characterisation by infecting N2 animals. In addition, we used differential interference contrast (DIC) microscopy to recognise the different stages of the oomycete's life cycle.

The distinguishing hallmark of *Myzocytiopsis* infections are the development of sporangia that occupy the body cavity of nematodes, which can develop within 24hrs post exposure to the pathogen (Figures 3.3A and B). At this final stage, each infected adult nematode contains a mean of 201±8 sporangia (Table 3.2). At first, the sporangia contain undifferentiated cytoplasmic mass, later, they differentiate to produce approximately 18±1 zoospores per sporangium (Figure 3.3C, Table 3.2). The zoospores are biflagellated (Glockling and Beakes, 2000; L. Barron and G. Percy, 2011), and develop within the sporangia until they are released through the evacuation tube of a fully matured sporangium (Figures 3.3D and E). Once outside of the host, the released zoospores encyst (Figure 3.3F) to produce adhesive 'bud'-like extensions (Figure 3.3G), and transform into the infection transmitting cytospores (Figure 3.3H). Later, the cytospores attach to the cuticle of passing nematodes (Figure 3.3I). After successfully penetrating the cuticle, the growth of septa-less hyphae termed thalli is initiated inside the nematode's body cavity (Figure 3.3J). Subsequently, the hyphae form complex networks that eventually partition into distinct sporangia (Figure 3.3K). The development of sporangia and the growth of hyphae happen exclusively within the host. See Figure 3.3L for a summary of the pathogen's life cycle.

Based on these morphological characterisations, which are consistent with previous reports of the *M. humicola* life cycle in other nematode species (Glockling and Beakes, 2000; L. Barron and G. Percy, 2011), we determined that the Lisbon isolated oomycete was morphologically undistinguishable from *M. humicola*. This was most evident when comparing mature spore and sporangia morphology, as well as the method of spore release, i.e. the presence of an evacuation tube, motile zoospores and the morphology of encysted 'budded' cytospores (Glockling and Beakes, 2000). As these results validated our phylogenetic analysis, we concluded that the Lisbon pathogen is a new isolate of *M. humicola*, and as such will be referred to as *M. humicola* (strain JUo1) for the remainder of this thesis. While *M. humicola* has been reported to be able to undergo both asexual and sexual reproduction in the wild (Glockling and Beakes, 2000; L. Barron and G. Percy, 2011), we only observed an asexual life cycle under lab culture conditions.

Table 3.2. Mean values (± SE) of sporangia per infected animal and zoospores per sporangium. The quantifications were performed using DIC.

Characterisation	No. Sporangia (per infected animal)	No. Zoospores (per sporangium)
Mean ± SE	201±8	18±1
Sample size	n=5	n=7

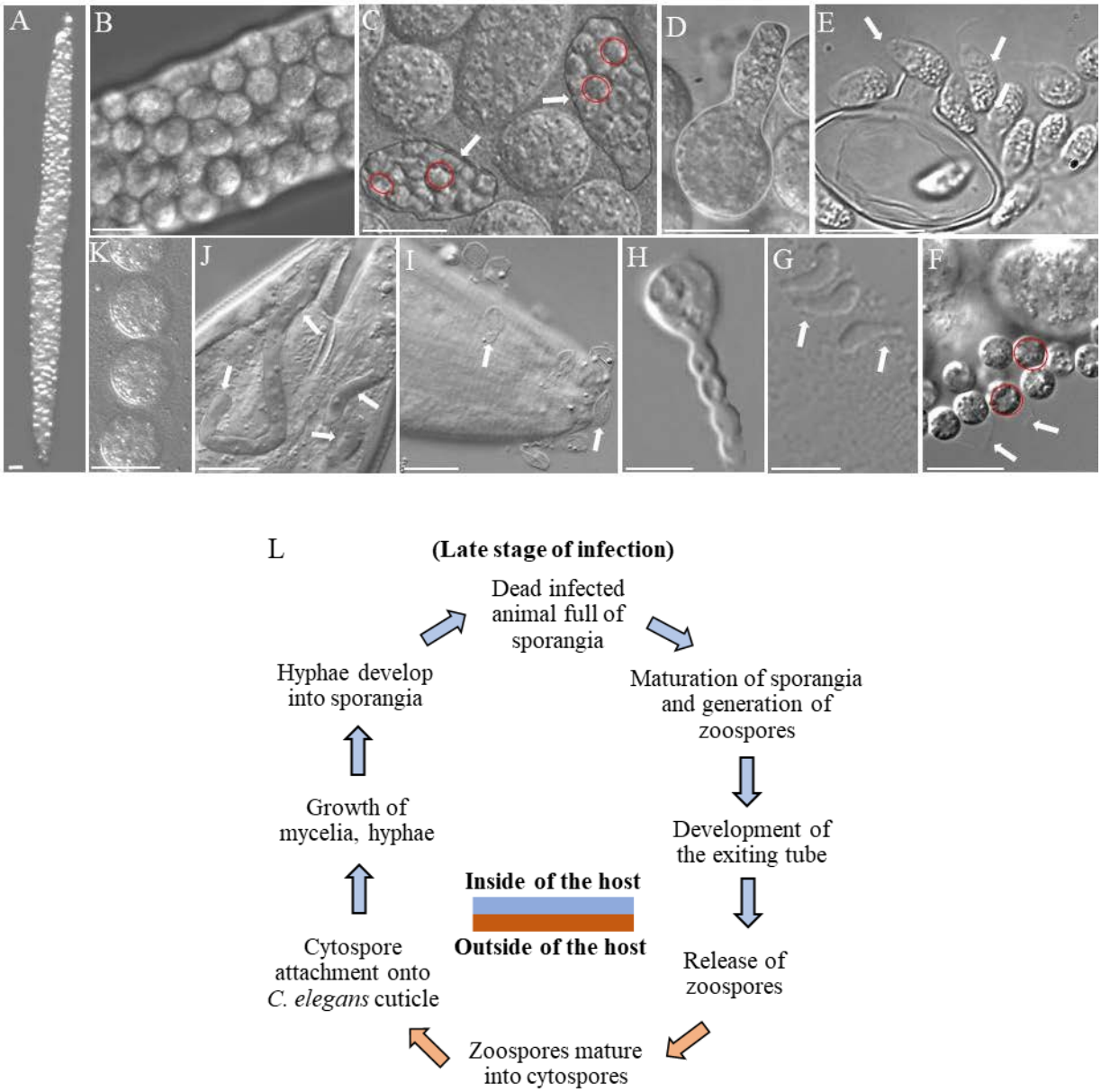

Figure 3.3: The *M. humicola* life cycle during the infection of *C. elegans*. The infection of *C. elegans* by *M. humicola* proceeds through distinct stages. **(A-B)** In the late stage of successful infection, the oomycete develops as sporangia that occupy the nematode's body. These 'sphere'-like structures initially contain an undifferentiated cytoplasmic mass. (A) An infected nematode. (B) Close-up of undifferentiated sporangia. **(C)** After maturation and differentiation of the cytoplasmic mass, zoospores are produced (mature sporangia are indicated with white arrows, and individual zoospores are marked with red circles). Following further development, an evacuation tube is then formed **(D)**, where later the biflagellated motile

zoospores exit **(E**, white arrows indicate flagellated zoospores**)**. Once outside of the host, the released zoospores encyst **(F**, red circles indicate individual zoospores and white arrows indicate flagellar**),** and begin to develop extensions **(G**, white arrows**)**. With the production of adhesive 'bud'-like extensions, the cysts mature into cytospores, which is the infection transmitting stage **(H)**. Upon successful attachment of the cytospores to the cuticle **(I**, white arrows**)**, and penetration, the growth of non-septate hyphal termed thalli is initiated inside the nematode's body cavity **(J)**. Subsequently, the thalli swell and partition into distinct sporangia **(K)**. The pathogen's life cycle was characterised by infecting *C. elegans* N2 hermaphrodites. Scale bars represent 100μm. **(L)** A summary of the *M. humicola* life cycle.

During the establishment of infection, *M. humicola* adheres to the integument of the host. Anatomically, the outermost layer of *C. elegans* is comprised of a tough but flexible cuticle. The cuticle acts as the primary barrier modulating *C. elegans* interaction with its environment, and also protects against a range of detrimental biotic and abiotic threats (Chisholm and Hsiao, 2012; Johnstone, 1994). Throughout our studies to characterise the *M. humicola* (strain JUo1) life cycle, we were able to detect cytospore attachments to the nematode's cuticle with DIC. However, visualising these attachment events proved difficult and time consuming, this limitation prevented us from addressing such questions as, do the *M. humicola* cytospores display any spatial attachment specificity? Therefore, to address this possibility, we employed scanning electron microscopy (SEM) to visualise pathogen sites of attachment. We observed that the *M. humicola* attachments were specific to regions around the mouth, along the longitudinal ridges of the cuticle, termed the alae and around the tail (Figure 3.4).

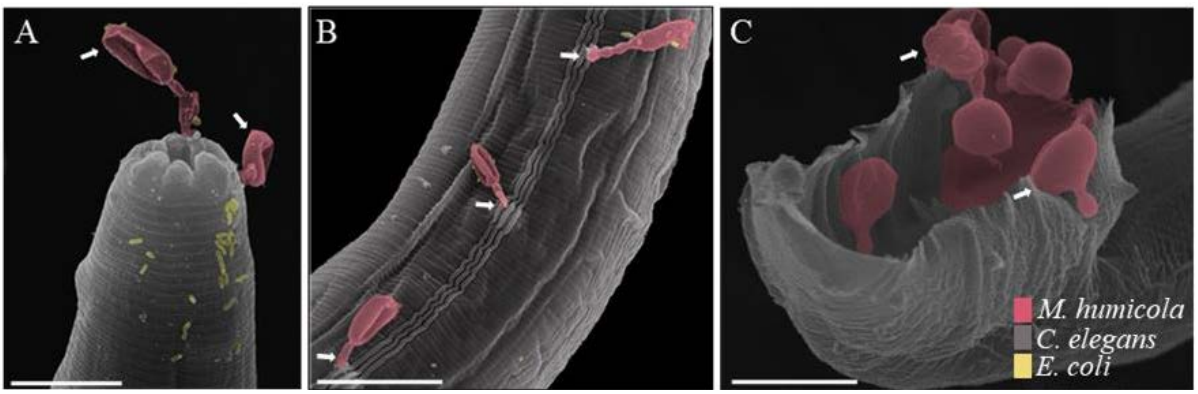

Figure 3.4: SEM reveals that *M. humicola* cytospores preferentially attach onto specific regions of the *C. elegans* cuticle. (A-C) Representative false colour scanning electron micrographs showing *M. humicola* cytospores preferentially attached around the mouth (A), along the alae (B) and around the tail (C) of adult nematodes. The white arrows indicate attached cytospores. The colour key is presented in panel C. Scale bars represent 10μm.

3.2.3. The development of a *M. humicola* infection assay.

Although previous studies have described the life cycle and characterised the morphological diversity of some nematophagous oomycetes, including members of the *Myzocytiopsis* genus (Glockling and Beakes, 2000, 2008; L. Barron and G. Percy, 2011), these studies were restricted to morphological analysis and did not focus on the identity of the host, or how the nematodes responded to an oomycete infection. As a consequence, the interactions of the host and pathogen were never studied at the molecular level. In addition, whether nematophagous oomycetes could infect *C. elegans* also had never been demonstrated, both in nature or in a controlled laboratory setting. With the observation that we could efficiently transmit the infection to the genetically tractable lab reference strain N2, by using dead infected animals as "vehicles" to inoculate populations of nematodes, we next sought to exploit this natural oomycete infection to establish a new pathosystem. To this end, we developed a method to reproducibly and accurately monitor the rate of *M. humicola* infection.

To study the mechanisms of *M. humicola* infection and *C. elegans* susceptibility in a controlled manner, we developed an infection assay to precisely measure the number of animals that show a defined symptom of infection over time, namely non-responsive animals that exhibit sporangia (Figure 3.3A). Due to the constraint of requiring infected animals as "vehicles" for transferring the *M. humicola* pathogen to populations of non-infected nematodes, and the low penetrance of infection observed within the pathogen maintenance plates, we decided upon inoculating populations of nematodes with 3 infected adult hermaphrodites. In this assay (Figure 3.5), we maintain 50 developmentally synchronized fourth larval stage (L4) hermaphrodites on NGM plates inoculated with 3 infected animals. Also, the nematodes are only exposed to the pathogen for the first 48 hours, and at 24-hour timepoints, we monitor the number of newly infected animals, whilst we censor the number of animals dead, missing or killed during transfers. We define dead animals as nematodes irresponsive to touch that fail to

develop sporangia. Additionally, we transfer the surviving animals at 24-hour intervals onto new NGM plates to ensure the availability of food, as well as to prevent new progeny from obscuring the assay. We monitor the assays for a period of 7 days. For each experiment, we used three technical replicates (three plates) per strain, and pooled the data, this was done to address reproducibility of results, potential variations between plates and to generate robust data. In turn, to determine if the event being studied was reproducible e.g. a mutation increased or decreased the hosts sensitivity to *M. humicola* infection, we repeated the assay at least once more. As a control, we simultaneously maintain the same population of synchronized animals on NGM plates not inoculated with the pathogen, and we monitor the number of dead animals, whilst censoring nematodes that are missing or killed. In both instances, the NGM plates contain small lawns of OP50 as the food source, this ensures the nematodes come in contact with the pathogen.

Using this method, we first optimised conditions, and investigated the effect of different culturing temperatures on the rate of *M. humicola* infection in *C. elegans*. We incubated N2 with *M. humicola* at 20ºC or 25ºC, both are standard culturing temperatures (Stiernagle, 2006). We found that *M. humicola* infections were reproducibly more penetrant at 25ºC compared to 20ºC (log-rank, $p<0.0001$, Figure 3.6A). In both cases, some animals survived at the end of the assay, with 54% of animals surviving at 20ºC as opposed to 34% at 25ºC. The different culturing temperatures did not affect the survival of nematodes maintained on the control plates, as 97% (20ºC) and 98% (25ºC) of animals survived at the end of the assay (log-rank, not significant, Figure 3.6B). These findings therefore establish 25ºC as the optimum temperature to conduct our infection assays, with the aim of obtaining higher rates of infection.

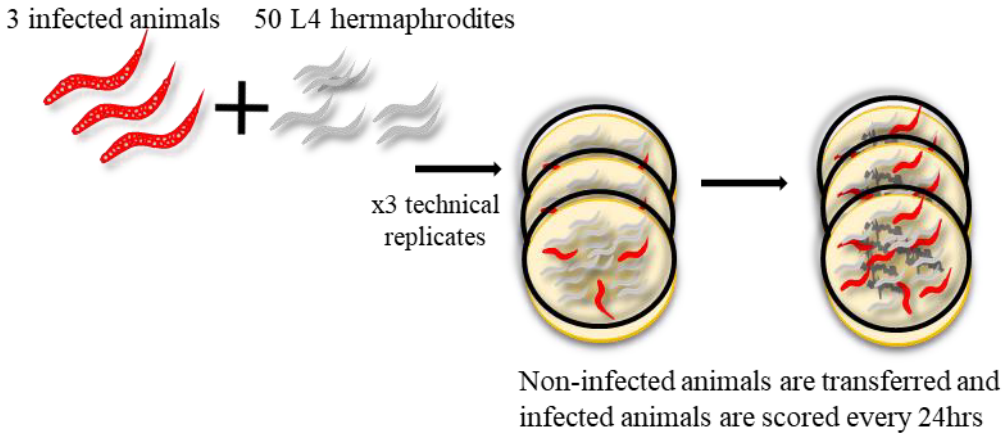

Figure 3.5: The design of the *M. humicola* infection assay. A cartoon depicting the infection assay designed to study the susceptibility of *C. elegans* to *M. humicola* infection. Initially, 50 developmentally synchronized L4's are transferred onto OP50 seeded NGM plates that contain 3 previously infected animals. The animals are only exposed to the pathogen for the initial 48hrs, and the rate of infection is monitored at 24hr timepoints. Each assay consists of 3 technical replicates per strain. The infection assays are maintained for a period of 7 days, and the surviving animals are transferred without the pathogen to new NGM plates every 24hrs.

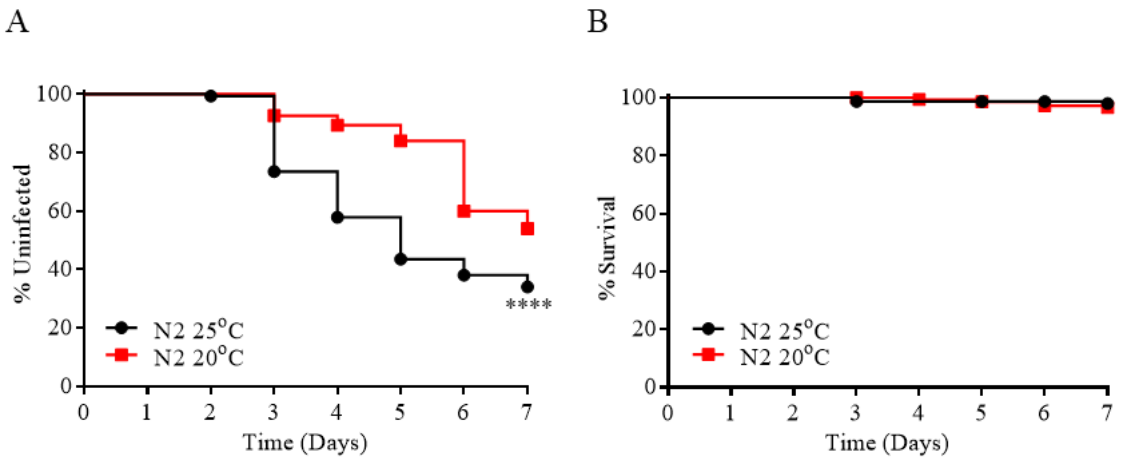

Figure 3.6: *C. elegans* is more sensitive to *M. humicola* infection at 25°C. (A-B) Characterising the effects of nematode culturing temperatures on host survival against *M. humicola* infection. (A) Infection plates containing wild-type L4's cultured on OP50 inoculated with *M. humicola*, and incubated at the indicated temperatures. The survival of N2 infected with *M. humicola* was significantly reduced at 25°C compared to 20°C ($p < 0.0001$). (B) Control plates containing L4's cultured on OP50 not inoculated with the pathogen. The animals cultured at 20°C or 25°C survived at a comparable rate during the short time of the assay. The infection assays were performed using 50 developmentally synchronized L4 hermaphrodites. Each survival curve represents pooled data from three technical replicates (N=150 per curve). The data shown is representative of three independent experiments. The survival curves were visualised using GraphPad prism 7. The statistical significance between the survival curves was determined using the log-rank analysis (**** $p<0.0001$).

3.2.4. The p38 MAPK pathway antagonises *M. humicola* infection.

With the establishment of a robust and reproducible infection assay, we next sought to determine if the well characterised p38 MAPK innate immunity pathway (Figure 3.7A), previously implicated to contribute towards *C. elegans* immunity to a range of fungal and bacterial pathogens (Kim et al., 2002; Liberati et al., 2004; Pujol et al., 2008; Troemel et al., 2006), could also confer *C. elegans* resistance against an oomycete infection. This pathway is principally comprised of the upstream Toll/IL-1 resistance (TIR) domain containing protein TIR-1, and a kinase signalling cascade; activated NSY-1 phosphorylates SEK-1, which in turn phosphorylates and activates PMK-1, this results in downstream regulators of the pathway, such as the transcription factor SKN-1, inducing the expression of defense genes and mechanisms that antagonise infection (Andrusiak and Jin, 2016; Inoue et al., 2005; Kim et al., 2002; Papp et al., 2012).

To achieve this aim, we examined the sensitivity of *C. elegans* strains harbouring stable genetic mutations attenuating the function of genes *sek-1*(*km4*) and *pmk-1*(*km25*). We found that both the *sek-1* ($p < 0.0001$) and *pmk-1* ($p < 0.0001$) mutants displayed reproducibly increased susceptibility to *M. humicola* infection compared to the wild-type N2 (Figures 3.7B-C). Whilst both mutations affect the function of the p38MPAK pathway, *sek-1* mutants displayed a significantly reduced rate of survival in comparison to the *pmk-1* mutants ($p<0.0001$), with all the *sek-1*(*km4*) animals succumbing to oomycete infection by day 4 compared to day 7 for the *pmk-1*(*km25*) mutants.

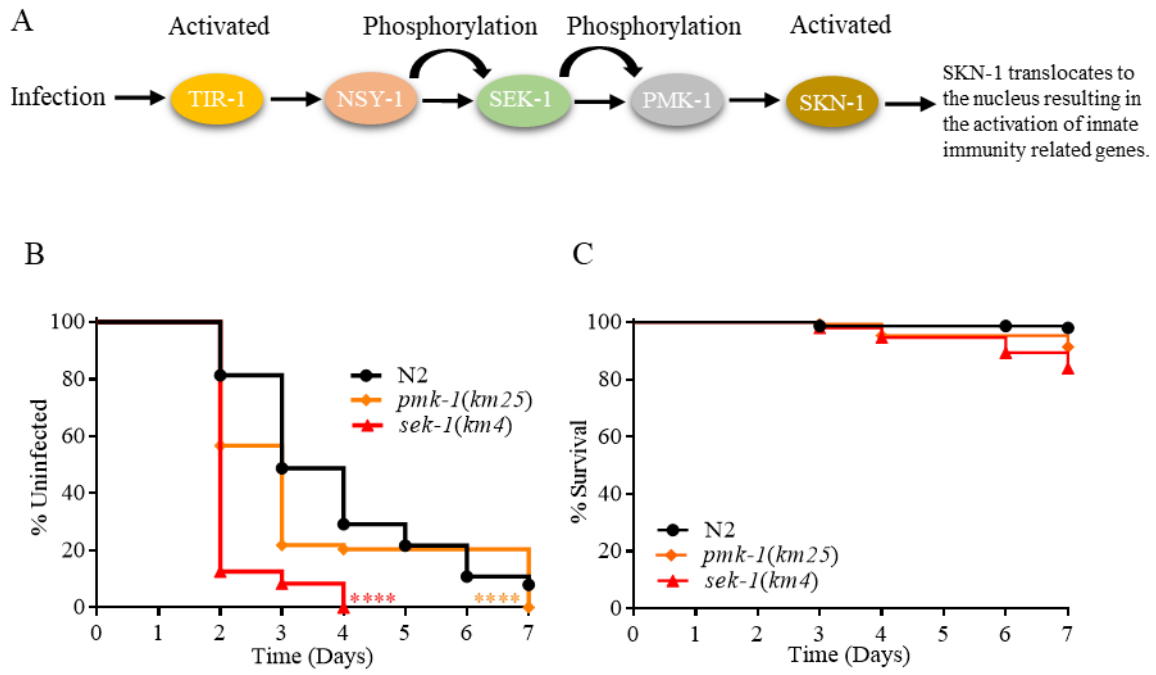

Figure 3.7: The p38MAPK pathway contributes towards *C. elegans* immunity against *M. humicola* infection. (A) A schematic diagram summarising the p38 MAPK pathway. **(B)** The p38MAPK pathway mutants *pmk-1*(*km25*) and *sek-1*(*km4*) display increased susceptibility to *M. humicola* infection compared to the wild-type N2 (both $p < 0.0001$). **(C)** The Mutant animals fed OP50 only, did not display significant differences in survival compared to N2 during the short time of the assay. The survival curves are representative of pooled data from three technical replicates (N=150 per curve). The data shown is representative of at least two independent experiments. The statistical analysis was performed using the log-rank analysis (**** $p<0.0001$).

3.3. Discussion.

3.3.1. *M. humicola* is a new natural pathogen of *C. elegans*.

The work presented in this chapter, represents, to our knowledge, the first report describing an oomycete as a natural pathogen of the nematode *C. elegans*. The nematophagous oomycete was isolated from a wild-caught *C. elegans* strain (JU2519). This discovery was aided by the improved understanding of *C. elegans* ecology over the last years, and in particular, its tendency to colonise microbe rich environments (Barrière and Félix, 2005; Félix and Braendle, 2010). This work presents a new perspective, and increases our understanding of the biotic challenges that *C. elegans* encounters in its natural habitat.

The newly isolated strain of *M. humicola* (JUo1), was initially molecularly identified by comparing multiple amplified rDNA sequences, including COX-2, ITS and 18S. As we have demonstrated, with regards to identifying members of the *Myzocytiopsis* genus, the nuclear 18S rDNA sequence was unable to give good resolution to the species level. This was due to the high genetic similarity between the various *Myzocytiopsis*-derived 18S sequences. Our identification was further validated with a comprehensive morphological characterisation of the pathogen's life cycle. It remains unknown whether natural infections of *C. elegans* by *M. humicola* are widespread around the world, or whether the recovery of this pathogen was a rare event. Undoubtedly, this question will be answered in the future when more *C. elegans* isolates are sampled. Conceivably, these efforts will also identify at the same time, other novel pathogens that naturally associate with *C. elegans*. In any case, the discovery of a diverse group of organisms infecting *C. elegans*, such as the oomycetes, offers researchers attractive opportunities to study host responses to infection, and host-pathogen co-evolved immune mechanisms.

3.3.2. *M. humicola* attaches onto specific regions of the *C. elegans* cuticle.

As demonstrated through characterisation of the oomycete's life cycle, *M. humicola* instigates infection by attaching in the form of cytospores to the host's cuticle, and later, they penetrate the integument and grow as hyphae within the body cavity. Presumably, this process is employed by the pathogen to both absorb nutrients and colonise the host. Next, these structures mature and develop into sporangia, whereby further cytospores are produced and released, ready to infect additional hosts, in an attempt to propagate the survival of the pathogen.

Through the use of SEM, we also revealed that the *M. humicola* cytospores attach to regions around the mouth, tail and along the alae. This latter spatial specificity, namely attachment to the alae, is rather unusual. As previously characterised pathogens of *C. elegans*, including fungal and bacterial pathogens, are shown to either attach over the entire surface of the cuticle, or more specifically in the vulva region, rectum and/or the mouth. For example, the fungal pathogen *D. coniospora* prefers the vulva, or displays whole body attachment (Jansson, 1994), and the bacterial pathogen *Y. pestis* forms biofilms on the nematodes anterior cuticle region and mouth (Darby et al., 2002), also *M. nematophilum* preferentially attaches to the *C. elegans* rectal and posterior cuticle regions (Nicholas and Hodgkin, 2004).

Why does the pathogen exhibit preferential attachment? Conceivably, this could be attributed to the pathogen targeting specific components of the cuticle. At present, the *C. elegans* cuticle biochemical composition, including that of the alae remains an under-studied field, and as a consequence, our understanding of the known components present in the exoskeleton is limited to that of collagen-like proteins, cuticlin (insoluble heavily cross-linked proteins) and glycoproteins (Fujimoto and Kanaya, 1973; Johnstone, 2000; Page and Winter, 2003; Politz et al., 1990; Sebastiano et al., 1991). Considering they are expressed in abundance across the whole cuticle, we can perhaps speculate that *M. humicola* most likely does not

exploit these components, otherwise, we would have observed cytospores binding non-specifically. Most likely, our findings imply the possibility of as yet identified components of the cuticle that appear to either be abundantly expressed, or specifically expressed at sites favoured by the oomycete. Alternatively, the cytospores could favour these sites due to some form of chemotropism, or due to the secretion of a 'chemoattractant', indeed, similar to other organisms, *C. elegans* has been shown to secrete a range of small molecules (Golden and Riddle, 1982; Jeong et al., 2005). Furthermore, due to the fact that spores from other pathogenic oomycetes, such as *Phytophthora cinnamoni* and *Phytophthora sojae* exhibit chemotactic activity, and display preferential attachment to root exudates, a region of root elongation, we reason this could also be a rational possibility (Zentmyer, 1961a, 1961b; Zhang et al., 2019). Considering we frequently observed pathogen attachment slightly off the exact position of the alae, we favour the possibility that the pathogen is chemically attracted to this region. Nonetheless, whether *M. humicola* attaches preferentially to the alae because of mechanical reasons, or due to some form of chemical attraction, remains to be determined.

3.3.3. The establishment of a new pathosystem to study oomycete infections of animals.

The isolation of *M. humicola* as a pathogen of *C. elegans*, has provided us, the opportunity to study a natural oomycete infection in a genetically tractable model host. We exploited this natural pathogen-host interaction, by developing a robust infection assay, which consisted of precisely monitoring the number of animals that showed the distinct late stage of *M. humicola* infection, a phenotype we defined as the presence of sporangia. This evident phenotype is important because, in contrast to most bacterial infection assays, it allows us to unambiguously detect infected animals, and censor animals that die due to technical reasons.

With this infection assay, and the employment of stable genetic mutants, we demonstrated that the p38 MAPK pathway is required for *C. elegans* resistance against *M. humicola*-mediated killing. The p38 MAPK pathway is thought to confer *C. elegans* resistance against a range of phylogenetically diverse pathogens, through the cell autonomous activation of PMK-1. This results in the activation of defense mechanisms, including the pathogen and tissue specific expression of antimicrobial peptides, in order to directly antagonise infections in the tissues targeted by the pathogen, and to also increase the host's capacity to cope (Pujol et al., 2008; Troemel et al., 2006). Perhaps in a similar manner, the *C. elegans* p38 MAPK pathway may also regulate the expression of resistance genes at initial sites of host-oomycete interaction, such as the hypodermis.

In summary, by exploiting *M. humicola* and *C. elegans* natural interaction, we have established a novel and robust pathosystem to study oomycete infections in whole animals. Using this system, we can now investigate the physiological mechanisms required to confer *C. elegans* resistance against *M. humicola* infection.

Chapter 4. Discovery of the *chitinase-like* genes, a new class of pathogen resistance genes

4.1. Introduction.

The nematode *C. elegans* has been successfully used as a system to study eukaryotic molecular responses to environmental stresses (Rohlfing et al., 2010). Pathogenic infections encompass one of the major environmental stresses faced by eukaryotes. In response to these biotic threats, *C. elegans* has been shown to activate inducible defense mechanisms, including the expression of resistance genes to both antagonise infection and increase the hosts survival (Mallo et al., 2002; Wong et al., 2007). Intriguingly, with the use of such techniques as comparative transcriptomics, *C. elegans* an invertebrate that relies exclusively on innate immunity, has been shown to induce pathogen specific transcriptional programs, indicating that *C. elegans* has the ability to distinguish between pathogens (Engelmann et al., 2011; Mallo et al., 2002). A trait previously only attributed to vertebrates harbouring an adaptive immune system (Litman et al., 2010). Moreover, the products of these resistance genes, such as the antimicrobial peptide *nlp-29*, are not only induced in response to specific pathogens, but they are also expressed in a tissue specific manner (Millet and Ewbank, 2004; Pujol et al., 2008), most plausibly, this is done to effectively combat the invading pathogens at primary sites of infection. These investigations have generally utilised non-natural pathogens of *C. elegans*, or when studying responses to natural pathogens, they were largely restricted to using fungal or closely related eukaryotes (Bakowski et al., 2014; Pujol et al., 2008). An extremely detrimental limitation, especially when considering how the genome of the laboratory reference *C. elegans* strain, has evolved in response to its natural habitat, which undoubtedly contained a range of pathogenic microbes (Félix and Braendle, 2010).

Of note, the *C. elegans* genome contains a plethora of genes that are yet to be functionally characterised. One possible explanation could be attributed to the laboratory conditions in which *C. elegans* is cultured. Furthermore, *C. elegans* genome encodes proteins that are homologous to proteins with defense roles in more complex organisms (Schulenburg

et al., 2004), such as the mitogen activated protein kinases, integral components of the *C. elegans* p38 MAPK innate immunity pathway that are also observed to be conserved in the mammalian p38 MAPK pathway (Kim, 2008; Matsuzawa et al., 2005). A reasonable posit would thus be that there are more homologs to be discovered, homologs that may also accomplish the same roles in *C. elegans* as they do for other organisms, but are yet to be validated.

To expand our knowledge of *C. elegans* genome-wide transcriptional response to a natural pathogen, we studied gene changes in the lab reference strain N2 post exposure to the nematophagous oomycete *M. humicola*. The oomycete belongs to a genus of pathogenic organisms that have previously been shown to infect a range of nematodes and rotifers (Glockling and Beakes, 2000). *M. humicola* instigates infection by attaching in the form of cytospores to the cuticle and growing as hyphae within the body cavity. Although previous studies have provided morphological characterisation of some nematophagous oomycetes, including members of the *Myzocytiopsis* genus such as *M. humicola* (Glockling and Beakes, 2008), how the host responds to an oomycete infection at the molecular level had not been examined.

With the use of comparative transcriptomic analysis, we identified the induction of members of the previously uncharacterised *chitinase-like* (*chil*) gene family. The *C. elegans chil* genes are not expressed under normal lab conditions. Unlike true chitinase proteins, chitinase-like proteins are enzymatically inactive, though are still predicted to have retained their carbohydrate binding ability (Kzhyshkowska et al., 2007). Interestingly, the *chitinase-like* genes have previously been reported to be involved in tissue remodelling and immunity in other organisms (Lee et al., 2011; Pesch et al., 2016). In this study, we demonstrate that the *chil* genes are highly specific to *M. humicola*, are induced in the hypodermis, and contribute towards increasing *C. elegans* survival against *M. humicola*-mediated killing. Also,

remarkably, we show that the protein encoded by *chil-27*, a member of this gene family, is expressed in a pattern reminiscent of the *C. elegans* cuticle structures, the initial site of host-oomycete interaction. Furthermore, with the use of gene attenuation and overexpression experiments, we show that the *chil* genes antagonise *M. humicola* infection by hindering the oomycetes ability to attach onto the cuticle. Our work presented here, encompasses the first recorded efforts to study an oomycete infection of nematodes at the molecular level. This study also expands our understanding of *C. elegans* innate immune responses to a natural pathogen, and reveals a new class of previously uncharacterised resistance genes.

4.2. Results.

4.2.1. The analysis of *C. elegans* transcriptional response to *M. humicola*.

Our efforts have thus far examined, the role that previously characterised innate immunity pathways play in conferring *C. elegans* resistance against *M. humicola* infection. Whilst such genetic approaches are important, nevertheless, limit our investigations to genes that have previously been characterised to play a role in immunity. Thus, to discover novel genes involved in conferring *C. elegans* resistance against *M. humicola*, we sought to comprehensively analyse *M. humicola* induced global gene changes in *C. elegans*. To this end, we combined RNA sequencing (RNA-seq) with our established *M. humicola* infection assay (Figure 4.1A). In summary, the assay consists of placing 50 developmentally synchronised N2 hermaphrodites onto OP50 seeded NGM infection plates, these plates contain three equally distributed infected animals full of sporangia (the distinct final stage of infection, and our method for transferring the pathogen in a control manner). The control plates lack the oomycete, but are identical to the infection plates in all other aspects. To capture both acute and long-term responses to *M. humicola*, we measured gene changes at 12 and 24 hour timepoints post exposure to the pathogen.

To identify differentially expressed genes, the transcript expression levels were compared between the *M. humicola* treated animals cultured on OP50, and the nematodes maintained on OP50 only (control treatment). Using stringent statistical criteria with DESEQ2, we identified 96 and 127 genes whose expressions were altered at the 12 and 24 hour timepoints respectively (Figure 4.1B). Overall, we observed a discreet yet statistically significant change in gene expression. At both timepoints, we noted the presence of classes of resistance genes that have previously been associated with a range of microbial infections, including the *c-type lectins* (*clc*) *clc-232*, *clc-95*, *caenacins* (*cnc*) *cnc-2* and *cnc-4*, *neuropeptide-like proteins* (*nlp*) *nlp-31* and *nlp-34*. In addition, we also noticed members of the protein containing ALS2CR12

(*pals*) genes family (*pals-26*, *pals-27*, *pals-28*, *pals-32* and *pals-39*) present in our data set. These *pals* genes have previously been shown to be significantly upregulated in response to both viral and microsporidia infections (Bakowski et al., 2014; Chen et al., 2017; Reddy et al., 2017; Sarkies et al., 2013). By functionally classifying and pooling our data at both timepoints, we noticed that the largest category of differentially expressed genes corresponded to those previously shown to be involved in *C. elegans* development, the second largest contained uncharacterised genes with no known function, followed by genes involved in a range of other roles, and the smallest category encompassed those known to play a role in immunity (Figure 4.1C).

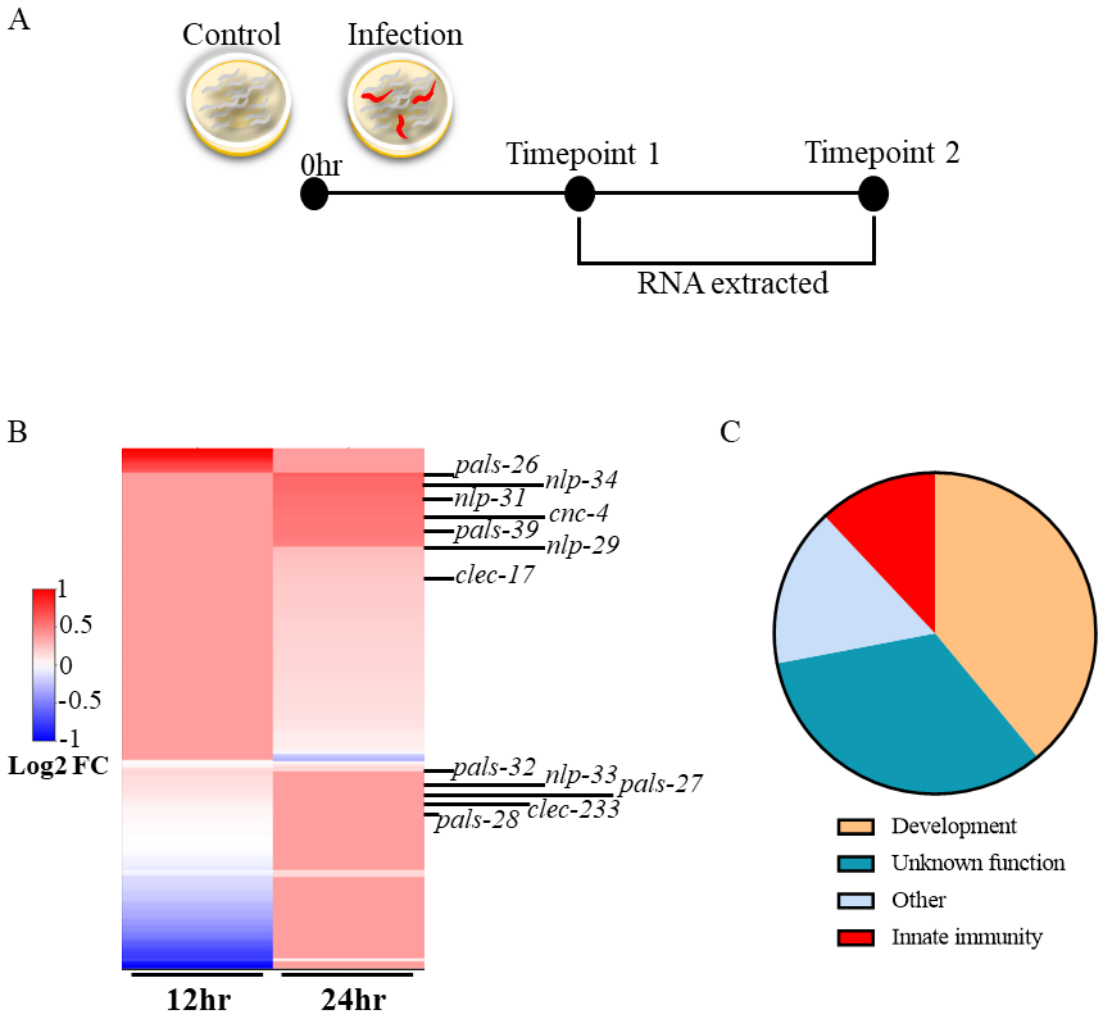

Figure 4.1: Exposure to *M. humicola* induces gene expression changes in *C. elegans*. (A) A cartoon depicting the experimental design for extracting total RNA. The assay consists of placing developmentally synchronised L4 hermaphrodites onto NGM plates either containing OP50 only (food source), or OP50 and 3 equally distributed infected animals. Afterwards, at the desired timepoints, the total RNA is extracted from the animals for transcriptomic analysis. **(B)** A heat map showing differentially expressed gene changes associated with *M. humicola* exposure at 12 and 24hr timepoints, a cut-off value of FDR-1% was used. The genes previously characterised to be involved in immunity are presented. **(C)** A pie chart depicting the categorisation of genes based on their known function, the figure is representative of pooled data comprised of both the 12 and 24hr timepoints.

To analyse whether our RNAseq data overlapped with previously published data sets, we compiled a list, which included only the upregulated responses to a diverse range of pathogens, and performed comparative transcriptomics analysis between *C. elegans* transcriptional responses to *M. humicola* and the compiled gene sets (Figure 4.2A). Intriguingly, we found in general, only modest, non-significant overlap. In most cases, we detected moderate rates of intersection between our data and gene sets generated with the use of other pathogens. This non-significant overlap was observed even when explicitly comparing our data to the response against the fungus *D. coniospora* (Figure 4.2B), a natural pathogen that also attaches to and infects *C. elegans* through the cuticle, a method superficially similar to *M. humicola*. The genes present in the overlap between our data and the *D. coniospora* generated gene set, included the aforementioned *nlp* genes, genes that have also been shown to be induced by cuticle damage (Pujol et al., 2008; Zugasti and Ewbank, 2009). Our comparative analysis compliments previous findings, i.e. pathogens with divergent modes of infection can initiate a shared "pan-microbial" host response, although, this can be modest (Wong et al., 2007).

A

Treatment	Pathogen class	% overlap	Source	Technique
N. parisii	Microsporidia*		(Bakowski et al., 2014)	RNA-seq
D. coniospora	Fungal*		(Engelmann et al., 2011)	Oligo-arrays
Harposporium sp	Fungal*		(Engelmann et al., 2011)	RNA-seq
Orsay-like virus	Viral*		(Sarkies et al., 2013)	RNA-seq
P. aeruginosa strain PA14	Bacterial		(Troemel et al., 2006)	RNA-seq
E. faecalis	Bacterial		(Engelmann et al., 2011)	RNA-seq
S. marcescens	Bacterial		(Engelmann et al., 2011)	RNA-seq
P. luminescens	Bacterial		(Engelmann et al., 2011)	RNA-seq
S. aureus	Bacterial		(Irazoqui et al., 2010)	Microarray, affymetrix
B. thuringiensis strain BT247	Bacterial		WormExp, (Yang et al., 2016)	Oligo-arrays

0% 100%

B

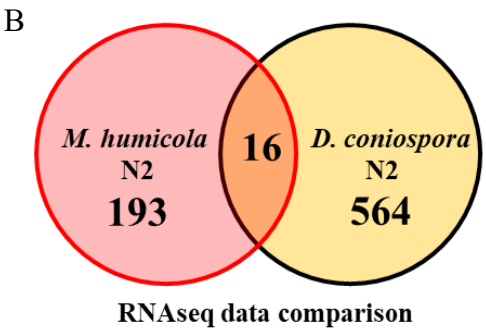

Figure 4.2: *M. humicola* induced gene changes do not display significant overlap with other pathogen generated data sets. (A) A table displaying the correlation between genes upregulated by *M. humicola* and genes upregulated by other pathogens. The natural pathogens are highlighted with a red asterisk. The gene sets were compared by percentage overlap. Red indicates significant overlap and high correlation with genes upregulated in response to *M. humicola* infection, while blue represents non-significant overlap, the colour key is presented below the table. The sources used to acquire the transcriptomics data sets are also included in the table. **(B)** Venn diagrams of genes differentially expressed post exposure to *M. humicola* and *D. coniospora*. The *D. coniospora* data was obtained from (Engelmann et al., 2011).

4.2.2. The identification of the *chitinase-like* genes.

Our analysis of *C. elegans* transcriptional response to *M. humicola* exposure, demonstrated that the oomycete initiates, a unique transcriptional profile in the host when compared to those generated with other extracellular, or intracellular pathogens. As a consequence, we next sought to examine the genes that were highly specific to our data, in order to find novel resistance genes. Considering *C. elegans* has been shown to rapidly respond to the presence of pathogens by inducing the transcription of hundreds of genes, including resistance genes that directly increase host survival against infection (Feinbaum et al., 2012; Pujol et al., 2008), we directed our attention to genes that were upregulated. Furthermore, we also limited our search to genes that were not previously reported to be involved in *C. elegans* immunity, uncharacterised and those encoding proteins that are homologous to proteins with defense roles in other organisms. Using the above stated criteria, we noticed amongst the most significantly upregulated genes at both timepoints, were members of a previously uncharacterised gene family, namely the *chitinase-like* (*chil*) genes *chil-18*, *chil-27* and *chil-28* (Figure 4.3A). We validated the induction of the *C. elegans chil* genes upon exposure to *M. humicola* with the use of microarray analysis (Figure 4.3B). For the microarray experiment, we used the same conditions and methods to obtain total RNA as those employed for our RNAseq, but, in this instance, we sought to capture a more chronic response, as such, we measured gene changes at 26 and 46 hours post exposure to the oomycete. For the microarray generated data set, we observed a greater number of *chil* genes expressed compared to our RNA-seq generated set. Conceivably, this may reflect an experimental difference in the strength of the infection, or the duration of time in which the nematodes were exposed to the oomycete. Although the *chitinase-like* genes have not been studied in the context of an oomycete infection, they have been linked to mammalian immunity against pathogenic nematodes (Sutherland et al., 2014).

During the course of our comparative transcriptomics analysis, we noticed that the *chil* genes expression was frequently absent in gene sets derived with the use of other pathogens (Table 4.1). Although, we did observe a comparable number of *chil* genes induced by *Enterococcus faecalis* (*E. faecalis*). In fact, with the use of WormExp (Yang et al., 2016), a web based tool to perform *C. elegans* specific gene expression enrichment analysis, the *chil* genes as a group appeared infrequently (1 out of 212 microbe generated gene sets), and they only appeared on average in 1.6 out of 42 gene sets as individually induced genes (Bakowski et al., 2014; Engelmann et al., 2011; Irazoqui et al., 2010a; Yang et al., 2016). Additionally, *chil-27*, the second most significantly upregulated *chil* gene in our RNA-seq data, and the most significantly upregulated in our microarray data, was absent from all other pathogen gene sets that were analysed, except for that of the *E. faecalis* generated data set, for which *chil-27* gene induction was reported to be present at 24 hours post exposure to the pathogen (Engelmann et al., 2011). Due to our analysis and previous efforts to use *chitinase-like* genes as biomarkers of various pathologies (Kzhyshkowska et al., 2007), we designated the *C. elegans chil* genes as a putative signature of *M. humicola* infection.

The *chil* genes encode proteins that contain a glycoside hydrolase 18 family (glyco-18) domain, as revealed by InterPro (https://www.ebi.ac.uk/interpro/) (Finn et al., 2017). In contrast to catalytically active chitinase proteins, enzymes that hydrolyse glycosidic bonds, CHIL proteins are likely to be catalytically inactive, due to the absence of a glutamate amino acid residue in the glyco-18 domain motif DxxDxDxE, the catalytic proton donor, which is required for the catalytic activity of true chitinase enzymes (Bussink et al., 2007; Chang et al., 2001; Houston et al., 2003; Renkema et al., 1998; Zaheer-ul-Haq et al., 2007). The CHIL proteins have also been shown to be conserved across plants, mammals and invertebrates (Bussink et al., 2007; Funkhouser and Aronson, 2007). In contrast to the *chil* genes, the expression of true chitinases were unaltered in response to the oomycete (Figure 4.3C). The *C.*

elegans genome contains a total of 28 annotated genes that are classified and or predicted to encode CHIL proteins (http://www.wormbase.org/). Curiously, while there are few in humans and mice (Kzhyshkowska et al., 2007), in comparison, the number of *chitinase-like* family members in *C. elegans* is expanded. Furthermore, they are largely genomically clustered (Figure 4.4), with 86% (24/28) of *chil* genes located on chromosome II, although in two distinct clusters, the remaining *chil* genes are present on chromosome V (*chil-12* and *chil-14*), chromosome IV (*chil-11*) and chromosome X (*chil-10*). Whilst *chil-28* is currently annotated as a pseudogene (http://www.wormbase.org/), in our lab, we have recovered with the use of a 3' RACE reaction post-infection, a putative functional transcript with an earlier stop codon than that of the current annotation on WormBase (Osman et al., 2018).

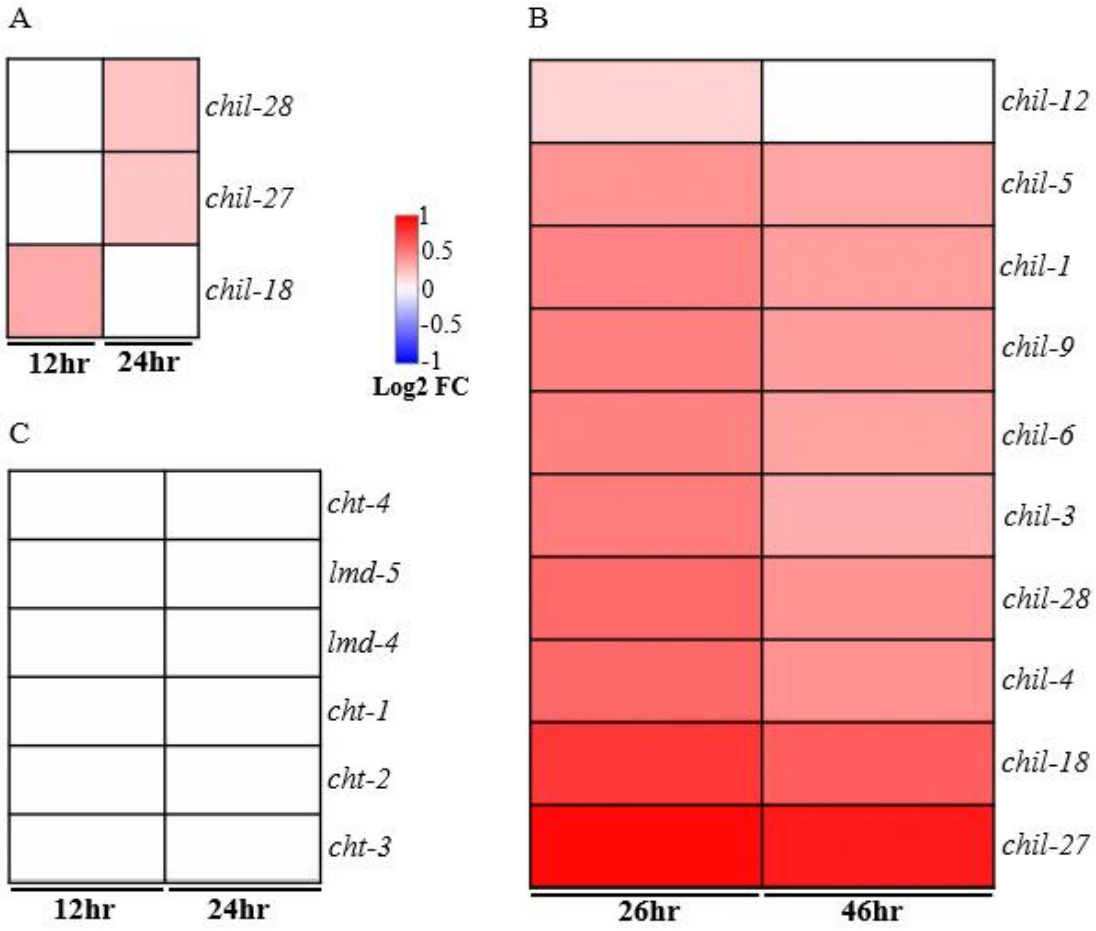

Figure 4.3: *M. humicola* induces the expression of *chil* genes in *C. elegans*. (A) A heat map showing the expression of *chil* genes at 12 and 24 hours post exposure to *M. humicola*. At the 12hr timepoint only *chil-18* expression is observed to be differentially expressed. At the 24hr timepoint, only genes *chil-27* and *chil-28* are induced, in contrast to the 12hr timepoint *chil-18* expression is absent. In both instances, differential changes are modest but statistically significant. The heatmap was generated using the RNA-seq data. **(B)** A heat map showing the expression of *chil* genes at 26 and 46 hours post exposure to *M. humicola*. At both timepoints, we observe the significant expression of genes *chil-27*, *chil-18*, *chil-4*, *chil-28*, *chil-3*, *chil-6*, *chil-9*, *chil-1* and *chil-5*, whilst *chil-12* is only present at the 26hr timepoint. The heatmap was generated using the microarray data**. (C)** A heat map showing the expression of true chitinase protein encoding genes at 12 and 24 hours post exposure to *M. humicola*. We observe no change

in the expression of *C. elegans* genes encoding catalytically active chitinase proteins, the figure was generated using the RNA-seq data.

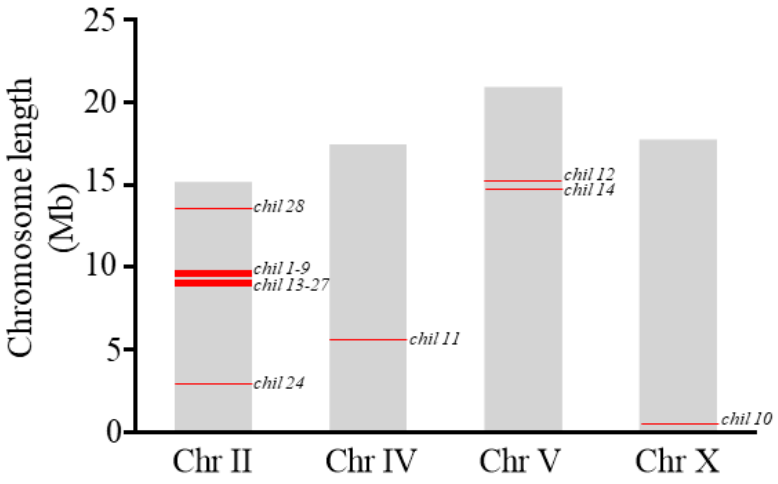

Figure 4.4: A diagram displaying the chromosomal locations of the *C. elegans chil* genes. The *C. elegans* genome is annotated to encode a total of 28 *chil* genes. The majority of *chil* genes are present in two large clusters on chromosome II (ChrII); genes *chil-1* to *chil-9* and *chil-13* to *chil-27* are clustered. ChrII also contains genes *chil-28* and *chil-24*. The remaining genes *chil-11*, *chil-12*, *chil-14* and *chil-10* are located on ChrIV, V and X respectively. The data is derived from (http://www.wormbase.org/).

Table 4.1. The *chil* genes that are induced by other pathogens.

Pathogen	Class of pathogen	Are *chil* genes present in the data set? (Yes/No)	The *chil* genes present in the data set
M. humicola [1]	Oomycete	Y	*chil-1*, *chil-3*, *chil-4*, *chil-5*, *chil-6*, *chil-9*, *chil-12*, *chil-18*, *chil-27* and *chil-28*
S. aureus [2]	Bacterial	N	Not applicable
Harposporium sp [3]	Fungal	Y	*chil-12*
D. coniospora [3]	Fungal	Y	*chil-3*, *chil-5*
E. faecalis [3]	Bacterial	Y	*chil-1*, *chil-3*, *chil-4*, *chil-5*, *chil-6*, *chil-12*, *chil-18*, *chil-27* and *chil-28*
P. luminescens [3]	Bacterial	Y	*chil-6*, *chil-12* and *chil-18*
S. marcescens [3]	Bacterial	N	Not applicable
B. thuringiensis [4]	Bacterial	Y	*chil-18*
Orsay-like virus [5]	Virus	N	Not applicable
N. parisii [6]	Microsporidia	N	Not applicable

Of note, *E. faecalis* and *M. humicola* induce a comparable number of *chil* genes. [1] Osman et al., 2018; [2] Irazoqui et al., 2010; [3] Engelmann et al., 2011; [4] Yang et al., 2016; [5] Sarkies et al., 2013; [6] Bakowski et al., 2014.

4.2.3. The *chil* genes antagonise *M. humicola* infection.

As discussed above, we have demonstrated that the novel *chil* genes are induced in response to *M. humicola* exposure. The *C. elegans chil* genes are comprised of an uncharacterized family of genes that are not expressed under standard lab conditions, nor have they previously been reported to be involved in *C. elegans* immune responses to infection (Engelmann et al., 2011; Mallo et al., 2002; Pujol et al., 2008; Troemel et al., 2006). Therefore, we next sought to address whether the *chil* genes could contribute towards *C. elegans* resistance against an oomycete infection. To this end, we assessed the consequences of either overexpressing or abrogating the expression of *chil* genes. Initially, we examined the consequence of *chil* gene overexpression on *C. elegans* ability to survive *M. humicola* infection.

Our analysis of the N2 genome revealed that the *chil* gene are present in clusters (Figure 4.4), this feature allowed us to overexpress multiple *chil* genes simultaneously with the use of fosmid clones WRM065aH01 and WRM0619bB10 (Source Bioscience). Fosmids are cloning vectors that contain large fragments of the *C. elegans* genome, on average ~ 40 kb, which permits the functional overexpression and analysis of target genes in their 'native' environment (Craig et al., 2013). With the respective fosmid clones, we generated transgenic N2 animals carrying super-numerous copies of genes *chil-1*, *chil-2*, *chil-3*, *chil-4*, *chil-5*, *chil-6*, *chil-7*, *chil-8* and *chil-9* (WRM065aH01), or *chil-18*, *chil-19*, *chil-20*, *chil-21*, *chil-22*, *chil-23*, *chil-25*, *chil-26* and *chil-27* (WRM0619bB10). In both cases (Figure 4.5), we found that the simultaneous overexpression of 9 *chil* genes significantly increased the hosts capacity to resist oomycete mediated-killing; *chil-1* to *chil-9* overexpression $p=0.0442$, or *chil-18* to *chil-27* overexpression $p<0.0001$. Interestingly, transgenic animals overexpressing genes *chil-18* to *chil-27* displayed greater resistance to *M. humicola* infection compared to the *chil-1* to *chil-9* overexpressing animals ($p=0.0013$). Additionally, as a control, we showed that the fosmid

constructs themselves did not confer resistance by overexpressing a random region of the chromosome with fosmid WRM0627dG07, the construct contained a ~34kb fragment of chromosome IV, which encompassed only one complete gene (*lin-22*) and a partial fragment of a second gene (*ndnf-1*).

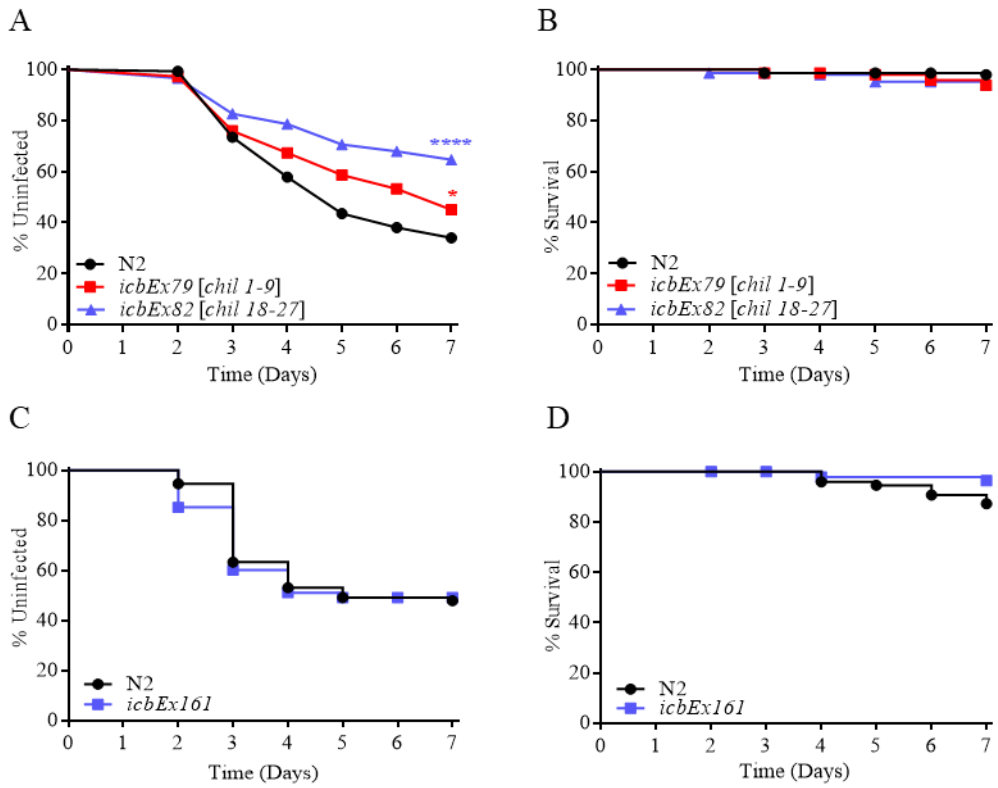

Figure 4.5: The overexpression of *chil* genes increases *C. elegans* resistance to *M. humicola* infection. (A) The transgenic nematodes carrying supernumerary copies of the *chil* genes, display significantly increased survival against *M. humicola* infection compared to the wild-type animals; *chil-1* to *chil-9,* p=0.0442, *chil-18* to *chil-27*, p< 0.0001. The animals overexpressing genes *chil-18* to *chil-27* survived at a slightly increased rate compared to the *chil-1* to *chil-9* overexpressing animals, p=0.0013. **(B)** Control plate, the transgenic animals fed OP50 only did not display differences in survival compared to the wild-type N2. **(C)** The transgenic animals carrying control fosmid WRM0627dG07 did not display increased resistance to *M. humicola* infection. **(D)** Control plate, the transgenic animals carrying the control fosmid WRM0627dG07 fed OP50 survived at a comparable rate to N2. The results are representative of two independently isolated transgenic overexpressing lines and two experimental repeats. The survival curves represent pooled data from three technical replicates (N=150 per curve). The statistical analysis was performed using the log-rank analysis (* p<0.05, **** p<0.0001).

As demonstrated in Figure 4.5, the simultaneous overexpression of 9 *chil* genes at a time, significantly decreased *C. elegans* susceptibility to *M. humicola*-mediated killing. To corroborate that the *chil* genes functionally contribute towards host immunity against the oomycete infection, we next attenuated *chil* gene function and assessed the host's capacity to overcome *M. humicola* infection. Towards this goal, we generated CRISPR genome edited N2 animals as an alternative to performing RNAi knock-down of *chil* genes, as this technique is known to have at times unintended off-target effects (Boutros and Ahringer, 2008). To produce the stable loss-of-function mutants, we utilised the antibiotic selection method developed by Chen and colleagues (Chen et al., 2013), a method that involves exploiting homologous recombination to insert a hygromycin resistance cassette within the coding region of a gene of interest, in order to disrupt the production of a functional gene (Figure 4.6). Using this method, we targeted genes *chil-4*, *chil-9*, *chil-18* or *chil-27*, and generated 2 independent CRISPR knock-in mutants for each gene of interest. In support of the overexpression infection assays, we found that in all cases, the CRISPR mutants displayed marginal, but a statistically significant increase in their susceptibility to *M. humicola* infection in comparison to the wild-type N2; *chil-4*; p=0.0314, *chil-9*; p= 0.0369, *chil-18*; p=0.0051 and *chil-27*; p=0.0060 (Figure 4.7). As a control, we also assessed the sensitivity of animals overexpressing the hygromycin resistance cassette. In support of the CRISPR infection assays, these transgenic animals did not display enhanced susceptibility to *M. humicola* infection. Taken together, these findings thus corroborate our overexpression experiments, and indicates that the *chil* genes functionally contribute towards *C. elegans* immunity against *M. humicola*-mediated killing.

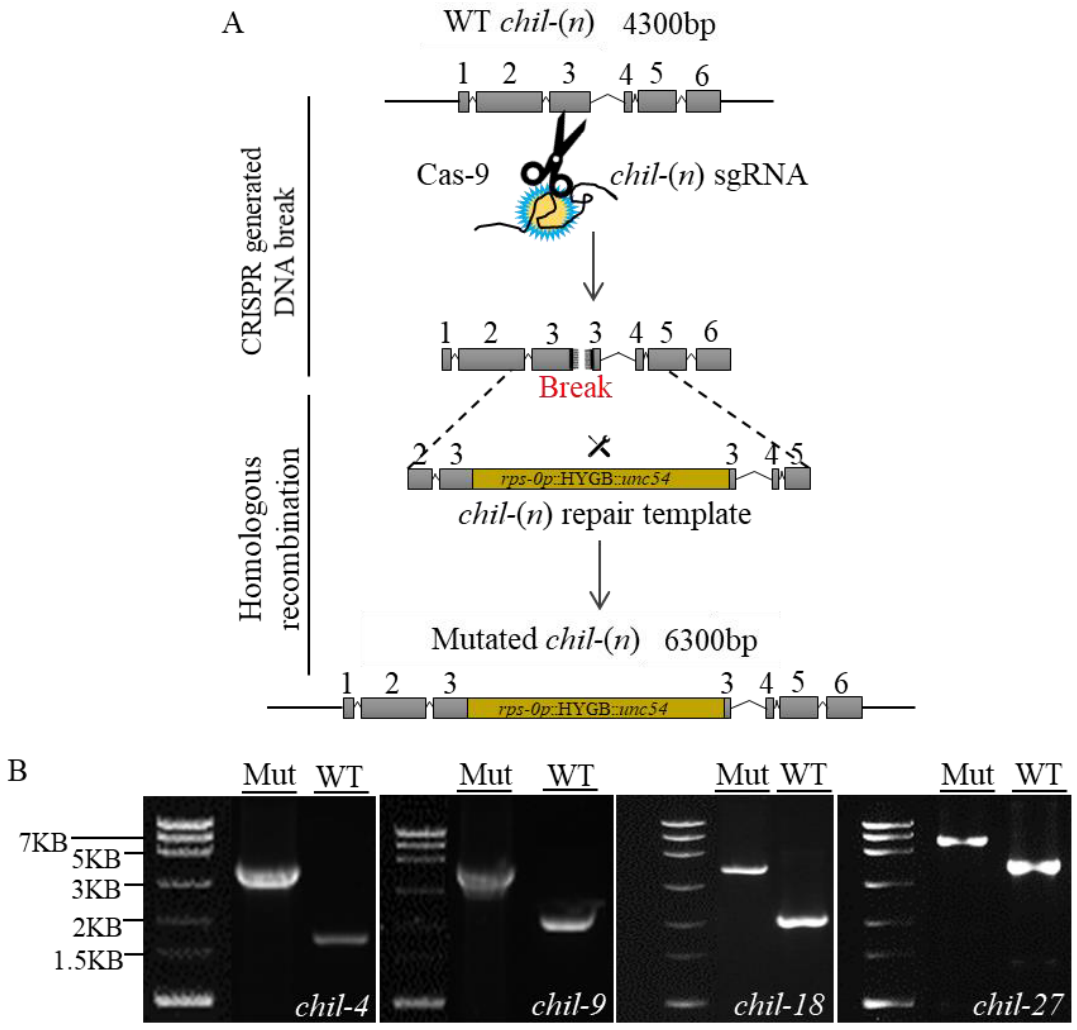

Figure 4.6: The generation of *chil* loss-of-function CRISPR mutants. (A) A schematic depiction of the procedure used to generate the CRISPR knock-in mutants. A double stranded break is induced within the coding region of a target *chil* gene using CRISPR-Cas-9 and the relevant guide sgRNA. Subsequently, due to the presence of a repair template containing the hygromycin gene (HYGB cassette, flanked by ~2kb genomic regions upstream and downstream of the target *chil*-(*n*) gene pam motif) and because of homologous recombination, the hygromycin cassette is knocked-in, rendering the gene non-functional. **(B)** Agarose gels depicting the successful generation of genome edited CRISP knock-in mutants for genes *chil-4*, *chil-9*, *chil-18* or *chil-27*. Successful conversion was confirmed by using primers that hybridised to sequences located outside of the repair template. The amplicons of the CRISPR modified *chil* genes (Mut) are larger than the wild-type (WT) genes.

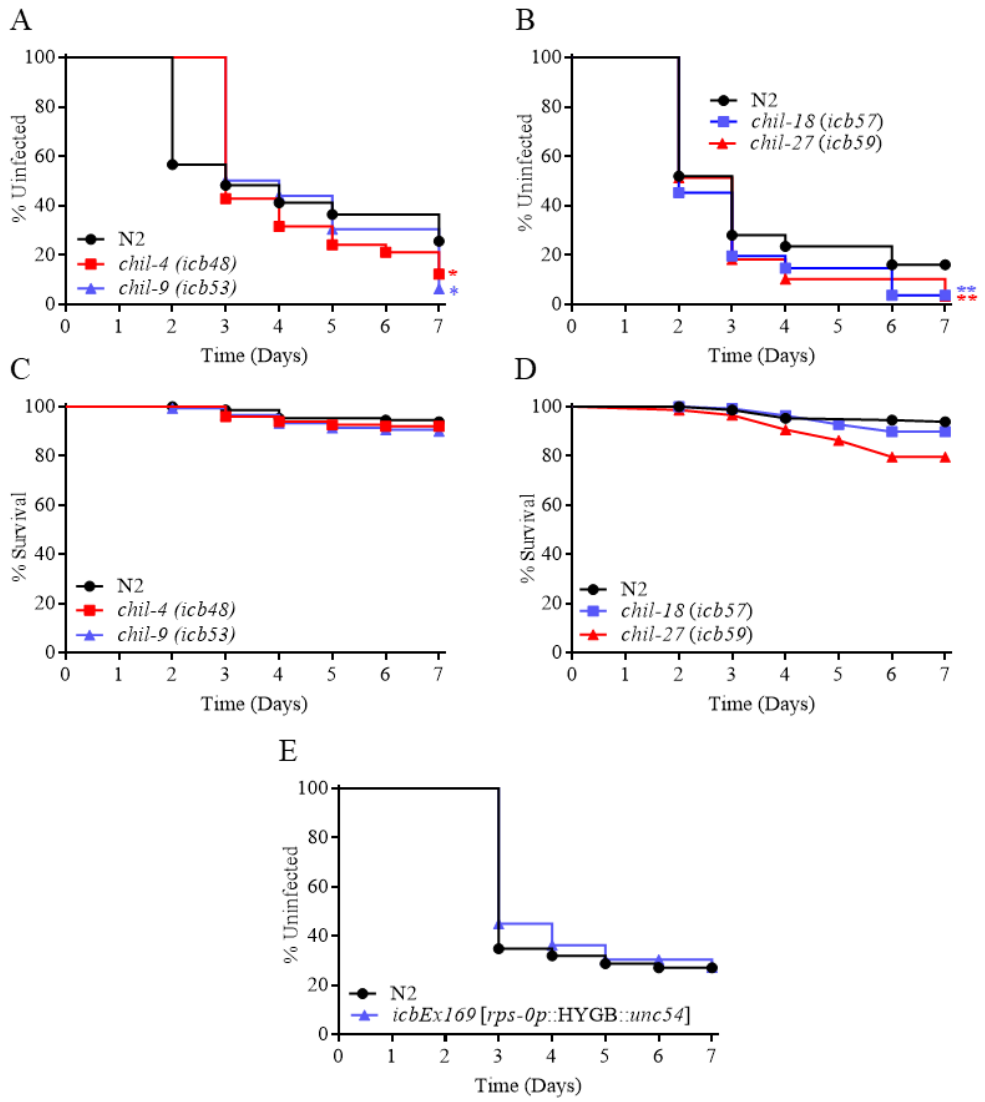

Figure 4.7: The *chil* loss-of-function CRISPR mutants display increased susceptibility to *M. humicola* infection. **(A-B)** Infection plates. In all cases, the insertion of the hygromycin resistance cassette to interrupt genes *chil-4*, *chil-9*, *chil-18* or *chil-27* increased host susceptibility to *M. humicola* infection. Log rank scores; *chil-4*, p=0.0314; *chil-9*, p=0.0369; *chil-18*, p=0.0051 and *chil-27*, p=0.0060. **(C-D)** Control plates. The CRSIPR mutants maintained on OP50 only survived at a comparable rate to N2. **(E)** The transgenic animals overexpressing hygromycin are not more susceptible to *M. humicola* infection compared to N2. The data shown is representative of two experimental repeats. The survival curves represent pooled data from three technical replicates (N=150 per curve). The statistical analysis was performed using the log-rank analysis (* $p<0.05$, ** $p<0.01$).

4.2.4. *chil-27* localises to the hypodermis.

Whilst RNA-seq is a powerful technique to profile the expression of genes at the whole-genome level, it does not provide the spatial expression of a gene, information that is often needed to characterise and determine the function of a novel gene. Therefore, to further characterize these novel resistance genes, we next sought to address in which tissue the most significantly upregulated *chil* genes are expressed upon induction. To this end, we created nuclear localized transcriptional reporters for genes *chil-27* and *chil-28*. The constructs consisted of the wild-type 5' untranslated region of the *chil-27* or *chil-28* gene fused to a commonly used minimal promoter *pes-10*, and a GFP::LacZ fusion (Figure 4.8 depicts the generation of a *chil* gene transcriptional reporter, in this instance, the construction of the *chil-27* reporter is presented as an example). The minimal *pes-10* promoter lacks basal transcriptional activity, and only enhances GFP expression in the presence of other cis-regulatory elements (Fire et al., 1990). To examine the expression pattern of these promoter GFP fusions, we transformed them together with a constitutively expressed nuclear localized *col-12* transcriptional reporter (*col-12p*::mCherry) (Perales et al., 2014) into wild-type N2 animals. This allowed us to positively identify transformed transgenic animals. The gene *col-12* encodes a *C. elegans* collagen gene that is expressed exclusively in the hypodermis (Johnstone and Barry, 1996).

To study whether the transcriptional reporters could be induced by *M. humicola* exposure, we introduced the pathogen to a population of transgenic animals harbouring either the *chil-27* or *chil-28* reporter, and examined for the activation of the GFP transgene. Consistent with our RNAseq data, we only observed the expression of the *chil-27* and *chil-28* reporters when the transgenic animals were exposed to *M. humicola* (Figure 4.9). Upon careful examination of the transgenic animals carrying either the *chil-27* or *chil-28* transgene, we noticed that the GFP reporters were expressed in an anterior to posterior gradient, and

completely co-localised with the constitutively expressed *col-12* transcriptional reporter (Figure 4.10, the *chil-27p*::GFP/*col-12p::*mCherry co-localisation is presented as an example), indicating that the genes *chil-27* and *chil-28* are exclusively expressed in the hypodermis.

Our work has so far demonstrated that the *chil* genes are part of the transcriptional program initiated by *C. elegans* to antagonize oomycete infection. Furthermore, we have demonstrated that the *chil-28* and *chil-27* genes site of transcription is the hypodermis. Considering the *chil* genes function have not been studied in *C. elegans*, we next sought to further characterise these novel genes by investigating the expression of a CHIL protein, as this might indicate how they function. Towards this goal, we decided to study and further characterise a single gene (*chil-27*), in order to understand how the products of other *chil* genes may confer resistance against *M. humicola* infection. For the remainder of the thesis, we have presented the *chil-27* gene as a candidate to understand *chil* gene transcriptional regulation and protein function. This was based on the facts; 1) *chil-27* was observed to be repeatedly and robustly expressed in comparison to the other *chil* genes during our transcriptomics analysis (Figure 4.3), and 2) at the time of our decision, *chil-28* was classified as a pseudogene, also, as we had not yet performed the 3' RACE reaction, the existence of a putative functional transcript was not yet known to us.

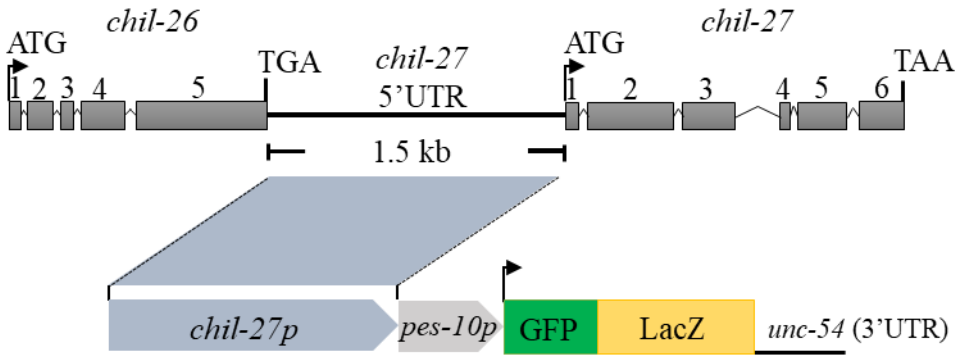

Figure 4.8: The generation of a GFP transcriptional reporter to monitor *chil-27* gene expression. A simplified plasmid map depicting the design of the nuclear localised *chil-27* transcriptional reporter. The promoter of *chil-27*, defined as the 1.5kb region distal to the ATG start site of *chil-27* was inserted upstream of *pes-10* (a minimal promoter) fused to GFP, LacZ and the generic *unc-54* 3'UTR. LacZ was used to ensure the nuclear localisation of the GFP reporter.

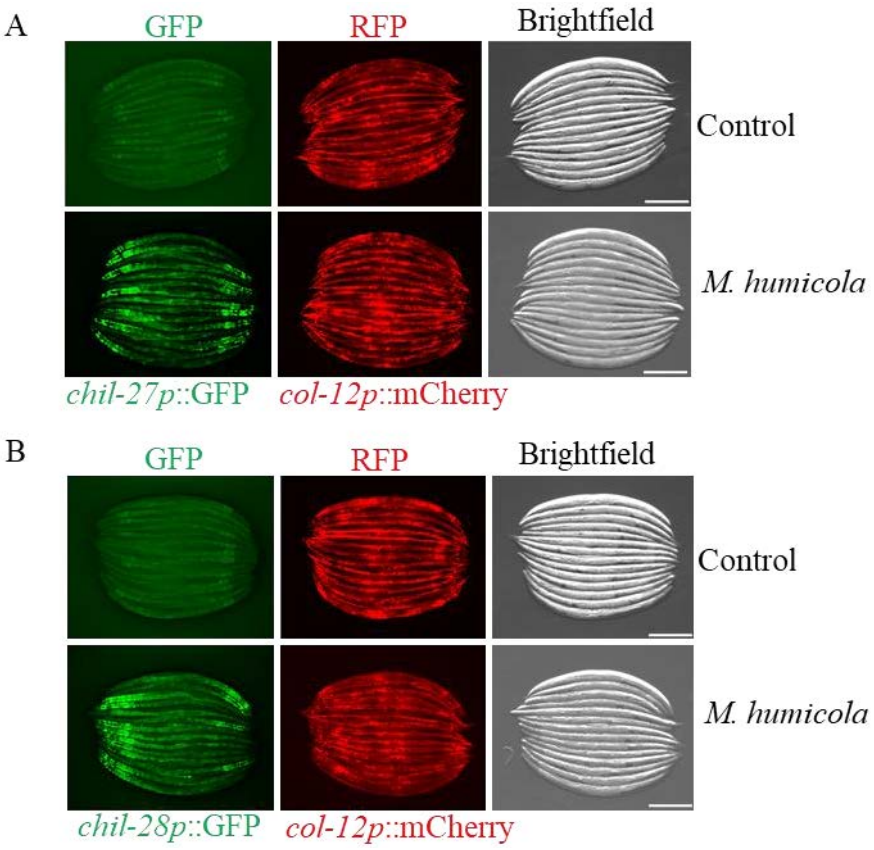

Figure 4.9: The *chil-27* and *chil-28* transcriptional reporters are robustly induced by *M. humicola*. (A-B) Micrographs of transgenic animals harbouring either the *chil-27* or *chil-28* transcriptional reporter. The nematodes also possess the constitutively expressed *col-12* transcriptional reporter. The animals were imaged after being maintained with (treated) or without the pathogen (control). The nematodes harbouring either the *chil-27* (A) or the *chil-28* (B) transcriptional reporter display intense, and robust activation of the GFP transgene upon exposure to the oomycete. In all instances, the transcriptional reporters were not active under normal (control) conditions, but we can observe mild GFP signal that denotes gut granule autofluorescence. Also, notice the absence of any signal reminiscent of the GFP reporter in the RFP channel. Developmentally synchronized L4 hermaphrodites were used at the start of the experiments. Scale bars represent 200µm.

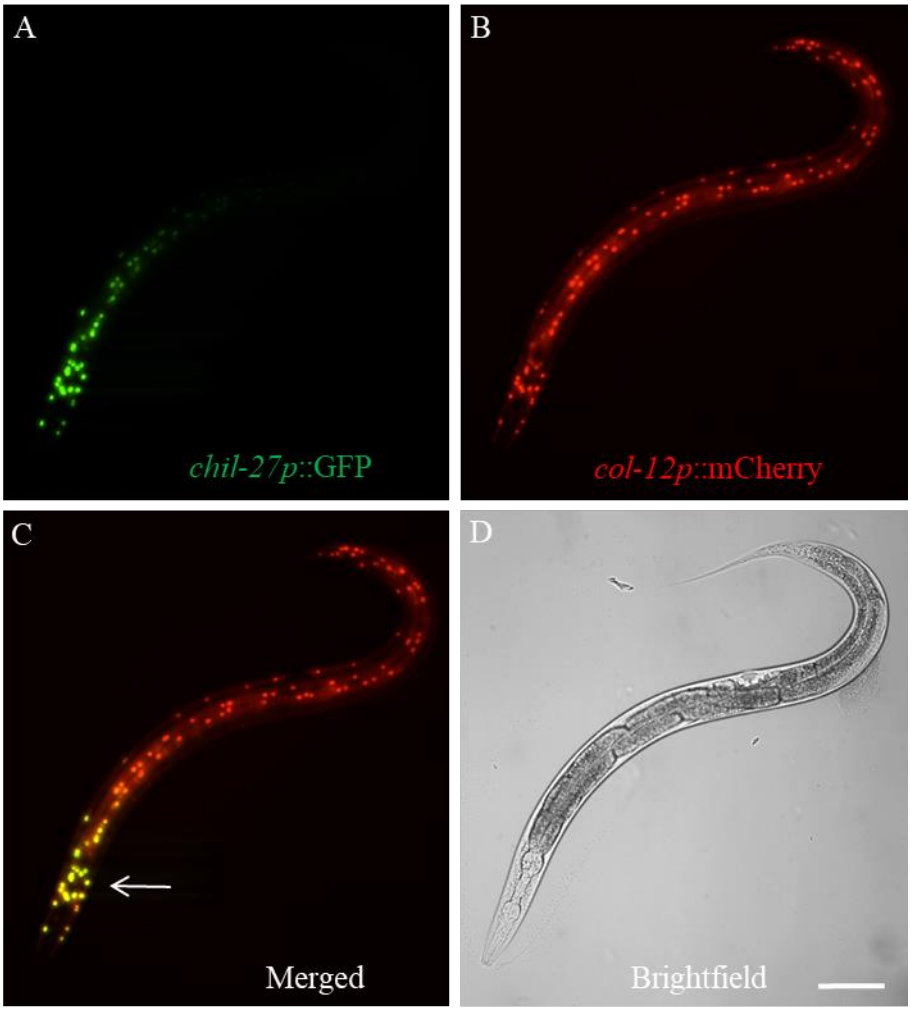

Figure 4.10: *chil-27* is expressed in an anterior to posterior gradient and localizes to the hypodermis. (A-C) Fluorescent micrographs of a transgenic L4 hermaphrodite harbouring the *chil-27* (*chil-27p*::GFP) and *col-12* (*col-12p*::mCherry) transcriptional reporters. The animal was imaged after being maintained with *M. humicola* for 48hrs. Upon induction, the *chil-27* reporter is observed to be expressed in an anterior to posterior gradient (A). In contrast, the constitutively expressed *col-12* reporter is expressed consistently throughout the entire hypodermis (B). Once the two fluorescent channels were merged (C), *chil-27* was revealed to completely localise with the *col-12* transcriptional reporter, which is expressed exclusively in the hypodermis. **(D)** The brightfield image of the transgenic animal. Scale bar represents 100µm.

4.2.5. CHIL-27 protein expression.

To further characterise *chil-27*, we next sought to analyse the localisation of CHIL-27 protein. Initially, in order to determine the optimal design of our transgene, we performed molecular analysis of the CHIL-27 protein sequence by examining the WormBase annotations, and by employing such bioinformatic tools as WoLFPSORT (https://wolfpsort.hgc.jp) and Interpro (https://www.ebi.ac.uk/interpro/ - Finn et al., 2017). Structurally, CHIL-27 is predicted to possess distinct domains; a C-terminal glyco-18 domain and a single transmembrane domain. Furthermore, CHIL-27 does not contain a signal peptide, which suggests that CHIL-27 is not likely to be secreted, at least not through canonical secretion pathways (Phobius - http://phobius.sbc.su.se/). Based on these findings, as well as the need to minimise affecting protein structure and function, we decided to avoid tagging the C-terminally located glycol-18 domain, and opted instead to generate an N-terminally GFP tagged translational reporter. The transgene encompassed the complete open reading frame including the introns of *chil-27* (ATG-TAG), and was under the control of the native *chil-27* promoter (all of the 5' intergenic sequences). The construct was injected into N2. Upon examining the induced reporter, we observed the CHIL-27 protein to be expressed in distinct localisations, represented as bright GFP puncta (Figure 4.11A). Furthermore, we observed no nuclear localised GFP expression. Comparable to our transcriptional reporter, the CHIL-27 translational reporter was only induced in the presence of the oomycete, and also distributed in a similar anterior to posterior graded manner. Interestingly, magnification revealed that the pattern of CHIL-27 expression was reminiscent to the circumferentially located grooves and ridges of the cuticle (Figures 4.11B-E), structures termed the annuli and furrows (Chisholm and Hsiao, 2012), remarkably, a primary site of interaction between *M. humicola* and *C. elegans*.

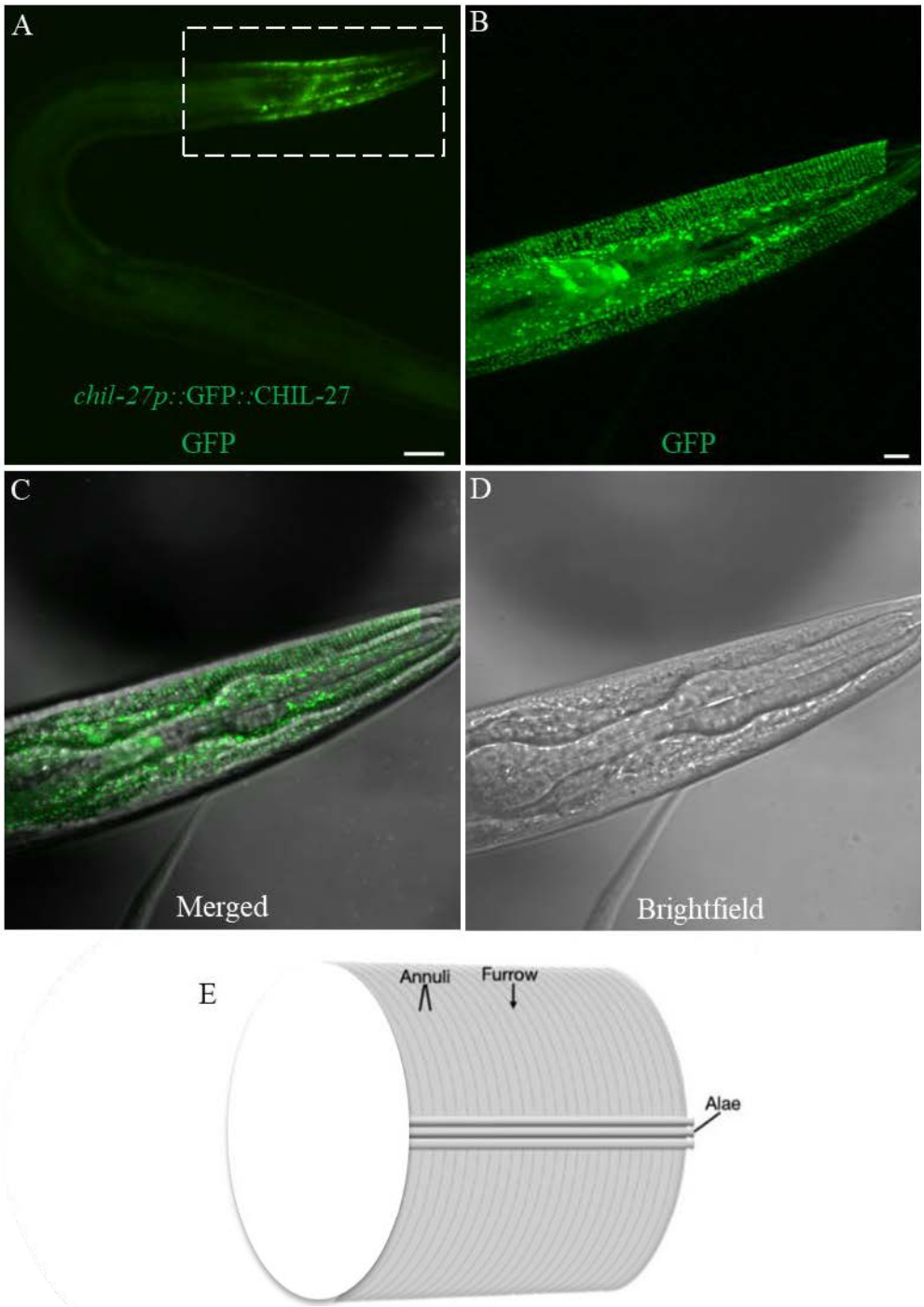

Figure 4.11: CHIL-27 protein expression. (A-D) Micrographs of a day-1 adult hermaphrodite that displays the induced CHIL-27 translation reporter. The animal was imaged after being maintained with *M. humicola* for 48hrs. Upon induction, the translational reporter is observed to be expressed in an anterior to posterior gradient (bright GFP puncta highlighted with the white rectangle), and in a manner reminiscent to the cuticle's annuli and furrows. Panel

(A) depicts the GFP channel displaying a transgenic animal with the activated CHIL-27 reporter. Panel (B) depicts the amplified section contained within the white rectangle of panel A. Panel (C) depicts a merger of the GFP and brightfield channels. Panel (D) depicts the brightfield channel. The images represent projections comprised of 9x0.5µm thick sections. Scale bars represent 50µm. **(E)** A cartoon depicting a simplified cross section of an adult *C. elegans* cuticle. The outermost layer of *C. elegans* is composed of a tough but flexible cuticle. The cuticle is morphologically comprised of circumferentially oriented structures termed the annuli and furrows, as well as longitudinal ridges called the alae. The image is adapted from WormAtlas.

4.2.6. The *chil* genes antagonise *M. humicola* infection by decreasing pathogen attachment.

Having demonstrated that the *chil* genes antagonise *M. humicola* infection, we next sought to investigate how the *chil* genes might accomplish this task. Considering, at least in the case of *chil-27*, transcription is localised to the hypodermis and protein expression is distributed in a pattern reminiscent to structures of the cuticle, both initial sites of host-pathogen interaction, we reasoned that the *chil* genes might directly antagonise the oomycete. Furthermore, we also postulated that the *chil* genes could either be employed to hinder the oomycetes ability to attach onto the cuticle, or are deployed to antagonise infection after attachment. To address these possibilities, we first developed a robust method to easily visualise the pathogen. To this end, we designed florescent *in situ* hybridisation (FISH) probes targeting abundant transcripts of the *M. humicola* 18S rRNA and L30 ribosomal protein genes (herein defined as M-FISH), a multivalent approach to detect the pathogen. As depicted in Figure 4.12, we were able to detect the oomycete, both at early stages as attached cytospores while entering *C. elegans* (Figure 4.12A), as well as at more progressed infection stages when growing as hyphae (Figure 4.12B) and sporangia (Figure 4.12C) within the host. Furthermore, these probes showed strong and specific staining of the pathogen only, and did not label non-infected animals (Figure 4.12D).

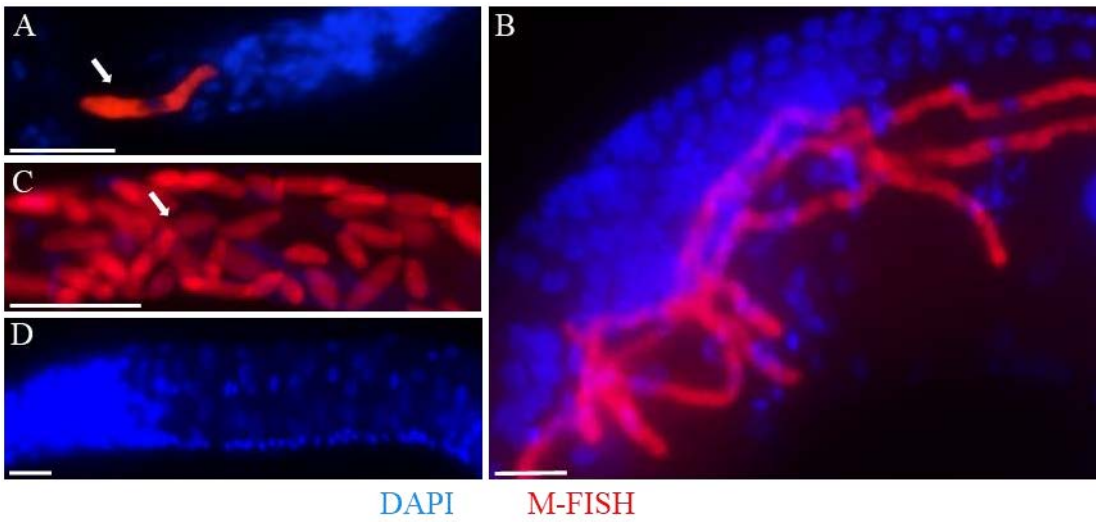

Figure 4.12: The detection of *M. humicola* infection in *C. elegans* by FISH. (A-C) The *M. humicola* Cy5 probes specifically label the pathogen. The animals were maintained with or without the oomycete for 48hrs prior to staining with the Cy5 probes. The probes target the pathogens L30 ribosomal subunit mRNA and 18S rRNA (red, M-FISH). The animals were also counterstained with DAPI (blue) to mark both the hosts and pathogens nuclei. As can be observed, the staining allows us to easily visualise *M. humicola* both at early stages while entering the host (A, an attached cytospore is indicated with a white arrow), as well as during later stages whilst growing inside the host as hyphae (B) and sporangia (C, white arrow). **(D)** The Cy5 signal cannot be observed in non-infected animals. Scale bars represent 50µm.

Using the above stated method, we also devised an attachment assay to address this question. The assays entails exposing developmentally synchronised populations of animals to the oomycete for 24 hours, followed by fixation and quantification of cytospore attachment events with the use of *M. humicola* specific FISH probes (Figure 4.13A). In a classical approach, we assessed the phenotypic consequence of either *chil* gene overexpression or attenuation on the number of oomycete attachment events. To this end, we utilised our *chil* gene overexpression animals and the CRISPR generated mutants. We found that the *chil* loss-of-function CRISPR knock-in mutants exhibited increased events of *M. humicola* cytospore attachments (Figure 4.13B), and conversely, transgenic animals overexpressing super-numerous copies of 9 *chil* genes at a time displayed reduced events of attachment. With this interesting result, we conjectured that perhaps the observed phenotypes could indicate a broader change to the cuticles composition and or mechanical properties. To investigate this possibility, and with the aid of Clara Essmann (UCL), we employed atomic force microscopy (AFM), a technique commonly used to characterise the mechanical properties of extracellular matrices, cells, and recently, the topographical and biochemical properties of the *C. elegans* cuticle (Essmann et al., 2017). With this method, we delivered exact and quantifiable forces to the cuticle of sample nematodes using a 10μm borosilicate bead tipless cantilever (Figure 4.14A), and measured the displacement of the cuticle, namely the stiffness. This data was then used to generate force-displacement curves. Remarkably, we found that the overexpression of *chil* genes *1-9* or *18*-27 significantly altered the properties of the cuticle (Figure 4.14B-C), this was displayed as a striking decrease in cuticle stiffness compared to wild-type N2 animals, i.e. the same force applied to the transgenic nematodes cuticle, results in a greater indentation compared to N2. In all instances, the animals were not exposed to *M. humicola* prior to AFM.

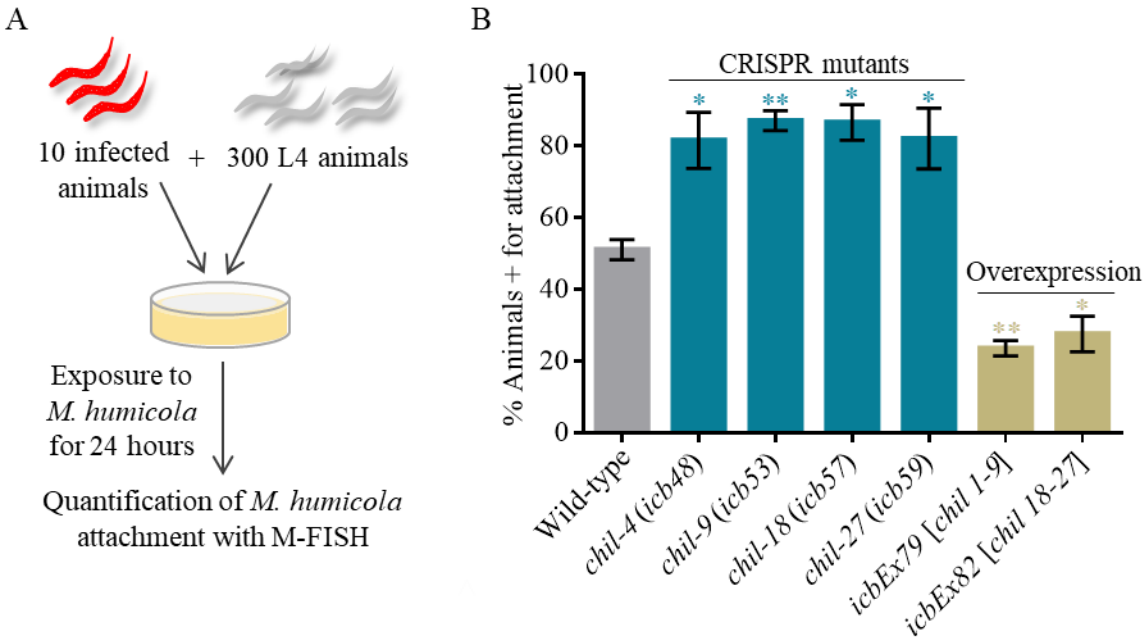

Figure 4.13: The *chil* genes antagonise *M. humicola* cytospore attachment. (A) A cartoon summarising the assay used to quantify *M. humicola* attachment events on the *C. elegans* cuticle. The assay entails exposing developmentally synchronised populations of animals to the oomycete for 24 hours, followed by the fixation, detection and the quantification of cytospore attachment events with the *M. humicola* specific FISH probes (M-FISH). **(B)** The quantification of oomycete attachment events for *chil-4*, *chil-9*, *chil-18*, and *chil-27* CRISPR loss-of-function mutants, as well as transgenic animals overexpressing *chil* genes *1-9* or *18-27*. The *chil* loss-of-function mutants exhibit increased events of cytospore attachment, and conversely, the transgenic animals overexpressing 9 *chil* genes at a time, display reduced oomycete attachment events. The data shown is representative of two technical replicates and two experimental repeats, and is shown as a mean frequency ± standard error of the proportion, n>100 animals. The statistical analysis was performed using the T-test (* $p<0.05$, ** $p<0.01$).

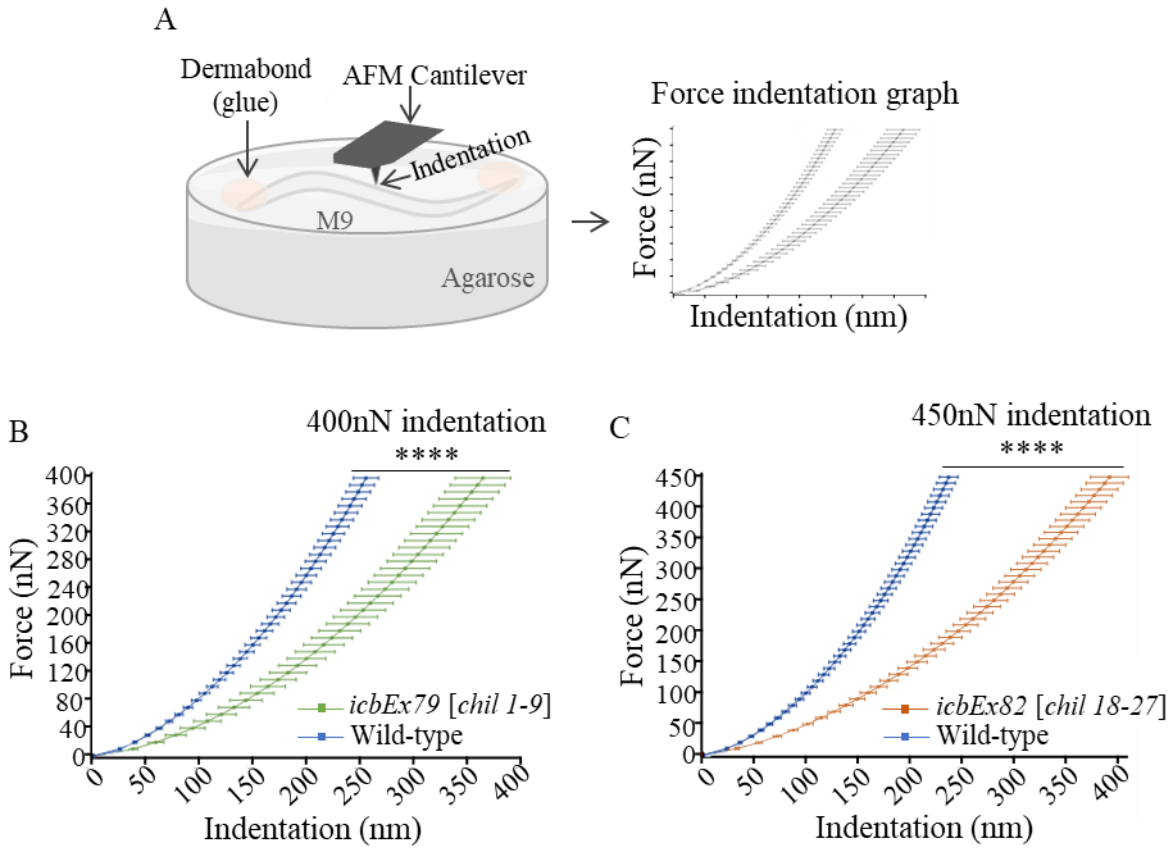

Figure 4.14: The *chil* overexpression animals display reduced cuticle stiffness. (A) A cartoon summarising how the nematode cuticle stiffness was measured using atomic force microscopy (AFM) and force-displacement analysis. In summary, exact and quantifiable forces were delivered to the cuticle of sample nematodes using a cantilever, and the resulting indentation (stiffness) was measured. The procedure was performed on animals that were paralysed and fixed onto an agarose pad with dermabond as a glue, also, the compartment was filled with M9 buffer to prevent dehydration of the specimens. **(B-C)** AFM Force-displacement analysis curves of transgenic animals carrying fosmids containing either *chil* genes *1-9* (B) or *18-27* (C). The *chil* overexpression nematodes display statistically significant reduction in cuticle stiffness compared to the wild-type animals, as indicated by the increased indentation at equivalent forces. In both instances, the animals were not exposed to *M. humicola* prior to AFM. The statistical analysis was performed using the T-test (**** $p < 0.0001$), n>20 animals per genotype, and at least 2 quantifications per animal.

4.3. Discussion.

4.3.1. *C. elegans* transcriptional response to *M. humicola*.

The nematode *C. elegans* has been extensively used as a model organism to study pathogen induced transcriptional changes in eukaryotes, these studies have generally utilised opportunistic pathogens, i.e. pathogens not shown to naturally interact with *C. elegans* (Engelmann et al., 2011; Wong et al., 2007). In contrast, comparatively little is known about *C. elegans* transcriptional responses to natural pathogens. Towards expanding our knowledge in this field, we have characterised changes in host gene expression after exposure to the oomycete *M. humicola*, an organism newly discovered to be a natural pathogen of *C. elegans*. We noted in our RNA-seq data set, the presence of classes of resistance genes previously associated with a range of microbial infections, including *c-type lectins*, *caenacins*, *neuropeptide-like proteins* and members of the *pals* genes family. These genes are thought to function as antimicrobial peptides (AMPs), or have been shown to be induced in *C. elegans*, observed to be upregulated in response to fungal, bacterial, viral and microsporidia infections (Engelmann et al., 2011; Mallo et al., 2002; Pujol et al., 2008; Troemel et al., 2006; Reddy et al., 2017; Sarkies et al., 2013).

Upon pooling and categorising the genes in our data set, we noticed that most genes corresponded to those previously characterised to play a role in *C. elegans* development. This is perhaps not unexpected, as L4 (fourth larval stage) hermaphrodites were used at the start of our infection assays, animals that were still undergoing development 12 and 24hrs later. As well as identifying common sets of genes that are differentially regulated by *M. humicola* and a range of taxonomically diverse pathogens (Bakowski et al., 2014; Engelmann et al., 2011; Sarkies et al., 2013; Yang et al., 2016), we also observed that *M. humicola* exposure initiated a highly specific transcriptional program, which showed very little overlap with other pathogen

generated gene sets, this was the case even when we directly compared to *D. coniospora* (Engelmann et al., 2011), a natural fungal pathogen that also infects in a superficially similar manner to *M. humicola*. Our observation that *C. elegans* can induce "pan-microbial" but distinct "microbe-specific" transcriptional programs supports previous published findings (Bakowski et al., 2014; Engelmann et al., 2011; O'Rourke et al., 2006; Wong et al., 2007). Presumably, this reflects *C. elegans* attempt to enhance survival, by initiating repertoires of genes to counter each pathogen's specific nature, for example, the virulence mechanisms employed by the pathogen.

4.3.2. The identification of the *chil* genes, a novel family of pathogen resistance genes.

Our analysis of the hosts transcriptome profile 12 and 24hrs post exposure to *M. humicola*, demonstrated that *C. elegans* initiates a unique transcriptional profile when compared to those generated with other extracellular or intracellular pathogens (Bakowski et al., 2014; Engelmann et al., 2011; Wong et al., 2007). Furthermore, we found that a large fraction of our RNA-seq data contained genes with no known function. In light of these results, and the fact that infection causes *C. elegans* to rapidly induce the expression of resistance genes (Feinbaum et al., 2012; Pujol et al., 2008), we reasoned that perhaps some of these genes could correspond to novel *M. humicola* induced resistance genes. In an attempt to prove this theory, we examined uncharacterised genes that were upregulated, but not previously reported to be involved in *C. elegans* immunity. In addition, we also directed our attention towards genes encoding proteins homologous to proteins with defense roles in other organisms. Using this criteria, we noticed the presence of members of the *chitinase-like* (*chil*) gene family. The *chil* genes encode proteins that contain a glycoside hydrolase 18 family (glyco-18) domain.

Interestingly, the *chil* genes have not previously been reported to be expressed under normal lab conditions, or shown to be involved in *C. elegans* immunity. Although *chitinase-like* genes have not been studied in the context of infection in *C. elegans*, their homologs have been linked to mammalian immunity against pathogenic nematodes, in addition, they have also been shown to play a role in tissue remodelling (Kzhyshkowska et al., 2007; Lee, 2009; Sutherland et al., 2014). Consequently, we postulated that perhaps the *chil* genes may also play similar roles in *C. elegans* immunity. Because *chil* gene induction was largely absent from previously reported pathogen generated, differential gene expression datasets, we also designated the *chil* genes as signatures, biomarkers to indicate the activation of *M. humicola* induced immune responses in *C. elegans*.

To investigate whether the *chil* genes contribute towards *C. elegans* resistance against *M. humicola* infection, we generated transgenic animals overexpressing genes *chil-1* to *chil-9*, or *chil-18* to *chil*-27. In both instances, we observed a significant increase in the hosts capacity to survive against *M. humicola*-mediated killing. During the course of these assays, we noticed that nematodes expressing supernumerary copies of genes *chil-18* to *chil-27* exhibited more of an enhanced resistance phenotype, than the animals overexpressing genes *chil-1* to *chil-9*. Possibly, this could either suggest that genes *chil-18* to *chil-27* play a more significant role than *chil-1* to *chil-9*, or that the transgenic animals harbour differing levels of extrachromosomal expression, and as a result, significant differences in the overexpression of target *chil* genes. We also studied the consequence of *chil-4*, *chil-9*, *chil-18* or *chil-27* loss-of-function on *C. elegans* ability to cope with *M. humicola* infection. Converse to the overexpression infection assays, we noticed that the CRISPR mutants exhibited modest, statistically significant decreases in their capacity to cope with *M. humicola* infection compared to the wild-type. The absence of a more pronounced phenotype could be explained by the phenomenon of genetic redundancy, i.e. the inactivation of a single gene that is performing the same function as two

or more genes has little or no effect on the biological phenotype in question (Nowak et al., 1997). Alternatively, the modest increase in susceptibility displayed by the CRISPR mutants, and the significant decrease exhibited by the overexpression transgenic animals, could also be attributed to cooperation, a mechanism whereby the phenotype of multiple genes or proteins executing their function together is greater, than when said tasks are performed independently (Chae et al., 2016; Playfair, 1971), e.g. 1 *chil* gene will contribute to conferring *C. elegans* considerably less resistance than 10 *chil* genes. Additionally, with the use of GFP transcriptional reporters, we have demonstrated that the two most significantly upregulated genes *chil-27* and *chil-28* are expressed in the hypodermis. Furthermore, by using *chil-27* as a model to study how *chil* genes may antagonise *M. humicola* infection, we discovered that CHIL-27 is expressed in a pattern reminiscent to the circumferentially located grooves and ridges of the cuticle, structures termed the annuli and furrows (Chisholm and Hsiao, 2012).

4.3.3. The *chil* genes enhance *C. elegans* survival by antagonising *M. humicola* attachment.

Having observed that CHIL-27 is expressed in a pattern reminiscent to the structures of the cuticle, the initial site of host-pathogen interaction, we hypothesised that the *chil* genes may confer resistance by antagonising the oomycetes ability to attach onto the host's cuticle. To address this possibility, we developed a FISH protocol to easily visualise and quantify *M. humicola* attachment events. In support of our theory, we found that the overexpression of *chil* genes resulted in a strikingly significant decrease in events of *M. humicola* attachment, and inversely, the attenuation of *chil* gene function lead to increased events. Also, with the use of AFM, we showed that the overexpression of *chil* genes noticeably decreased the stiffness of

the cuticle, signifying a broader change to the composition and or mechanical properties of the cuticle.

How exactly do the CHIL proteins mechanisms of action give rise to these associated phenotypes? Perhaps by examining homologs, namely members of the glyco-18 domain superfamily in other organisms we can speculate. Conceivably, the *C. elegans* CHIL proteins may remodel the extracellular matrix in a comparable manner to that of the human YKL-40 protein; CHIL proteins modify components of the cuticle that are exploited by the pathogen (Bussink et al., 2007; Kzhyshkowska et al., 2007; Lee et al., 2011). Also, considering chitinase-like proteins have retained their ability to bind similar to true chitinase proteins, CHIL proteins may bind and mask 'epitopes' that are normally expressed on the surface of the cuticle, components that are usually exposed to the environment and exploited by the pathogen to initiate infection.

The model organism *C. elegans* has been extensively used to study eukaryotic host innate immune responses to a range of opportunistic and natural pathogens (Engelmann et al., 2011; Mallo et al., 2002; Troemel et al., 2006; Sarkies et al., 2013). The work presented in this chapter, expands our knowledge of *C. elegans* immune responses and advocates for the use of natural pathogens. I argue here that natural pathogens are required to understand a model organisms immune system, especially as pathogens can be significant drivers of evolution (Black, 1970; Bozkurt et al., 2012). Undoubtedly, with the use of more natural pathogens to study *C. elegans* immune responses, researchers may discover other specialised defense mechanisms that have evolved to combat microbe-specific infections.

Chapter 5. *chil-27* is expressed in response to pathogen detection

5.1. Introduction.

The ability to detect biotic threats and mount an appropriate immune response, is crucial for an organisms survival. *C. elegans* innate immune system is comprised of both constitutively expressed and inducible elements (Bakowski et al., 2014; Feinbaum et al., 2012; Mallo et al., 2002). Intriguingly, whilst *C. elegans* lacks classical pathogen associated molecular pattern receptors that are found in more complex multicellular organisms such as humans, mice and *D. melanogaster* (Chamy et al., 2008), *C. elegans* has nevertheless been shown to mount highly specific transcriptional programs based on the nature of the invading pathogen (Alegado and Tan, 2008; Zugasti and Ewbank, 2009), and has also been shown to possess the ability to discriminate between pathogenic and non-pathogenic bacteria (Beale et al., 2006; Meisel and Kim, 2014; Pradel et al., 2007; Pujol et al., 2001; Wong et al., 2007).

In chapter 4, to expand our knowledge of *C. elegans* transcriptional response to a natural pathogen, we profiled genome-wide host gene expression changes post exposure to the oomycete *M. humicola*. Through comparative transcriptomic analysis, we discovered a novel class of *C. elegans* resistance genes, the *chitinase-like* (*chil*) family of genes. The *chil* genes are not expressed under standard lab conditions. Due to their role in contributing towards *C. elegans* resistance against the oomycete, we designated the *chil* genes putative effectors, and useful biomarkers for detecting *M. humicola* induced immune responses.

In this chapter, we sought to further characterise the transcriptional regulation of *chil-27*, the most significantly and reproducibly induced *chil* gene. Towards this goal, we transferred a *chil-27p*::GFP transcriptional reporter to a range of mutant backgrounds, and assessed their consequence to normal transgene activation. Using this method, we demonstrate that *chil-27* is transcriptionally regulated by the p38 MAPK innate immunity signalling pathway and ELT-3, a GATA transcription factor (Gilleard et al., 1999; Kim et al., 2002; Pujol

et al., 2008). We also show that *chil-27* can be induced with autoclaved, inactivated *M. humicola*, or an oomycete extract. Taken together, our results demonstrate that *chil-27* induction is likely to be as a consequence of pathogen recognition as opposed to infection, and that this process involves the anteriorly located amphids, the main *C. elegans* chemosensory organ (Oikonomou et al., 2011). The work presented in this chapter, indicates that there are some as yet unknown mechanisms used by *C. elegans* to detect pathogens in its environment.

5.2. Results.

5.2.1. The *chil-27* transcriptional reporter accurately depicts native *chil-27* expression.

In response to *M. humicola* infection, we have shown that *C. elegans* employs the *chil* genes to increase host survival. Considering the *chil* genes are a novel super family of resistance genes that are not expressed under normal lab conditions, nor have they previously been shown to be involved in *C. elegans* response to infections, we sought to further characterise these genes by studying the transcriptional regulation of *chil-27*. To this end, we used stable transgenic nematodes carrying the *chil-27p*::GFP transcriptional reporter. Initially, we examined whether the GFP nuclear localised reporter, accurately depicts the spatial expression of the native *chil-27* gene.

Whilst transcriptional reporters provide a tentative expression pattern of an endogenous gene under study, promoter GFP fusions may not reflect the endogenous expression pattern of a gene, both spatially and or temporally (Dolphin and Hope, 2006). Therefore, to address this concern, we used single molecule fluorescent *in situ* hybridization (smFISH), as an independent method to verify the site of *chil-27* transcriptional activity, and designed smFISH probes tagged with the fluorophore Cy5 that hybridise to *chil-27* mRNA. In order to accomplish this goal, we fixed stable transgenic animals harbouring the transcriptional reporter that had either been exposed, or not exposed to the pathogen, and examined whether the induced *chil-27* mRNAs co-localised with the activated, nuclear localised GFP reporter. Analogous to our previous findings (chapter 4), exposure to *M. humicola* resulted in the activation of the transcriptional reporter (Figure 5.1A). In validation of our GFP reporter, the transgenic animals exposed to the pathogen also expressed *chil-27* mRNAs, this was represented as distinct and intense Cy5 fluorescent puncta (Figure 5.1B). Also, the white spots significantly co-localised

with the activated GFP reporter (Figures 5.1C). In agreement with our transcriptomics analysis, and the transcriptional reporter assays, we failed to detect *chil-27* mRNAs in the absence of the oomycete (Figure 5.1D). Taken together, these results indicate that the GFP reporter accurately depicts both the spatial endogenous domain, and the induction of the native *chil-27* gene.

The hypodermis, the endogenous site of *chil-27* expression is predominantly comprised of a multinucleated cylindrical syncytium, which surrounds and encompasses seam cells. The seam cells generate and are overlaid by the alae, which are the longitudinal ridges that interrupt the circumferentially oriented grooves of the cuticle (Chisholm and Hsiao, 2012; Johnstone, 1994), and, as revealed by SEM, the alae are a site for *M. humicola* attachment. Therefore, to address whether *chil-27* transcription could also be initiated in the seam cells, we exposed transgenic animals harbouring a GFP reporter that labelled seam cell nuclei to *M. humicola*, and examined whether we could detect induced *chil-27* mRNAs in the seam cells with smFISH. As shown in Figure 5.2, we observed *chil-27* to be distinctly excluded from the seam cells and confined to the surrounding syncytium (hypodermis).

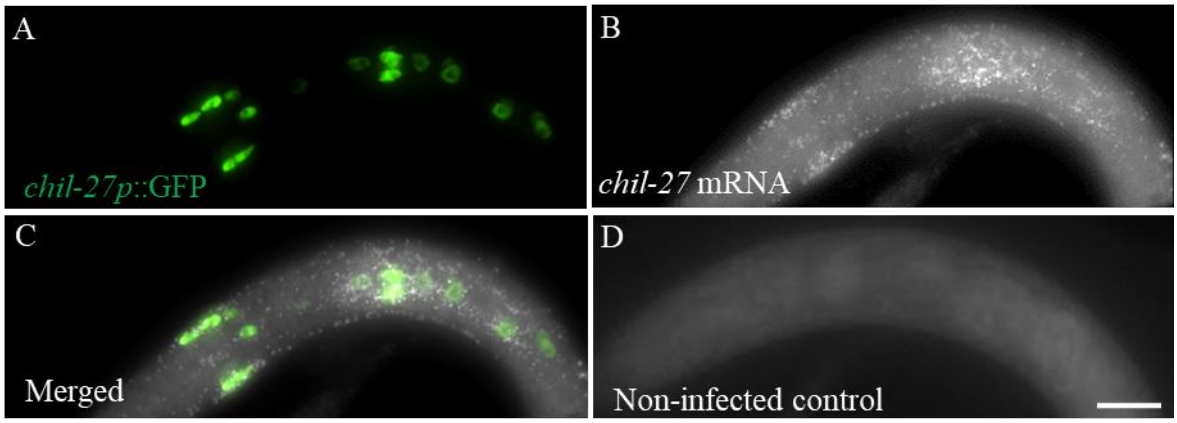

Figure 5.1: The *chil-27* transcriptional reporter accurately depicts *chil-27* expression. (A-D) Micrographs of transgenic animals carrying a *chil-27* GFP reporter maintained with or without *M. humicola*, and subjected to *chil-27* smFISH. (A) In the presence of the oomycete, we can observe the activation of the GFP nuclear localised reporter (white arrows point towards the marked nucleus and unlabelled nucleolus), and detect the presence of distinct white spots that correspond to the Cy5 labelled *chil-27* mRNAs (B). (C) Upon merger of the two channels, we can observe that the *chil-27* mRNAs co-localise with the *chil-27* GFP reporter. (D) In the absence of the pathogen, *chil-27p*::GFP expression is neither induced, nor can we detect *chil-27* mRNAs with smFISH. The data shown is representative of at least two independent experiments. Identical settings were used to acquire, process and display the images. The images are representative of projections comprised of 15x1μm thick sections. Scale bars represent 10μm.

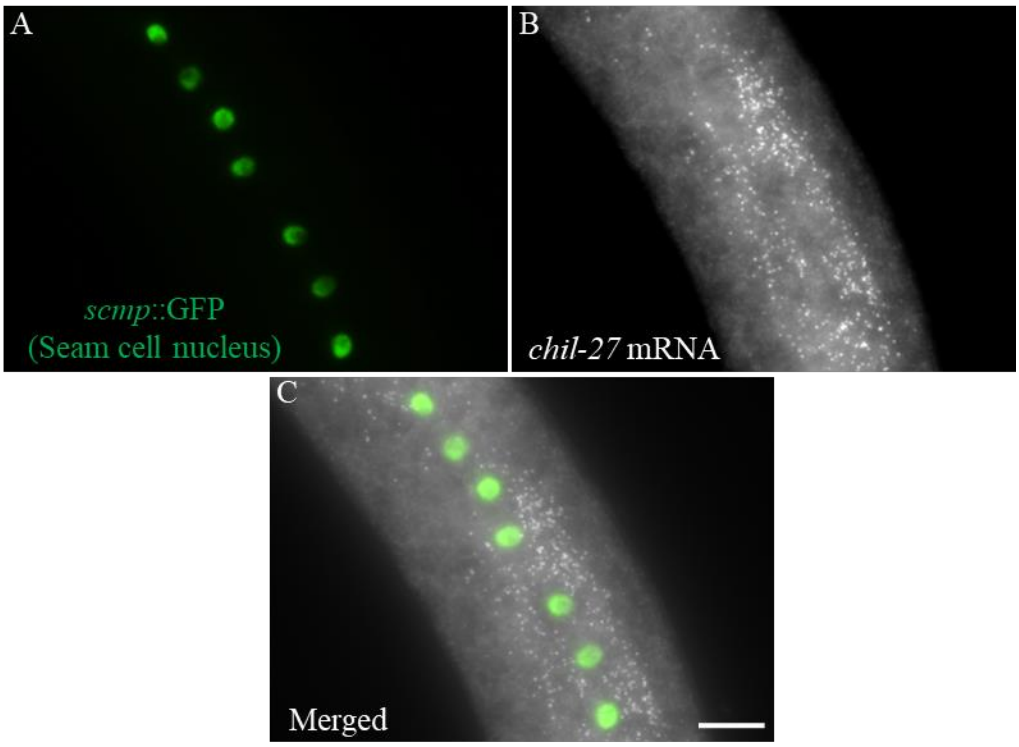

Figure 5.2: *chil-27* expression is distinctly excluded from the seam cells. **(A-C)** smFISH detection of *chil-27* mRNAs in transgenic animals containing a GFP transgene labelling the seam cell nucleus. The images are of an animal fixed 48hrs post exposure to *M. humicola*. (A) The GFP channel displaying the fluorescently labelled seam cell nucleus. (B) The Cy5 channel displaying the detection of *chil-27* mRNAs (white spots). (C) Merger of the two fluorescent channels. As can be observed, *chil-27* transcription can only be detected in the surrounding hypodermis, and is distinctly excluded from the seam cells. The images are representative of projections comprised of 10x1µm thick sections. Scale bar represents 10µm.

5.2.2. *chil-27* expression in response to abiotic stresses.

With the validation that our transcriptional reporter, accurately represents native *chil-27* gene expression, we next sought to characterise the specificity of the reporter, and examined whether *chil-27* could also be induced by stress conditions other than exposure to *M. humicola*. Towards this goal, we subjected animals carrying the transgene to a variety of abiotic stresses. Our reasoning was based on the fact that abiotic stresses, such as mechanical damage and hyperosmotic environments can induce the same effector genes in *C. elegans*, as those observed to be induced by infection (Pujol et al., 2008; Rohlfing et al., 2010). The substantial overlap between the genes observed to be induced by infection and abiotic stresses, could possibly be as a result of comparable physiological perturbations being triggered, for example, the disruption of similar basic cellular mechanisms, such as protein synthesis. Intriguingly, all the abiotic stresses that we subjected the transgenic animals with, including starvation (animals maintained at 20^{o}C for 24hrs in the absence of food), osmotic stress (exposed to 300mM NaCl for 24hrs), chemically induced endoplasmic reticulum stress (0.5µg/ml Tunicamycin for 48hrs), heat shock (animals maintained at 33^{o}C for 4hrs) and mechanical damage (pricked with a micro-injection needle) failed to induce the expression of *chil-27* (Figure 5.3).

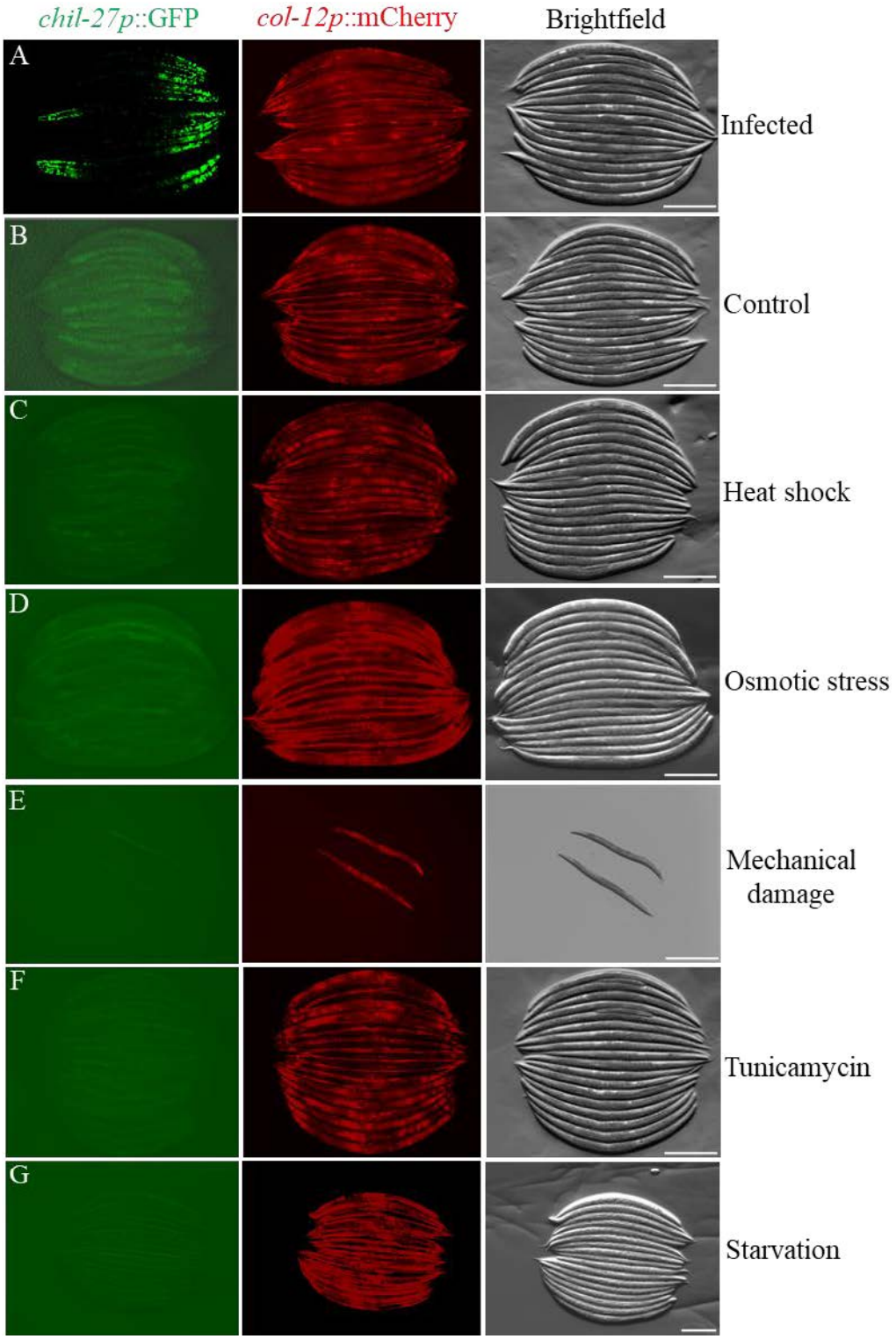

Figure 5.3: Assays to examine *chil-27* expression specificity to abiotic stresses. (A-G) Fluorescent micrographs of transgenic nematodes carrying a *chil-27* (*chil-27p*::GFP) and a *col-12* (*col-12p*::mCherry) transcriptional reporter exposed to *M. humicola*, and to a range of abiotic stresses. As depicted, the *chil-27* GFP reporter was only activated when the transgenic

animals were exposed to *M. humicola* (A), and was not active under control conditions (B), or induced when the animals were subjected to a range of abiotic stresses including heat shock (C), osmotic stress (D), mechanical damage (E), chemically induced endoplasmic reticulum stress (F), or starvation (G). The assays were set-up using 50 developmentally synchronized L4 animals, the data shown is representative of at least two technical replicates and two independent experiments. Identical settings were used to process, display and acquire the images. Scale bars represent 200μm.

5.2.3. *chil-27* expression is transcriptionally regulated by the p38 MAPK pathway and the GATA transcription factor ELT-3.

C. elegans possesses an innate immune system that is comprised of both inducible and constitutively expressed components. The inducible immune system, has previously been shown to modulate the tissue specific induction of resistance genes (Alper et al., 2007; Zugasti and Ewbank, 2009). Our work has demonstrated that *chil-27* is not expressed at a basal level in N2. Furthermore, induction of *chil-27* requires the host to be exposed to *M. humicola*, thus indicting that *chil-27* is part of the inducible defense mechanisms employed by *C. elegans* to counter the oomycete infection. As such, we reasoned that the p38 MAPK innate immunity pathway, may contribute to the transcriptional regulation of *chil-27*, as this pathway has previously been shown to control the expression of inducible resistance genes (Hesp et al., 2015; Kim et al., 2002; Kimura et al., 1997; Liberati et al., 2004; Pujol et al., 2008; Troemel et al., 2006).

To study the mechanisms of *chil-27* transcriptional regulation in a controlled manner, including the consequence of targeted gene attenuation on *chil-27* expression, we first developed an induction assay. The assay consists of quantifying the number of GFP positive animals, from a population of 50 transgenic animals that have been maintained with the oomycete for 48 hours.

Using the above stated method, we first investigated whether transgenic animals harbouring a *sek-1*(*km4*) mutation, exhibited any change in their ability to induce the expression of *chil-27*. SEK-1 constitutes an integral component of the p38 MAPK pathway (Kim et al., 2002). As depicted in Figure 5.4, the population of animals with abrogated *sek-1*, displayed a significant reduction in the number of GFP+ animals compared to the wild-type

(Fischer's exact test, $p<0.0001$). In all instances, the GFP reporter was not observed to be induced under control conditions.

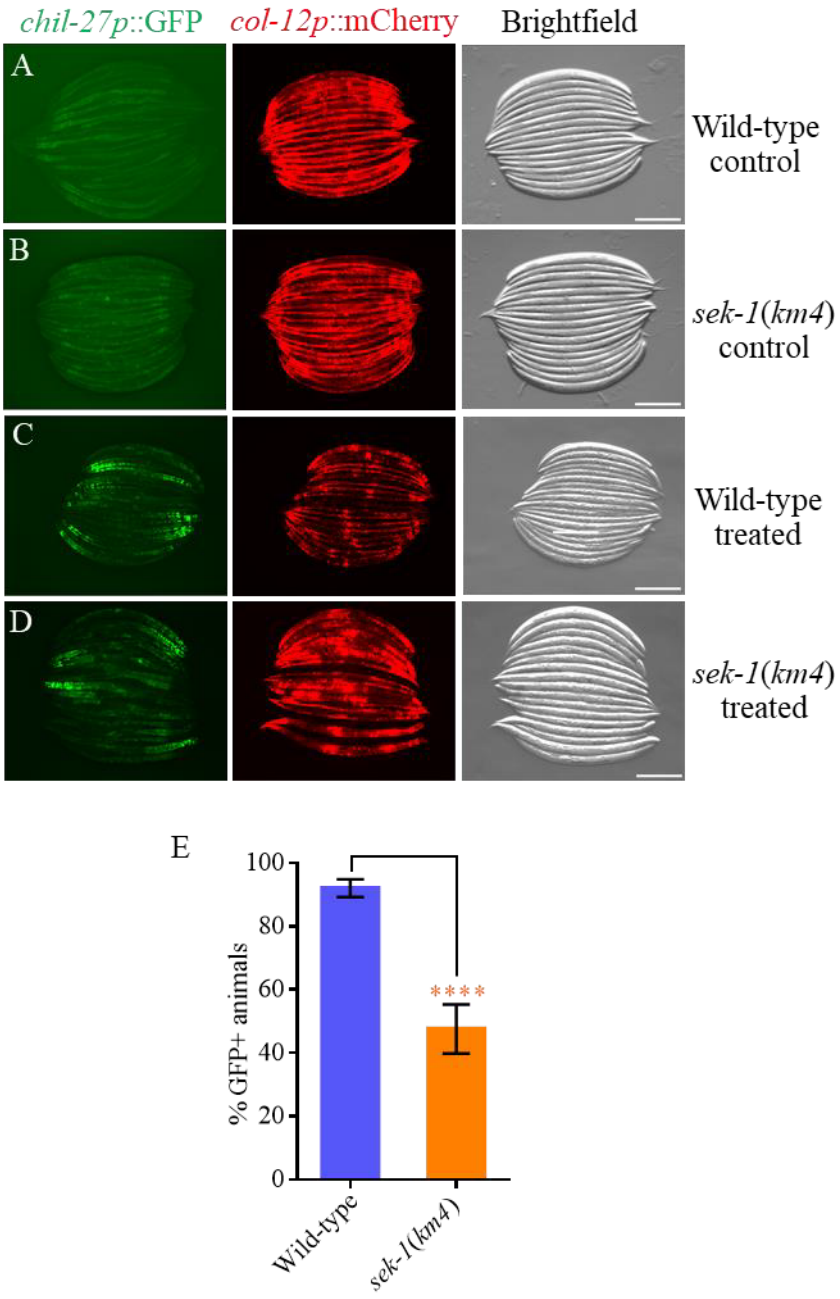

Figure 5.4: The p38 MAPK pathway transcriptionally regulates *chil-27* expression. (A-E) Characterising the effect of *sek-1* abrogation on *chil-27* expression post exposure to *M. humicola*. The panels show controls not exposed to the pathogen (A) wild-type animals and (B) *sek-1*(*km4*) mutants, as well as *M. humicola* treated animals (C) wild-type and (D) *sek-1*(*km4*). The transgenics harbouring the *sek-1*(*km4*) mutation display a significant reduction in the number of GFP+ animals compared to the wild-type (Fischer's exact test, $p < 0.0001$). In all instances, the animals that were cultured under control conditions without the pathogen did

not show activation of the reporter. The assays were set-up using 50 developmentally synchronized L4 animals. The data shown is representative of two technical replicates and two independent experiments. Identical settings were used to process, display and acquire the images. Scale bars represent 200μm. (E) A bar graph displaying the representative data from panels C and D. The data was visualised and analysed with GraphPad Prism 7. The error bars display 95% confidence intervals for the proportion of GFP+ animals. The statistical significance was determined using the Fischer's exact test (**** $p<0.0001$).

Additionally, to identify other mechanisms that transcriptionally regulate the expression of *chil-27*, we next examined the proximal promoter region of *chil-27*, for motifs that might mediate the binding of transcriptional regulators. We found in the upstream sequence of *chil-27*, the presence of the consensus sequence (A/T) GATA (A/G), a conserved putative binding site for members of the GATA transcription factor family (Reece-Hoyes et al., 2005). We reasoned that this suggested a GATA transcription factor could play a role in regulating the expression of *chil-27*. Previous findings have demonstrated that the GATA transcription factors, can regulate the expression of inducible innate immunity genes in a tissue specific manner, for example, ELT-2 controls the expression of *clec-67*, an antimicrobial peptide that is expressed in the intestine to antagonise *Salmonella enterica* infection (Kerry et al., 2006; Shapira et al., 2006). Because *chil-27* is expressed in the hypodermis, we focused on the GATA transcription factor ELT-3, which has also been shown to be expressed in the hypodermis (Gilleard et al., 1999). Furthermore, previous studies have demonstrated that ELT-3 regulates the expression of *nlp-29* in the hypodermis, a gene that encodes an antimicrobial peptide that is induced to increase host survival against *D. coniospora* infection (Pujol et al., 2008). To assess whether ELT-3 may also regulate the expression of *chil-27*, we transferred the *chil-27p*::GFP transgene into an *elt-3*(*gk121*) null mutant background. Interestingly, we found that abrogating *elt-3*, significantly reduced the number of GFP+ animals present in the population (Fischer's exact test, $p < 0.001$) (Figure 5.5).

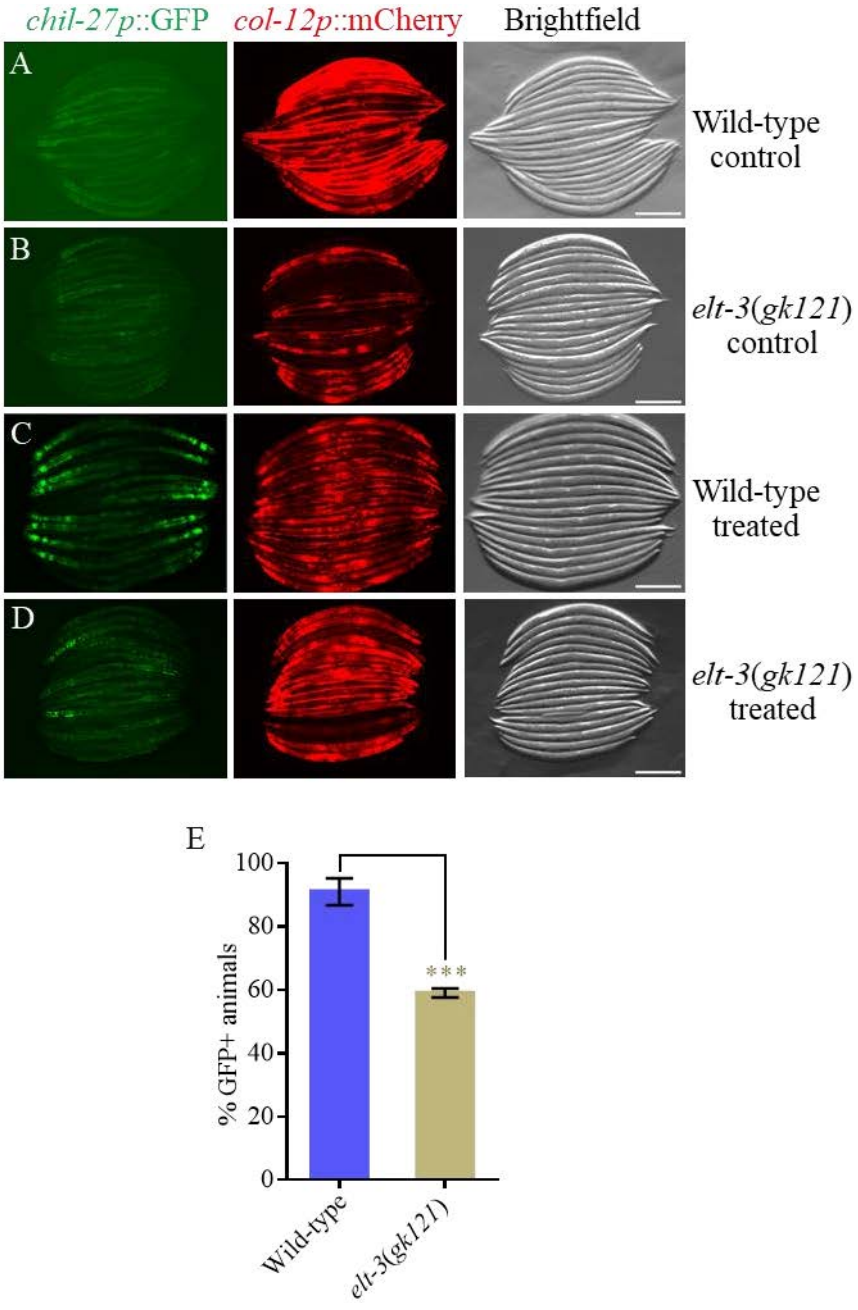

Figure 5.5: The GATA transcription factor ELT-3 is required for normal *chil-27* expression. (A-E) Characterising the effects of *elt-3* abrogation on *chil-27* expression post exposure to *M. humicola*. The panels show controls not exposed to the pathogen (A) wild-type animals and (B) *elt-3*(*gk121*) mutants, as well as *M. humicola* treated animals (C) wild-type and (D) *elt-3*(*gk121*). The transgenic nematodes harbouring the *elt-3*(*gk121*) mutation, display a significant reduction in the number of GFP+ animals compared to the wild-type (Fischer's exact test, $p<0.001$). The assays were set-up using 50 developmentally synchronized L4

animals. The data shown is representative of two technical replicates and four independent experiments. Identical settings were used to process, display and acquire the images. Scale bars represent 200μm. (E) A bar graph displaying the representative data from panels C and D. The error bars display 95% confidence intervals for the proportion of GFP+ animals. The statistical significance was determined using the Fischer's exact test (*** $p<0.001$).

5.2.4. *chil-27* is induced in response to pathogen detection.

Whilst imaging transgenic animals harbouring the *chil-27* transcriptional reporter during an induction assay, we observed something previously overlooked, some GFP+ animals did not display any signs of infection. This finding raised an intriguing question: could *chil-27* expression be induced because of *M. humicola* detection and not infection?

To address this possibility, we decided to examine whether exposure to the pathogen and not solely infection could induce *chil-27* expression. To this end, we exposed animals carrying the *chil-27* reporter to live pathogen, heat killed pathogen (autoclaved) and an oomycete extract (Figure 5.6). The oomycete extract consisted of filtered, autoclaved water that had been used to wash plates containing the pathogen. Intriguingly, we observed a comparable number of GFP+ animals between the nematodes exposed to the live pathogen and the other treatments. To validate our findings, we utilised our *M. humicola* specific M-FISH probes to detect signs of infection, in a population of GFP+ animals that had been exposed to the live pathogen (Figure 5.7). We discovered that *chil-27* expression could still be detected in animals that were neither showing pathogen attachment, or other symptoms of infection. Taken together, our results indicate that *chil-27* induction is likely to be as a consequence of pathogen recognition, as opposed to a response to infection. To elucidate how *C. elegans* may detect *M. humicola*, we next examined if the main *C. elegans* chemosensory organ could be involved in this process.

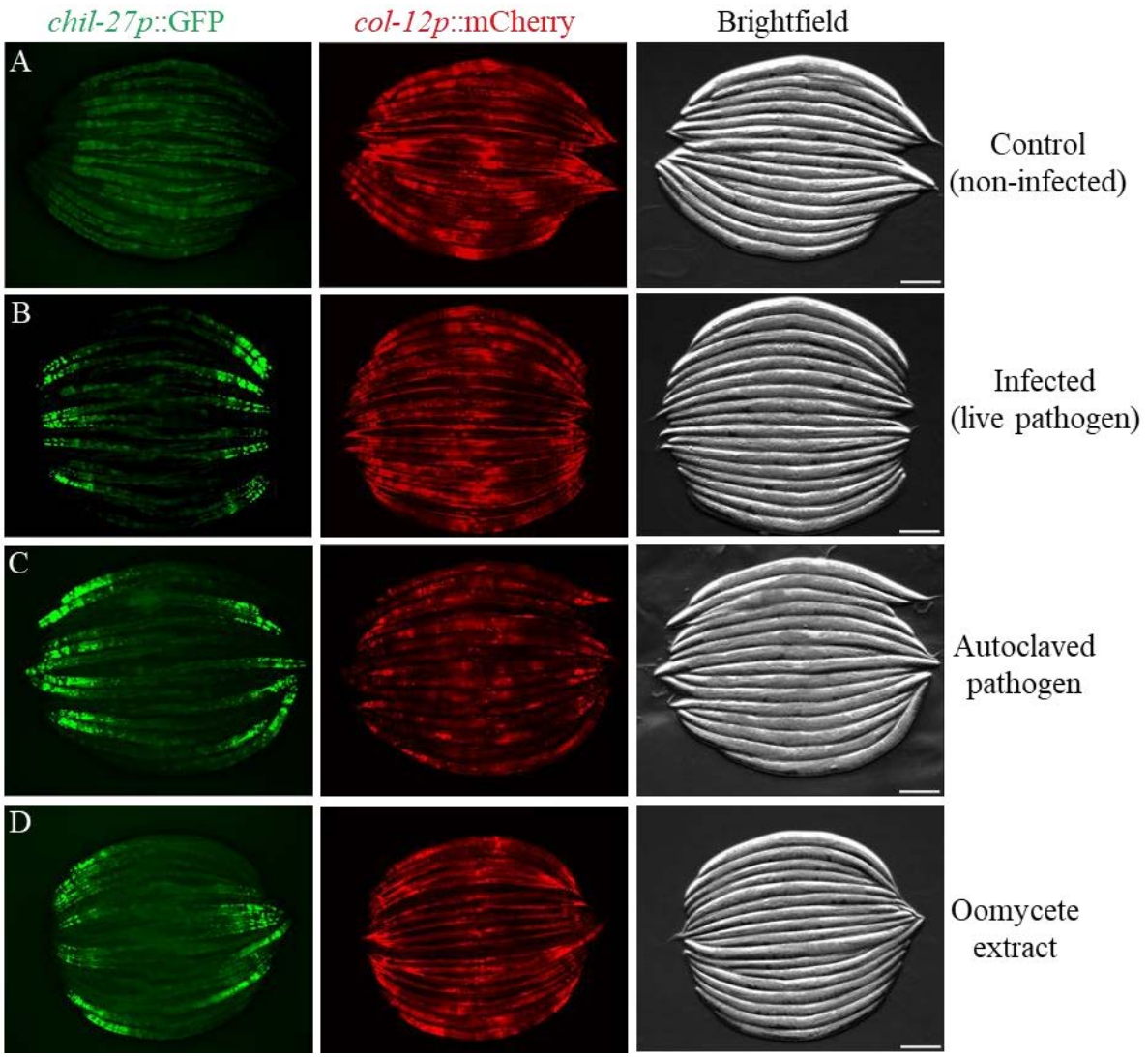

Figure 5.6: *chil-27* can be induced by inactivated pathogen. (A-D) Fluorescence micrographs of transgenic animals exposed to (A) control conditions, (B) live pathogen, (C) autoclaved pathogen and (D) an oomycete extract. The treatments did not induce a difference in the number of GFP+ animals. The induction assays were performed using 50 developmentally synchronized L4 animals. The data shown is representative of four independent experiments. Scale bars represent 200µm.

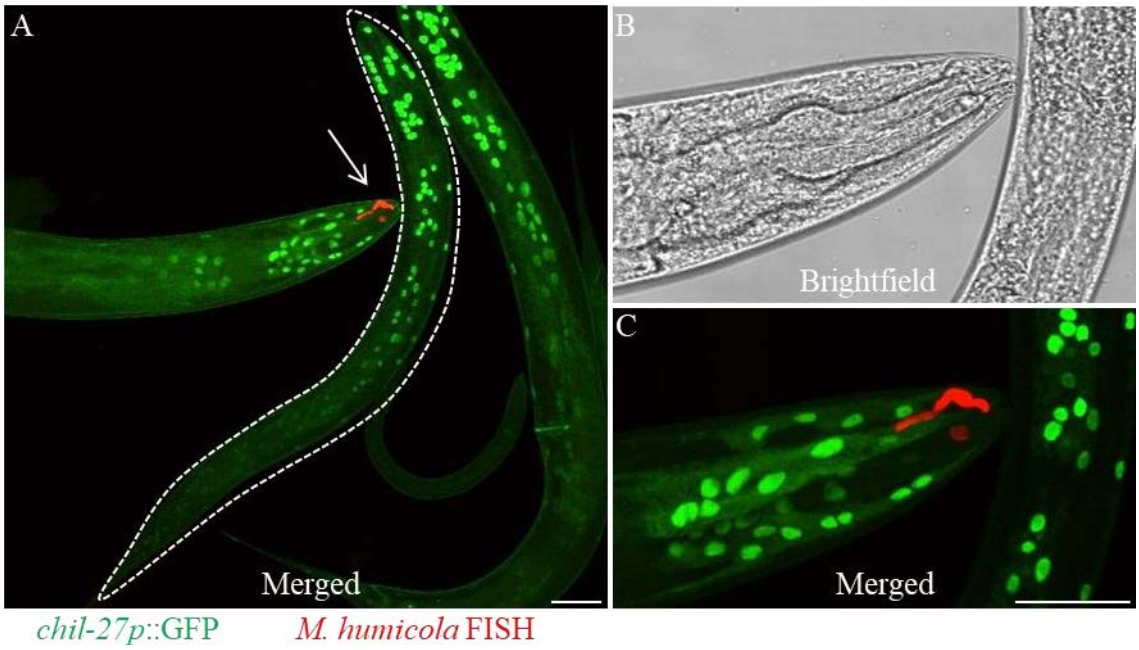

Figure 5.7: Infection is not required for the expression of *chil-27*. (A-C) The detection of *M. humicola* infection in *chil-27p*::GFP expressing animals by FISH. (A) Note that *chil-27* expression is observed in all three nematodes, but only the animal on the far left shows signs of infection (white arrow points towards the pathogen). The entire outline of a GFP+ animal devoid of any signs of infection is indicted with dashed lines. (B) The brightfield channel. (C) The close-up of the infected animal in panel A. The green represents the induced *chil-27p*::GFP reporter and red represents the M-FISH stained oomycete. Scale bars represent 50μm.

5.2.5. The chemosensory defective *daf-6* mutants exhibit reduced *chil-27* expression.

In *C. elegans*, the anteriorly located amphids, represent the main chemosensory organ used to detect a variety of water soluble and volatile environmental cues (Bargmann and Avery, 1995; Bargmann et al., 1993). The ampids contain 12 glial ensheathed sensory neurons, eight of which are ciliated and exposed to the environment. To assess whether the amphids also play a role in the detection of *M. humicola*, we monitored changes in GFP expression in a population of *daf-6*(*e1377*) mutants carrying the *chil-27* transgene. Nematodes harboring this strong loss-of-function mutation, have previously been shown to develop large and deformed amphids. In addition, the ciliated sensory neurons that are normally exposed to the environment in wild-type animals are instead bent, and enclosed within a channel pocket. Consequently, these mutants exhibit a markedly diminished capacity to detect both water soluble and volatile environmental cues (Oikonomou et al., 2011). Interestingly, when subjecting the *daf-6*(*e1377*) mutants to our induction assay, we observed a statistically significant decrease in the number of GFP+ animals compared to the wild-type (Fischer's exact test, $p<0.0001$) (Figure 5.8). To determine whether this phenotype is because of a deformed amphid, with ciliated neurons that are not exposed to the environment, or as another consequence of the molecular attenuation of *daf-6* would require further research.

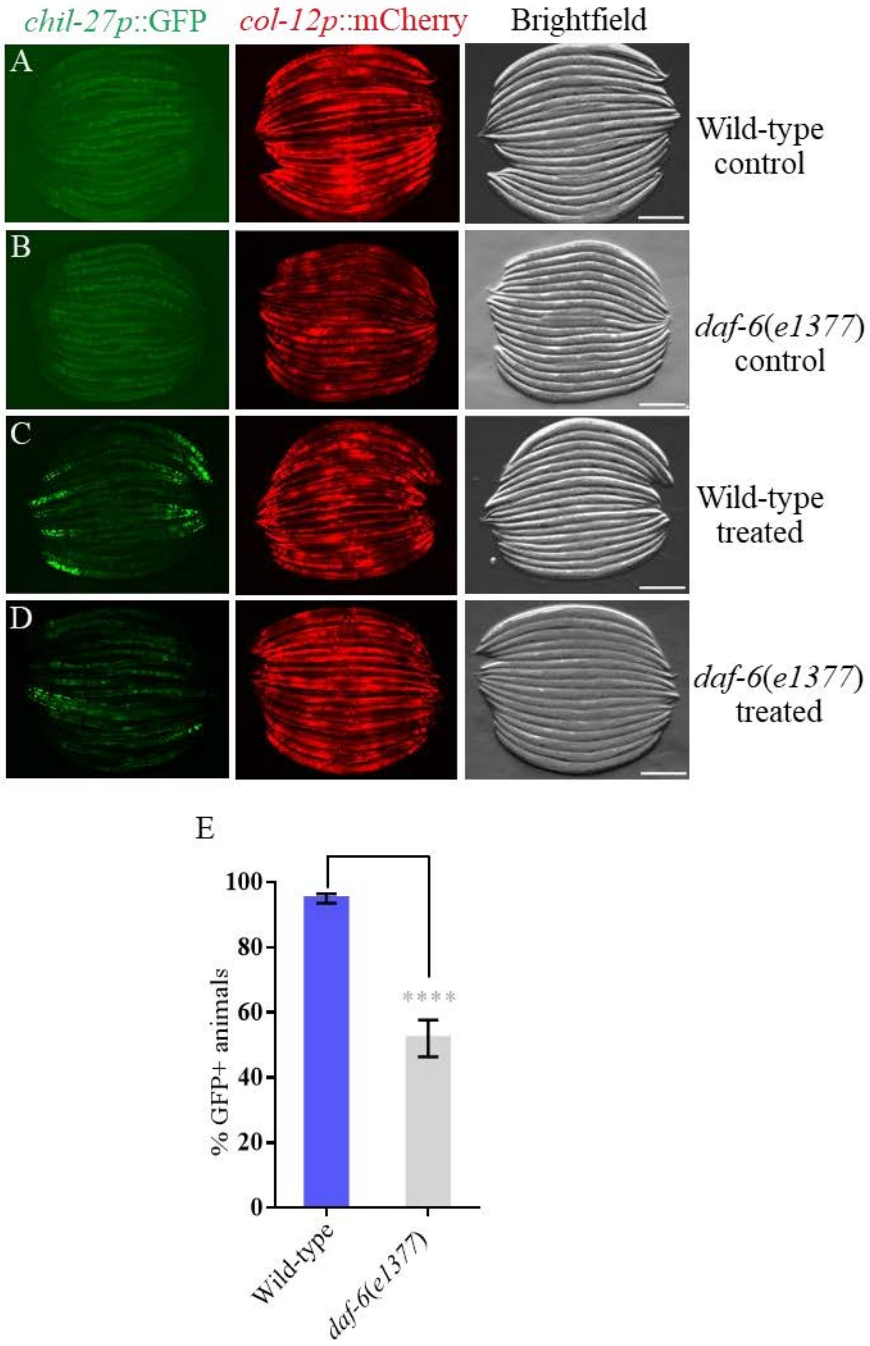

Figure 5.8: The chemosensory defective *daf-6* mutants display a reduced capacity to induce *chil-27*. (A-E) Characterising the effects of *daf-6* abrogation on *chil-27* expression post exposure to *M. humicola*. The panels show controls not exposed to the pathogen (A) wild-type animals and (B) *daf-6*(*e1377*) mutants, as well as *M. humicola* treated animals (C) wild-type and (D) *daf-6*(*e1377*). The transgenic nematodes harbouring the *daf-6*(*e1377*) mutation display a significant reduction in the number of GFP+ animals compared to the wild-type (Fischer's

exact test, p< 0.0001). The induction assays were performed using 50 developmentally synchronized L4 animals. The data shown is representative of two technical replicates and four independent experiments. Scale bars represent 200μm. (E) A bar graph displaying the representative data from panels C and D. The error bars display 95% confidence intervals for the proportion of GFP+ animals. The statistical significance was determined using the Fischer's exact test (**** p<0.0001).

5.3. Discussion.

5.3.1. *chil-27* is transcriptionally regulated by ELT-3 and the p38 MAPK pathway.

To characterise the transcriptional regulation of *chil-27*, we employed a *chil-27p*::GFP transgene, a reporter that accurately depicts both the spatial domain and induction of the native *chil-27* gene. Through a targeted reverse genetic approach, we have discovered that the GATA transcription factor ELT-3, and the p38 MAPK innate immunity pathway, both previously shown to regulate the expression of inducible defense genes in the hypodermis (Alegado and Tan, 2008; Pujol et al., 2008), are also required for normal *chil-27* induction. The observation that not a single mutation was sufficient to completely inhibit the activation of the reporter, suggests that *chil-27* is regulated by multiple mechanisms.

5.3.2. *chil-27* is induced as a consequence of pathogen detection.

Remarkably, we also discovered that the *chil-27* gene is induced in response to pathogen detection as opposed to infection, as both autoclaved pathogen and an oomycete extract, could induce the expression of *chil-27* as efficiently as the live pathogen. The observation that inactivated *M. humicola* could induce the expression of a putative defense effector, as well as the requirement for normal amphid morphology and thus indirectly chemosensation, implies that *C. elegans* possess the ability to survey its environment and pre-emptively initiate defense mechanisms. It would be interesting to observe if animals exposed to the inactivated pathogen can be inoculated, and gain increased resistance to *M. humicola* infection. As *C. elegans* lacks the classical pathogen associated molecular pattern recognition receptors that are found in more complex multicellular organisms (Chamy et al., 2008), but can still induce pathogen specific transcriptional programs (Alegado and Tan, 2008; Zugasti and

Ewbank, 2009), and is able to discriminate between pathogenic and non-pathogenic bacteria (Beale et al., 2006; Meisel and Kim, 2014; Pradel et al., 2007; Pujol et al., 2001; Wong et al., 2007), leads us to speculate that *C. elegans* possess as yet unknown mechanisms to detect pathogens in its environment.

Chapter 6. Forward genetic screens reveal *pals-22* and *pals-25* transcriptionally regulate *chil-27*

6.1. Introduction.

Caenorhabditis elegans is widely used as a model system to study host-pathogen interactions (Bakowski et al., 2014; Engelmann et al., 2011; Sarkies et al., 2013). Comparable to other multicellular organisms, *C. elegans* responds to infection by expressing defense genes to increase survival (Mallo et al., 2002). The *chitinase-like* (*chil*) family of genes, described herein this thesis, are one such group. The *chil* genes enhance *C. elegans* survival by antagonising the oomycetes ability to attach onto the cuticle. Furthermore, we have also shown that *chil-27* is induced in response to pathogen detection.

In this chapter, to further understand how *chil-27* is transcriptionally regulated, we performed forward genetic screens. By using strains carrying a *chil-27p*::GFP reporter, we were able to isolate mutants exhibiting changes in *chil-27* expression. In addition, we describe the discovery of a *C. elegans* specific mechanism controlling growth and immunity. A mechanisms that is regulated by the protein containing ALS2CR12 signature (*pals*) genes *pals-22* and *pals-25*. The *C. elegans pals* are comprised of a large family of novel genes, whose functions are poorly understood. Interestingly, whilst *pals-25* and *pals-22* are under the same operon, they appear to act antagonistically and direct opposing phenotypes. We find that the loss of *pals-22* results in an enhanced immunocompetent phenotype, which is also accompanied with significant developmental delays. We also show that this phenotype is dependent on functional *pals-25*, as the loss of *pals-25* in a *pals-22* mutant background, completely supresses the characteristic phenotypes of a *pals-22* null allele. Therefore, we conclude that the *pals-22* gene, acts as a negative transcriptional regulator of *chil-27* expression, and inversely that the *pals-25* gene is a positive regulator of *chil-27* expression. Our conclusions were further supported by the isolation of a weak gain-of-function *pals-25* mutant. Interestingly, mutants harbouring null alleles for both *pals-22* and *pals-25* were still able to induce *chil-27* expression when exposed to the oomycete, as such, we propose that the

antagonistic paralogs regulate the expression of *chil-27* independent to other, as yet identified mechanisms that are employed by *C. elegans* to detect *M. humicola* and induce the expression of *chil-27*. In summary, in this chapter, we present the discovery of *C. elegans* specific antagonistic paralogs that govern a novel mechanism regulating defense and developmental programs.

6.2. Results.

6.2.1. *pals-22* negatively regulates *chil-27* expression.

To discover key and perhaps novel factors that control the transcriptional regulation of *chil-27*, we took a forward genetic approach, and performed ethyl-methanesulfonate (EMS) mutagenesis screens on *chil-27p*::GFP integrated *C. elegans* strains. Our aim was to identify mutations that would cause the constitutive expression of the GFP reporter, but that would not alter the expression of the co-injection marker *col-12p*::mCherry. In our screens, we examined the F2 progeny of the mutagenised animals, and identified three independent dominant mutant alleles, *icb88*, *icb89* and *icb90*. All three strains were constitutively expressing the GFP reporter, whilst the expression of the co-injection marker remained unaltered (Figure 6.1). Intriguingly, under normal culture conditions, all three mutants displayed significant delay in development, with only ~20-30% of animals reaching the fourth larval stage at the expected 48-hour timepoint, this was in comparison to ~90% for N2, the wild-type reference strain (Figure 6.2).

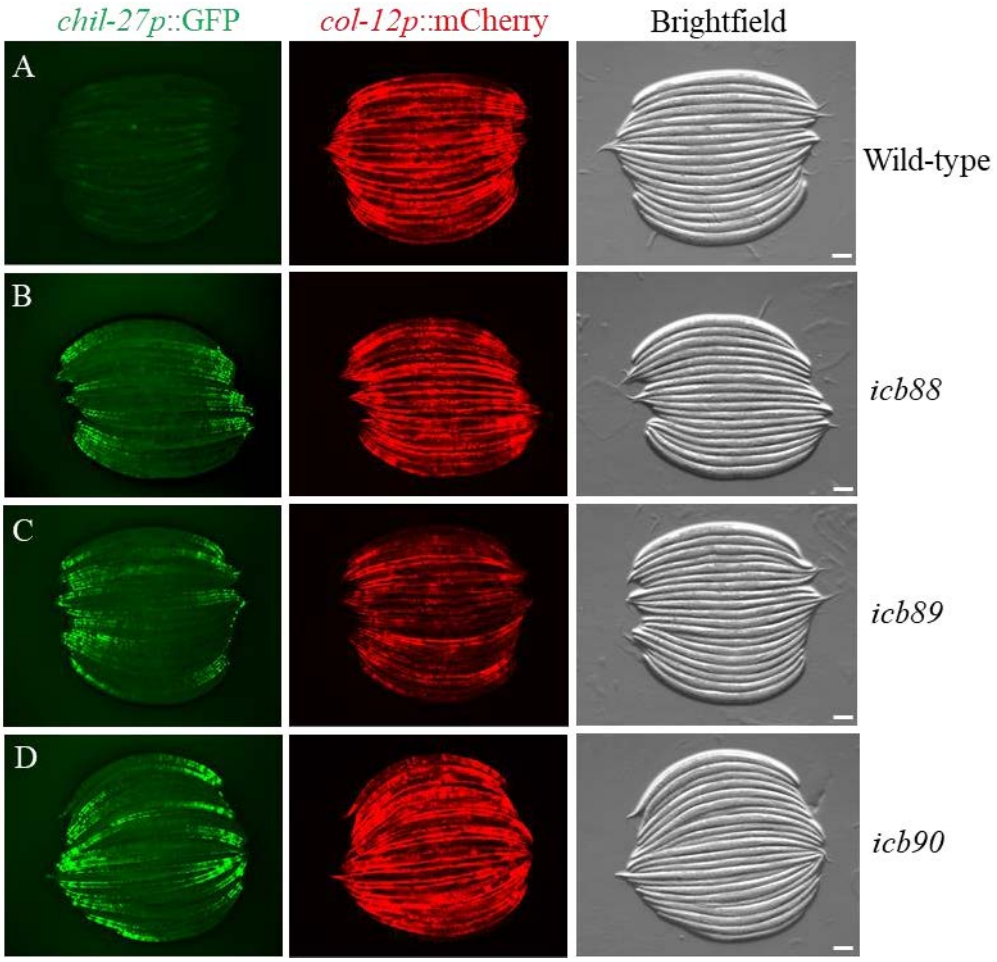

Figure 6.1: The isolation of mutants constitutively expressing *chil-27p*::GFP. (A-D) Micrographs of EMS generated mutants constitutively expressing the *chil-27* transcriptional reporter. The panels show (A) wild-type, (B) *icb88*, (C) *icb89* and (D) *icb90*. Under normal conditions, the *chil-27* reporter is not active. The transgenic animals also carry a naturally constitutively expressing *col-12p*::mCherry transcriptional reporter as the co-injection marker. Scale bars represent 100μm.

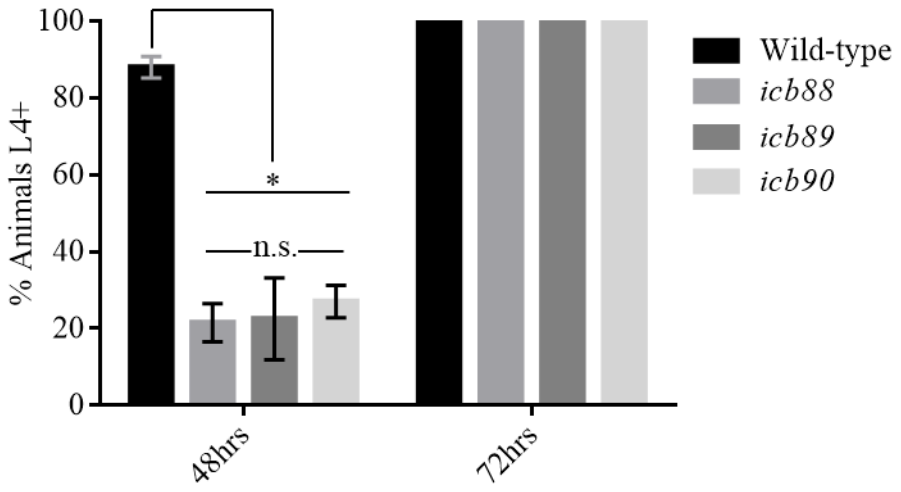

Figure 6.2: The isolated mutants display developmental delay. The percentage of animals reaching the fourth larval (L4) stage or later at 48 and 72hrs after egg laying. The isolated mutants display developmental delay reaching the L4 stage by 48hrs compared to the wild-type. At the 72hrs mark, mutants do not display developmental delay. The data shown is representative of two technical replicates and two experimental repeats, n=50. The error bars represent standard deviation. The statistical analysis was performed using the T-test (* $p<0.05$).

To identify the causative mutations, we performed Hawaiian SNP mapping (Doitsidou et al., 2008; Minevich et al., 2012). This entailed crossing the mutants to CB4856, a polymorphic isolate, followed by whole genome sequencing of the F2 recombinant animals that displayed the constitutive *chil-27p*::GFP expression, and unaltered *col-12p*::mCherry expression. For all three alleles, molecular lesions were mapped to chromosome III, and furthermore, all were predicted to harbour loss-of-function mutations affecting the same locus, *pals-22* (Figure 6.3A). The alleles *icb88* and *icb90* were predicted to harbour nonsense mutations that introduced early stop codons (G to A substitutions, W110STOP and W96STOP respectively), and the third allele *icb89*, contained a 200bp deletion spanning exons 1 and 2. All three predicted mutations were confirmed with PCR and sanger sequencing. To investigate whether *pals-22* transcriptionally regulates *chil-27* expression, we used the RNAi by feeding method (Timmons and Fire, 1998), to knockdown *pals-22* in wild-type animals carrying the *chil-27* transcriptional reporter. We found that the *pals-22* RNAi treated wild-type animals, displayed constitutive GFP expression (Figure 6.3B and C), thus verifying the *pals-22* null alleles as the causative mutations. To validate that the *chil-27* reporter was accurately representing native gene transcription, we used smFISH to detect *chil-27* expression in *pals-22* mutants not exposed to *M. humicola*. In endorsement of the reporter (Figure 6.4), we could detect intense and distinct spots corresponding to the presence of *chil-27* mRNAs.

pals-22 is part of an expanded family of *C. elegans* genes, named protein containing ALS2CR12 signature. The genes are so named because of a domain homology to the human gene ALS2CR12. ALS2CR12 was once attributed to be the causative gene underlying the human disease amyotrophic lateral sclerosis 2 (ALS), but has since been thought to not play a role in ALS (Hadano et al., 2001; Hentati et al., 1994). *pals-22* encodes a protein that is enriched in the cytoplasm and is broadly expressed in most tissues (Leyva-Díaz et al., 2017). Intriguingly, *pals-22* has recently been shown to contribute towards host thermotolerance, as

pals-22 null mutants display increased resistance to heat shock stress compared to wild-type (Reddy et al., 2017). In addition, *pals-22* has been shown to be involved in small RNA-mediated transgene silencing (Leyva-Díaz et al., 2017). Both studies have also reported that *pals-22* null mutants exhibit developmental delay, and a reduced life-span compared to the wild-type N2.

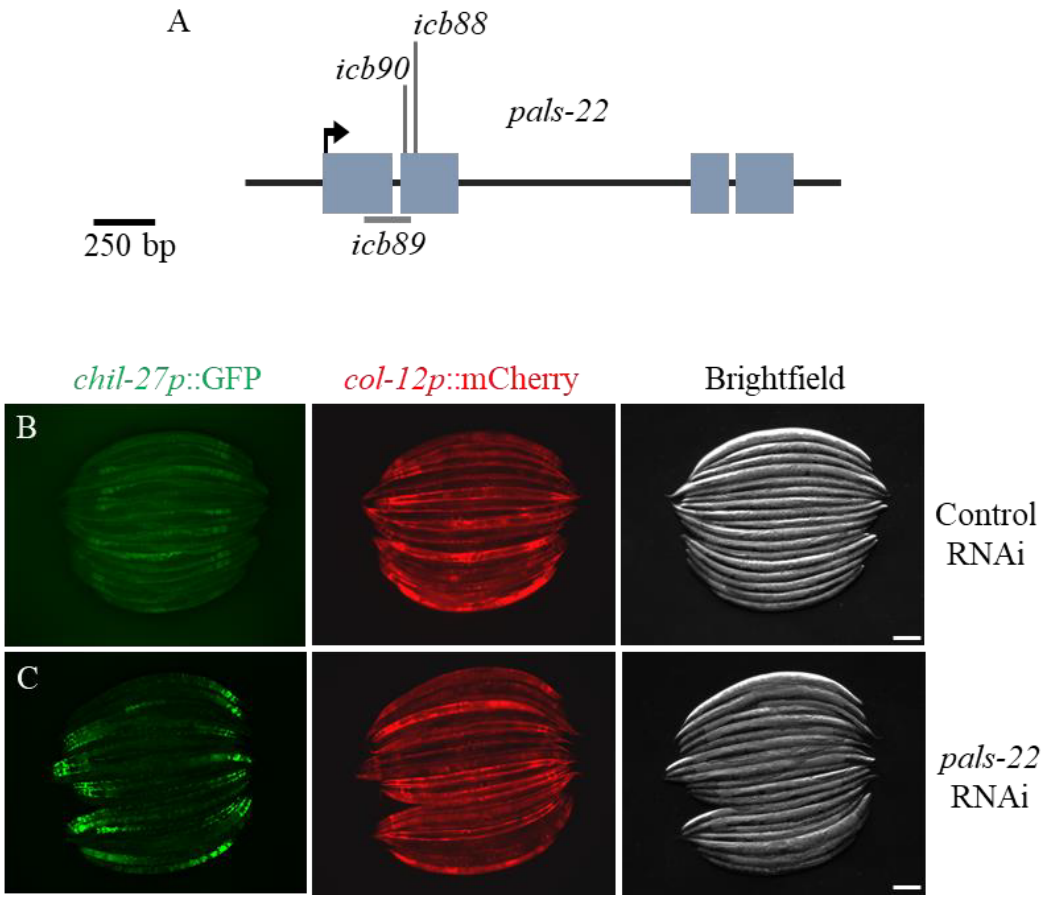

Figure 6.3: *pals-22* is a negative transcriptional regulator of *chil-27* expression. (A) A schematic cartoon showing the *pals-22* gene structure, and locations of the isolated mutations represented by their respective alleles. **(B-C)** *pals-22* RNAi induces the constitutive expression of the *chil-27* transcriptional reporter. (B) Wild-type animals carrying the *chil-27p*::GFP transgene treated with the control RNAi. (C) Wild-type animals carrying the *chil-27p*::GFP transgene treated with the *pals-22* RNAi. The results are representative of at least three independent experiments. Scale bars represent 100µm.

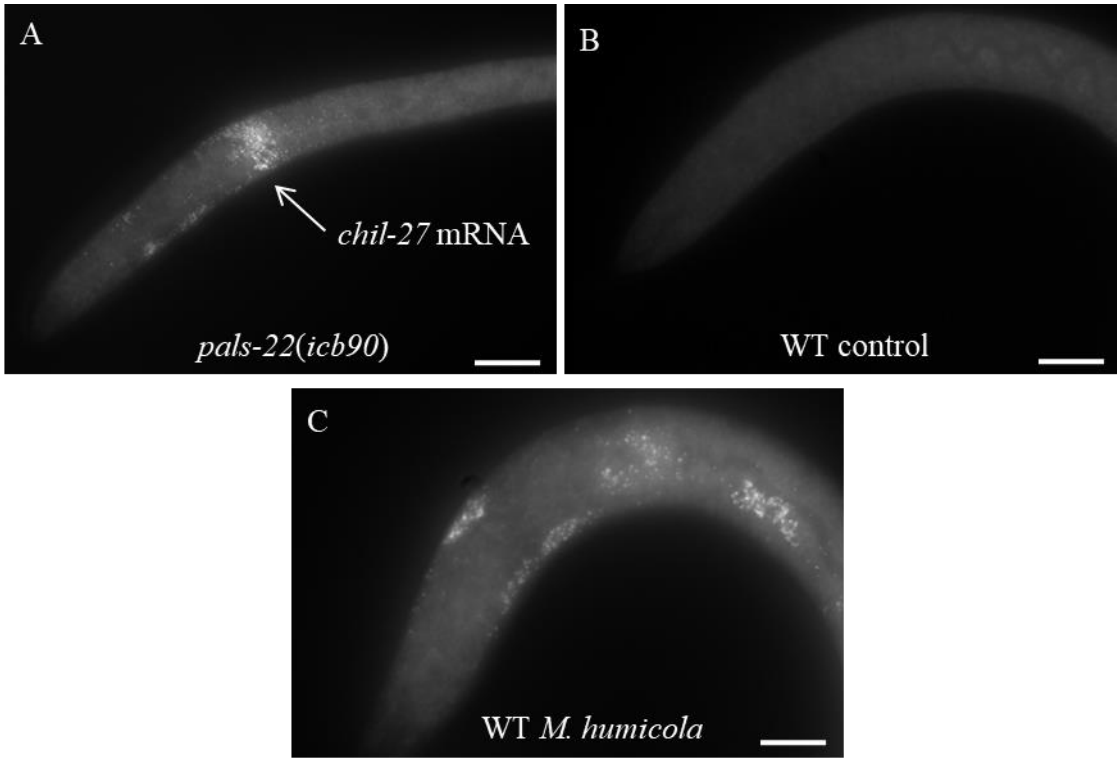

Figure 6.4: *chil-27* expression can be detected in *pals-22* mutants with smFISH. (A-C) Micrographs of a *pals-22*(*icb90*) mutant and wild-type animals maintained with, or without *M. humicola* and subjected to *chil-27* smFISH. (A) In the absence of the oomycete, we can detect *chil-27* mRNAs in a *pals-22*(*icb90*) mutant (white spots, white arrow). (B) A wild-type animal maintained under standard conditions and not exposed to the oomycete shows no expression of *chil-27*. (C) A wild-type animal exposed to *M. humicola* shows the induction of *chil-27*. In all instances, the Cy5 channel was used to detect smFISH probes that had hybridised to *chil-27* mRNAs. The data shown is representative of at least two independent experiments. Identical settings were used to acquire, process and display the images. The images are representative of projections comprised of 7x1µm thick sections. Scale bars represent 10µm.

Considering that the *pals-22* mutants constitutively express *chil-27*, a member of a super family of resistance genes, we postulated that the mutants could also exhibit greater resistance to *M. humicola* infection compared to the wild-type. To test this hypothesis, we examined the sensitivity of the *pals-22* mutants *icb89* and *icb90* to *M. humicola* infection, we found that the mutants exhibited strikingly increased resistance to the oomycete compared to the wild-type (Figure 6.5A and B). During the course of infection, *M. humicola* attaches to the cuticle of *C. elegans* to initiate infection. As we have previously shown, the overexpression of *chil* genes can reduce *M. humicola* attachment events (chapter 4), and considering the *pals-22* null mutants overexpress *chil* genes, we next examined if the increased resistance was attributed to reduced pathogen interaction. We found that the *pals-22* mutants showed markedly decreased *M. humicola* attachment events compared to the wild-type (Figure 6.5C).

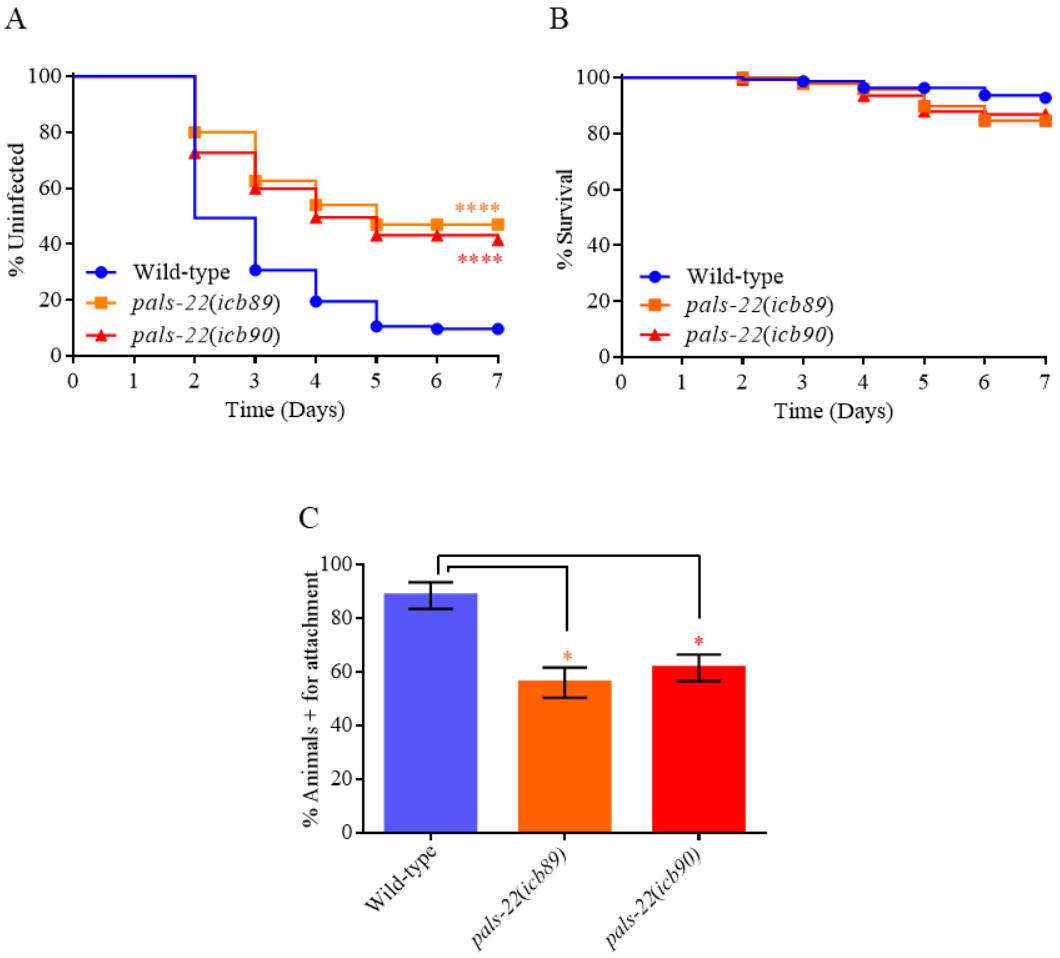

Figure 6.5: *pals-22* mutants display increased resistance to *M. humicola* infection. (A-B) Infection assay to examine the sensitivity of *pals-22* mutants to *M. humicola* infection. (A) The *pals-22* mutants display increased resistance to *M. humicola* infection ($p<0.0001$) compared to the wild-type animals. (B) The *pals-22* mutants maintained on OP50 only survived at comparable rates to N2. The data shown is representative of three technical replicates (N=150 per curve) and at least two independent experiments. The statistical analysis was performed using the log-rank analysis (**** $p<0.0001$). **(C)** The quantification of oomycete attachment events for *pals-22* mutants and wild-type animals. The *pals-22* mutants display statistically significant decrease in *M. humicola* attachment events compared to the wild-type ($p<0.05$). The data shown is representative of two technical replicates, and is presented as a mean frequency ± standard error of the proportion, n>100 animals. The statistical analysis was performed using the T-test (* $p<0.05$).

6.2.2. *pals-25* is required for the *pals-22* loss-of-function phenotypes.

In this chapter, we have discovered the *pals-22* gene to be a negative transcriptional regulator of *chil-27*, as indicated by the constitutive expression of *chil-27* when animals harbour a *pals-22* null allele. Furthermore, this phenotype is accompanied with a significant increase in resistance to *M. humicola* infection. To further understand how *pals-22* may regulate *chil-27* transcription, we mutagenised a *pals-22* null mutant, and screened for the loss of GFP expression in the F2 generation. The suppressor screen was performed with allele *pals-22*(*icb90*), as all three alleles displayed comparable phenotypes. From one screen, we isolated 2 independent alleles (*icb90icb91* and *icb90icb92*) that displayed complete suppression, a reversal of the constitutive GFP expression phenotype shown by the *pals-22*(*icb90*) mutant (Figure 6.6). Through genetic experiments (crossing *icb90icb91* or *icb90icb92* with *icb90* and quantifying segregation of phenotypes, i.e. GFP+ and GFP- animals), we determined that the *icb91* and *icb92* alleles represented recessive mutations. Also, they failed to complement when crossed together, suggesting that a gene on the same chromosome as *pals-22* was most likely affected, and that perhaps, they were alleles of the same gene.

To identify the causative mutations, we used whole genome sequencing, following analysis, interestingly, we found that both the alleles *icb90icb91* and *icb90icb92* harboured predicted loss-of-function mutations affecting the same locus, *pals-25* (A116V and G40D respectively, Figure 6.7A). Considering, *pals-25* and *pals-22* are paralogs that appear to be in an operon, and share very little sequence similarity, we hypothesised that the *pals-22* loss-of-function phenotypes would only be displayed in the presence of a functional *pal-25* gene. In validation of our theory, when *pals-25* was knocked-down using RNAi, we observed the complete suppression of the constitutively expressed GFP reporter in *pals-22*(*icb90*) animals, this phenotype was comparable to that of the *icb90icb91* and *icb90icb92* alleles (Figure 6.7B

and C). Thus, we concluded that the two alleles corresponded to *pals-25* loss-of-function mutations [*pals-22*(*icb90*)*pals-25*(*icb91*) / *pals-22*(*icb90*)*pals-25*(*icb92*)].

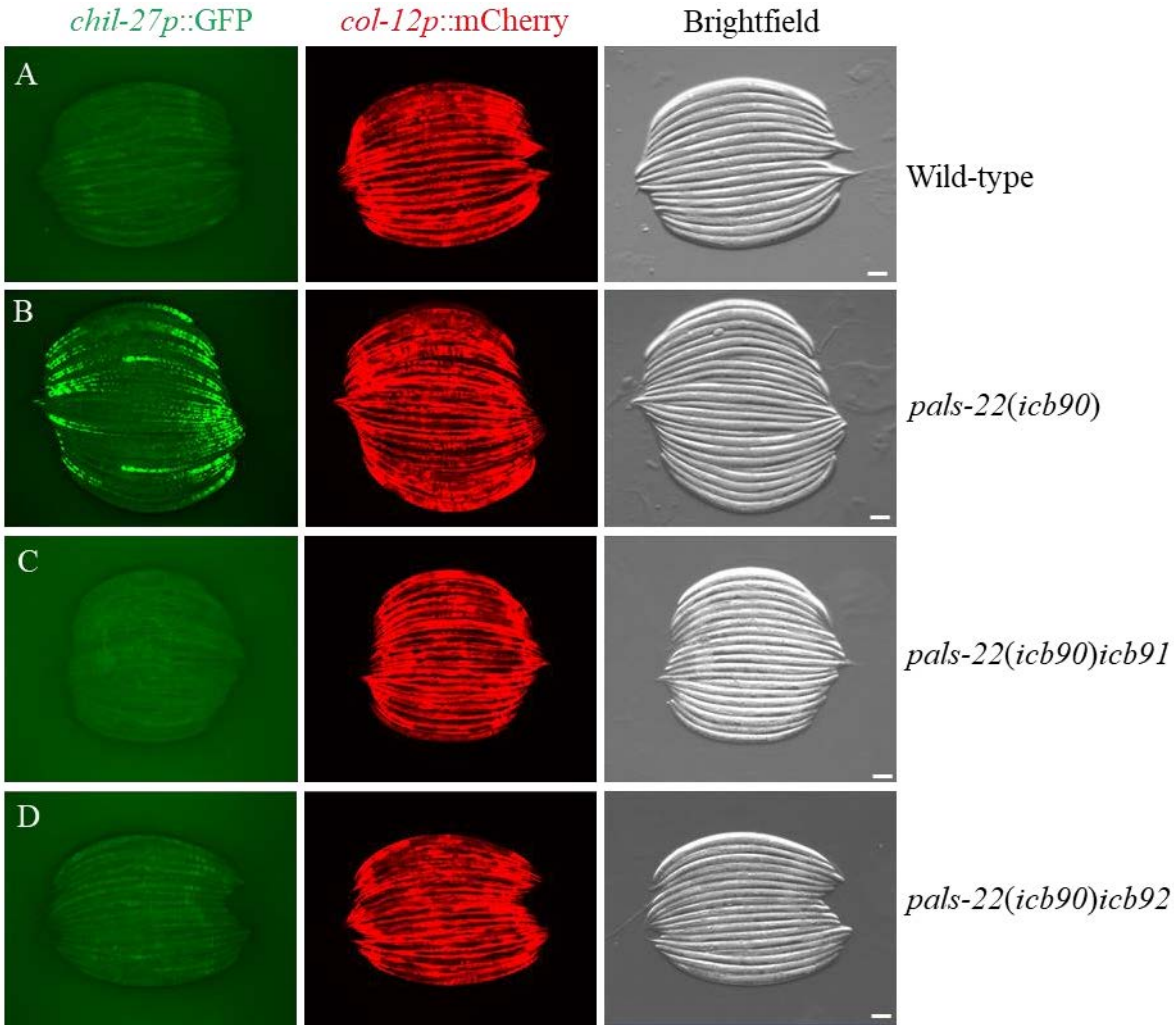

Figure 6.6: *pals-22* suppressor screen. (A-D) The isolation of mutations supressing the *chil-27* constitutive expressing phenotype of *pals-22*(*icb90*). The panels show (A) wild-type, (B) *pals-22*(*icb90*), (C) *pals-22*(*icb90*)*icb91* and (D) *pals-22*(*icb90*)*icb92*. The transgenic animals also carry a naturally constitutively expressing *col-12p*::mCherry transcriptional reporter as the co-injection marker. Scale bars represent 100µm.

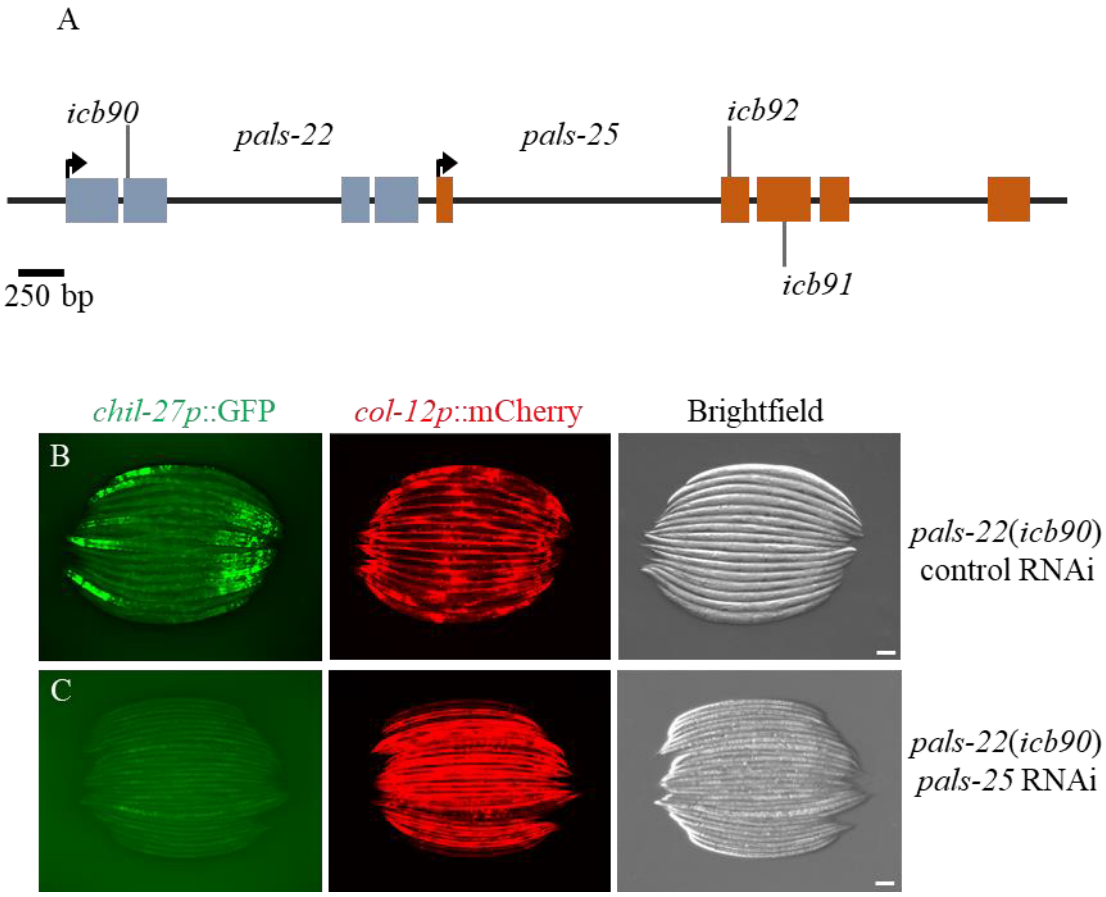

Figure 6.7: *pals-25* is required for the constitutive *chil-27* expression exhibited by the *pals-22* mutants. (A) A schematic cartoon showing the *pals-22* and *pals-25* gene structure, as well as the locations of the *pals-25* alleles isolated in a *pals-22*(*icb90*) mutant background. **(B-C)** The *pals-25* RNAi supresses the constitutive *chil-27* expression exhibited by the *pals-22* mutants. (B) *pals-22* mutants treated with the control RNAi. (C) *pals-22* mutants treated with the *pals-25* RNAi. The results are representative of at least three independent experiments. Scale bars represent 100µm.

6.2.3. *pals-25* acts as a positive transcriptional regulator of *chil-27* expression.

Next, we examined if the attenuation of *pals-25* in the *pals-22* mutant background had broader implications, such as if it also affected the enhanced immunity phenotype exhibited by the *pals-22* null mutants. To this end, we examined one of the alleles, and found that the *pals-22*(*icb90*)*pals-25*(*icb91*) mutants, exhibited a comparable level of resistance to *M. humicola* infection as the wild-type animals, a phenotype significantly different to the *pals-22*(*icb90*) mutants (Figure 6.8A and B). We also found analogous results when examining pathogen attachment events (Figure 6.8C) and consequences to development (Figure 6.8D). In summary, we concluded that the *pals-25* gene plays a role inverse to that of *pals-22*, and acts as a positive regulator of *chil-27* expression and immunity.

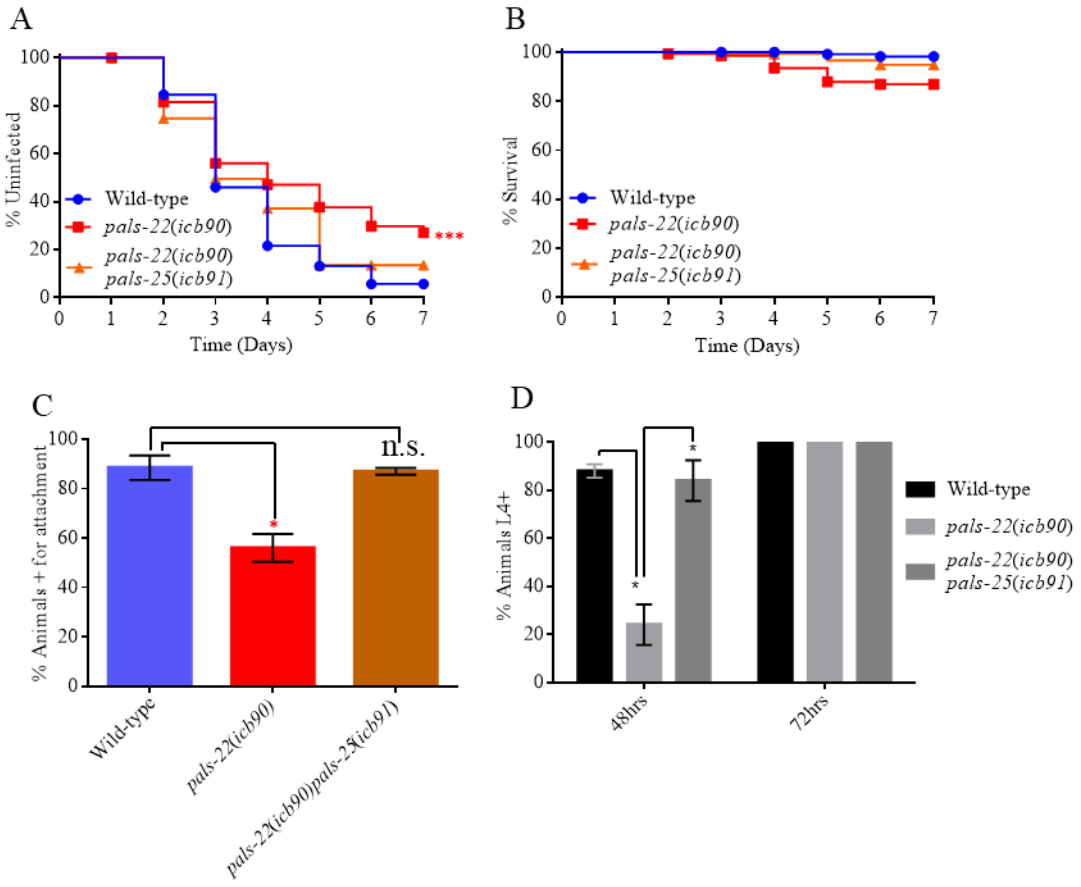

Figure 6.8: The loss of *pals-25* supresses the *pals-22* null mutant phenotypes. (A-B) Infection assay to examine the sensitivity of the *pals-22*(*icb90*)*pals-25*(*icb91*) mutants to *M. humicola* infection. (A) The *pals-22*(*icb90*)*pals-25*(*icb91*) mutants display similar sensitivity to *M. humicola* infection as the wild-type animals, but exhibit increased susceptibility when compared to the *pals-22*(*icb90*) mutants. (B) The *pals-22*(*icb90*)*pals-25*(*icb91*) mutants maintained on OP50 only survived at a comparable rate to the wild-type and *pals-22*(*icb90*) animals. The data shown is representative of three technical replicates (N=150 animals per curve) and at least two independent experiments. The statistical analysis was performed using the log-rank analysis (*** $p<0.001$). **(C)** The quantification of oomycete attachment events for the *pals-22*(*icb90*)*pals-25*(*icb91*), *pals-22*(*icb90*) and wild-type animals. The *pals-22*(*icb90*)*pals-25*(*icb91*) mutants display no difference in attachment events compared to the wild-type animals, a reversal of the *pals-22*(*icb90*) phenotype ($p<0.05$). The data shown is

representative of two technical replicates and two experimental repeats, and is shown as a mean frequency ± standard error of the proportion, n>100 animals. The statistical analysis was performed using the T-test (* $p<0.05$). **(D)** The percentage of animals reaching the fourth larval stage (L4) 48 and 72hrs after egg laying. The *pals-22*(*icb90*)*pals-25*(*icb91*) mutants develop at a comparable rate to the wild-type, this is in contrast to the *pals-22*(*icb90*) mutants that display delayed development. The data shown is representative of two technical replicates, n=50. The error bars represent standard deviation. The statistical analysis was performed using the T-test (* $p<0.05$).

In support of our conclusions, we independently isolated allele *icb98* a mutant constitutively expressing the *chil-27p::*GFP reporter. Intriguingly, upon whole genome sequencing, the allele *icb98* was found to harbour a stop codon (Q293STOP), just 40 base pairs before the native stop codon of *pals-25* (Figure 6.9A). With the understanding that *pals-25* acts downstream of *pal-22*, and the knock-down of *pals-25* in wild-type animals using RNAi does not affect *chil-27* expression, we reasoned that this most likely indicated a gain-of-function mutation. As predicted, *pals-25* RNAi completely abolished the GFP expression observed in *icb98* animals (Figures 6.9B-E). Considering that unrepressed *pals-25* acts as a positive regulator to induce the expression of *chil-27*, and enhance immunity in a *pals-22* null background, we next examined the sensitivity of *pals-25*(*icb98*) mutants to infection, and characterised other phenotypes associated with unrepressed *pals-25*. We found that the *pals-25*(*icb98*) mutants, exhibited increased resistance to *M. humicola* infection compared to the wild-type N2, but modest in comparison to the *pals-22* loss-of-function mutants (Figures 6.10A and B). In addition, the *pals-25*(*icb98*) mutants did not display any differences in *M. humicola* attachment events or delays in development when compared to the wild-type (Figures 6.10C and D). Based on these results, and the fact that only a quarter of the offspring, from a cross between *pals-25*(*icb98*) mutants and wild-type animals harbouring the *chil-27* reporter were GFP+, we reasoned that *pals-25*(*icb98*) most likely represented a recessive, weak gain-of-function mutation.

Considering that *pals-25* is required to activate the expression of *chil-27* in a *pals-22* loss-of-function mutant background, we wondered if these mutants could still induce *chil-27* when exposed to *M. humicola*, an external stimuli. To answer this question, we exposed the *pals-22*(*icb90*)*pals-25*(*icb91*) and *pals-22*(*icb90*)*pals-25*(*icb92*) mutants to the oomycete, and examined for the activation of the GFP transgene. Interestingly, we found that these mutants displayed comparable levels of expression to that of the wild-type animals (Figure 6.11). This

indicated that the antagonistic paralogs regulate *chil-27* expression independent, or in parallel to *C. elegans* pathogen detection “machinery”.

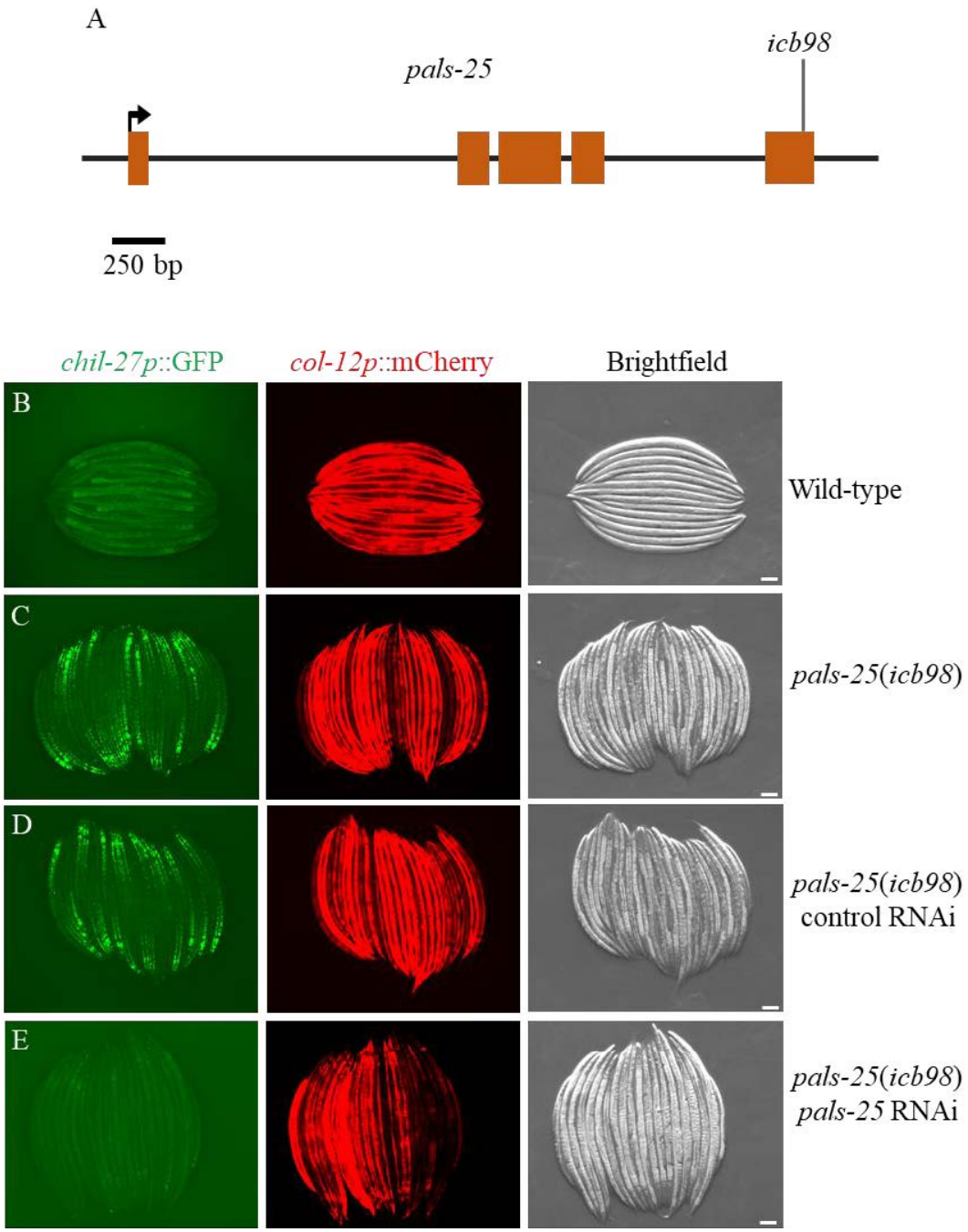

Figure 6.9: *pals-25* is a positive transcriptional regulator of *chil-27* expression. **(A)** A schematic cartoon showing the *pals-25* gene structure, and location of the *pals-25*(*icb98*) allele. **(B-C)** The isolation of a mutant constitutively expressing the *chil-27p*::GFP reporter. The panels show (B) wild-type and (C) *pals-25*(*icb98*) animals. The transgenic animals also carry a naturally constitutively expressing *col-12p*::mCherry transcriptional reporter as the co-injection marker. **(D-E)** *pals-25*(*icb98*) is a gain-of-function mutation. The *pals-25* RNAi

supresses the constitutive expression of *chil-27* in *pals-25*(*icb98*) mutants. (D) *pals-25* mutants treated with the control RNAi. (E) *pals-25* mutants treated with the *pals-25* RNAi. The results are representative of at least three independent experiments. Scale bars represent 100μm.

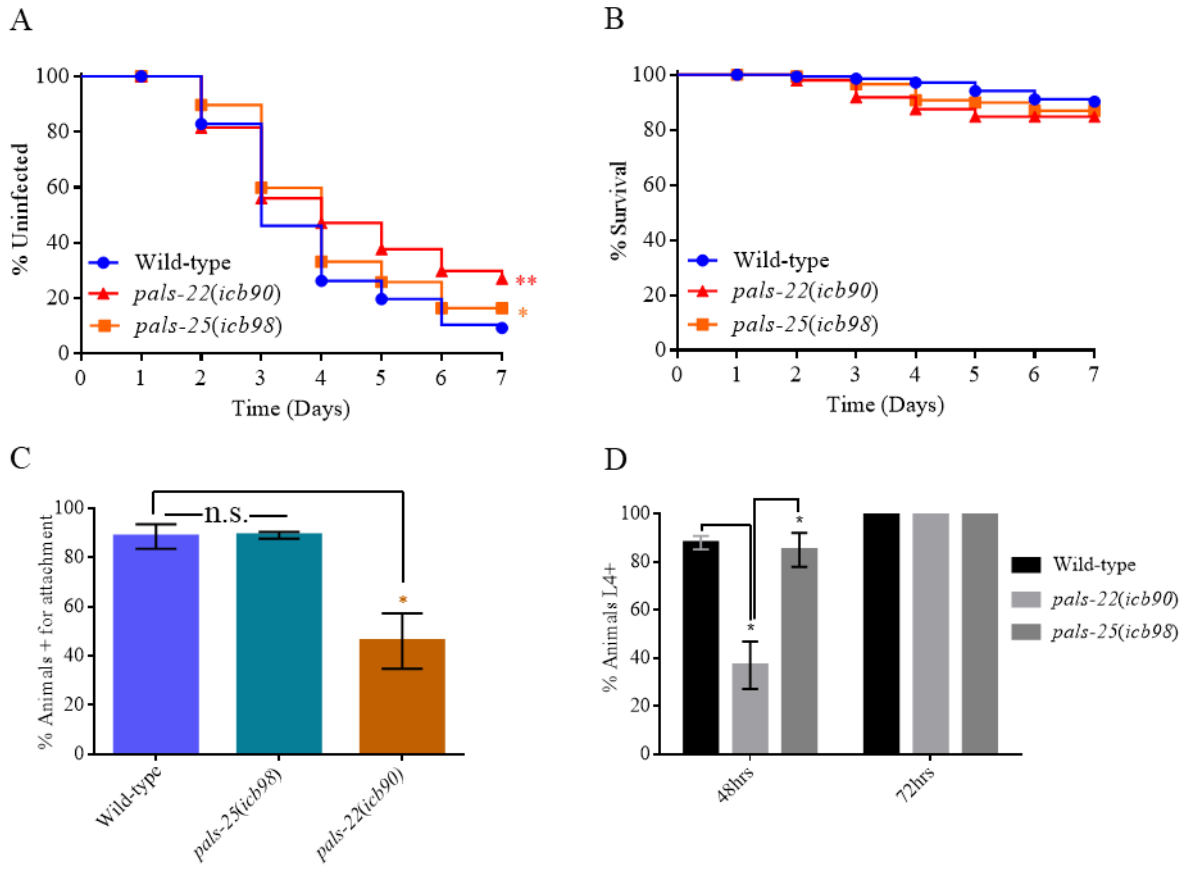

Figure 6.10: The *pals-25*(*icb98*) mutants exhibit modest phenotypes compared to the *pals-22* null mutants. (A-B) Infection assay to examine the sensitivity of the *pals-25*(*icb98*) mutants to *M. humicola* infection. (A) The *pals-25*(*icb98*) mutants display increased resistance against *M. humicola* infection compared to the wild-type nematodes, although this phenotype is modest when compared to the *pals-22*(*icb90*) mutants. (B) The *pals-22*(*icb90*) and *pals-25*(*icb98*) mutants maintained on OP50 only survived at comparable rates to the wild-type animals. The data shown is representative of three technical replicates (N=150 animals per curve) and at least two independent experiments. The statistical analysis was performed using the log-rank analysis (** $p<0.01$, * $p<0.05$). **(C)** The quantification of oomycete attachment events for the *pals-25*(*icb98*), *pals-22*(*icb90*) and wild-type animals. The *pals-25*(*icb98*) mutants displayed no difference in attachment events compared to the wild-type, a contrasting phenotype to the *pals-22*(*icb90*) mutants ($p<0.05$). The data shown is representative of two

technical replicates and two independent experiments. The data is presented as a mean frequency ± standard error of the proportion, n>100 animals. The statistical analysis was performed using the T-test (* $p<0.05$). **(D)** The percentage of animals reaching the fourth larval stage (L4) 48 and 72hrs after egg laying. The *pals-25*(*icb98*) mutants developed at a comparable rate to that of the wild-type nematodes, this is in contrast to the *pals-22*(*icb90*) animals that display delayed development. The data shown is representative of two technical replicates, n=50. The error bars represent standard deviation. The statistical analysis was performed using the T-test (* $p<0.05$).

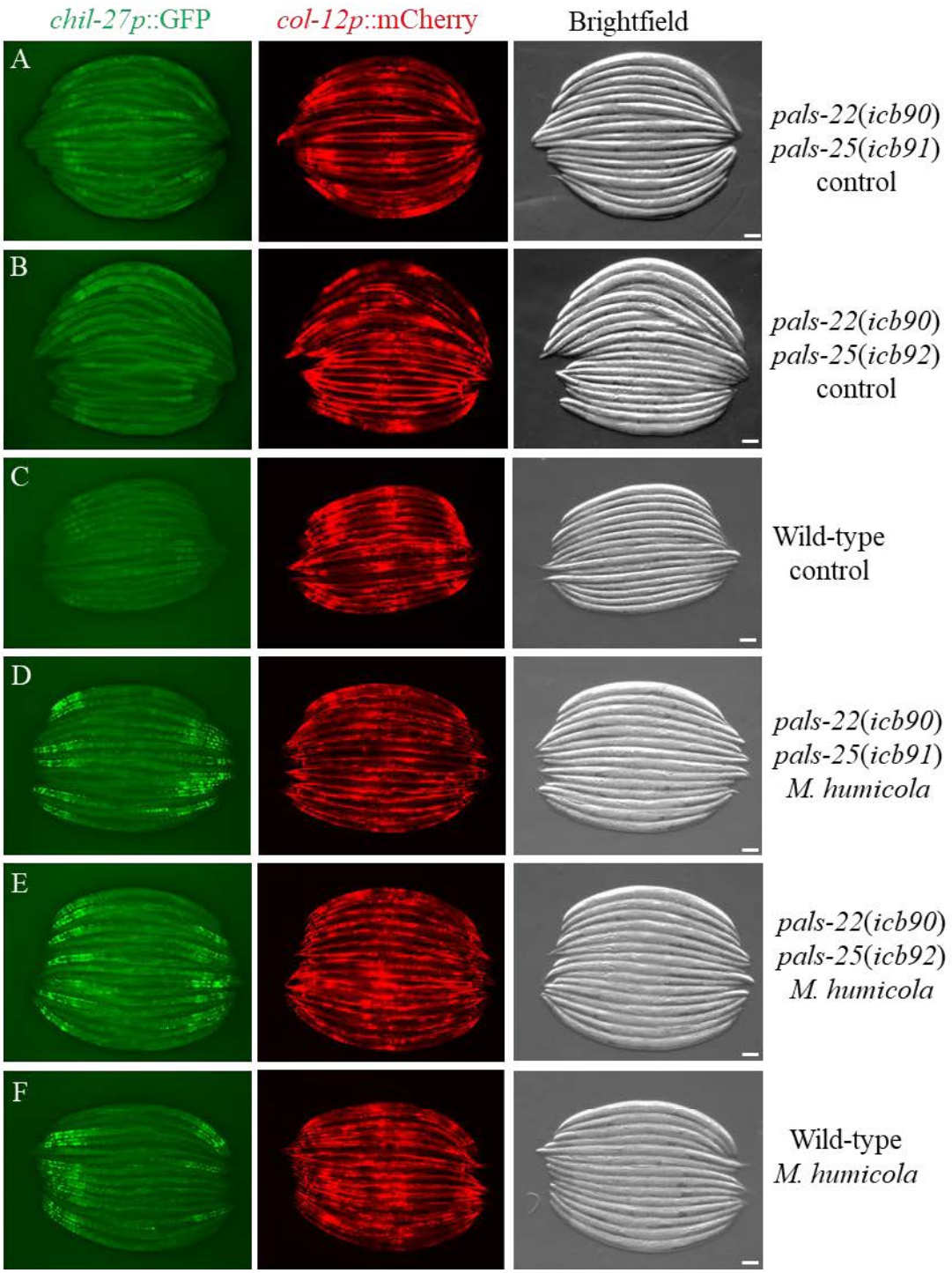

Figure 6.11: Mutants with abrogated *pal-22* and *pal-25* genes can still induce *chil-27* when exposed to the oomycete. (A-F) The *pals-22*(*icb90*)*pals-25*(*icb91*) and *pals-22*(*icb90*)*pals-25*(*icb92*) mutants can induce the expression of *chil-27* when exposed to *M. humicola.* The panels show (A) *pals-22*(*icb90*)*pals-25*(*icb91*), (B) *pals-22*(*icb90*)*pals-25*(*icb92*) and (C) wild-type animals treated with control conditions, and the panels (D) *pals-22*(*icb90*)*pals-25*(*icb91*),

(E) *pals-22*(*icb90*)*pals-25*(*icb92*) and (F) wild-type show animals exposed to the oomycete. The data shown is representative of at least three independent experiments. The transgenic animals also carry a naturally constitutively expressing *col-12p*::mCherry transcriptional reporter as the co-injection marker. Scale bars represent 100μm.

6.3. Discussion.

6.3.1. *pals-22* is a negative transcriptional regulator of *chil-27*.

pals-22 is part of a large family of genes whose functions are poorly understood. Intriguingly, the *pals* genes have previously been reported to be induced by a range of pathogens and abiotic stresses (Bakowski et al., 2014; Chen et al., 2017). Recently, through two independent mutagenesis studies, the novel *pals-22* gene has also been implicated in playing a role in small RNA-dependent transgene silencing (Leyva-Díaz et al., 2017), regulating thermotolerance and promoting proteostasis in *C. elegans* (Reddy et al., 2017).

We show here, through a forward genetic approach, *pals-22* also transcriptionally regulates the expression of the hypodermal effector gene *chil-27*, a member of a *C. elegans* family of resistance genes that are induced to antagonise *M. humicola* infection. We reason that the *M. humicola* infection resistance phenotype, can most likely be attributed to more than just the induction of the *chil* genes, as the *pals-22* mutants have also been shown to possess increased resistance against *P. aeruginosa* infection (Reddy et al., 2019). Additionally, as *M. humicola* and *P. aeruginosa* display quite divergent routes of infection, and initial sites of tissue tropism, we postulate that the mutants most likely exhibit "pan-microbial" resistance, a phenotype that can be ascribed to the broad, general change in the genes expressed and the transcriptional programs initiated.

The resistance phenotype was also accompanied with severe developmental delay, a trait recently reported for other *pals-22* null alleles (Leyva-Díaz et al., 2017; Reddy et al., 2017). Conceivably, this could be attributed to the constitutive induction of genes that are normally tightly regulated, or not expressed under standard conditions. As a consequence, resources normally allocated for development and other fundamental physiological tasks, are diverted to costly immune processes, and are thus rendered unavailable. This phenomena, a

trade-off between acquiring immunocompetence and developing normally, the need to prioritise defense over growth, has often been observed in organisms facing external pressures, such as pathogens in conditions where resource availability is limited (Greer, 2008; Hoi-Leitner et al., 2001; Lochmiller et al., 1993; Moret and Schmid-Hempel, 2000; Rantala and Roff, 2005).

6.3.2. *pals-25* is an antagonistic paralog of *pals-22*.

To understand how *pals-22* may regulate the expression of *chil-27*, we performed mutagenesis screens in a *pals-22* mutant background. By using the constitutive expression of the GFP reporter as a readout, we were able to isolate mutations suppressing the *pals-22* null allele phenotypes. Intriguingly, we found that the *pals-25* gene, a paralog of *pals-22*, was required for the *pals-22* loss-of-function phenotypes. Taken together with the fact that *pals-25* RNAi fails to induce *chil-27* expression in a wild-type background, we concluded that the *pals-25* gene is a positive regulator of *chil-27*, playing a role inverse to that of *pals-22*. A conclusion that was further supported, by the independent isolation of a weak gain-of-function *pals-25* mutant, a mutant that exhibited increased resistance to *M. humicola* infection compared to N2, but a reduced, significantly lower level when compared to the *pals-22* mutants.

Interestingly, the *pals-22*/*pals-25* paralogs, have also recently been independently discovered to regulate, the expression of genes induced by the intracellular microsporidia pathogen *N. parisii* (Reddy et al., 2019). Therefore, *pals-22*/*pals-25* appear to play a broad role in regulating resistance against a range of biotic threats. How might the antagonistic paralogs interact to regulate *chil-27* transcription? We have shown that *pals-25* is genetically downstream of *pals-22*, as *pals-22* loss-of-function mutations seem to have no obvious phenotypes in a *pals-25* null background. Furthermore, Reddy et al., 2019 have shown that the loss of *pals-22* had no effect on *pals-25* mRNA levels and vice versa. Thus, given these genetic

results, we propose that the antagonistic paralogs interact by way of their respective proteins (see Figure 6.12): PALS-22 and PALS-25 interact directly or perhaps indirectly as part of a complex, and under normal conditions, PALS-22 represses the activity of PALS-25. This theory appears likely, especially as we have isolated a *pals-25* gain-of-function mutant that harbours an early stop mutation, just 40 base pairs upstream of the original stop codon. This mutation may alter the ability of PALS-25 to interact with PALS-22, which in turn reduces or completely abrogates its repression. Nonetheless, these are purely speculations and further experimentation would be needed to prove or disprove these theories. In summary, this chapter discusses, the discovery of a new *C. elegans* specific mechanism that regulates immunity and growth, governed by novel antagonistic paralogs.

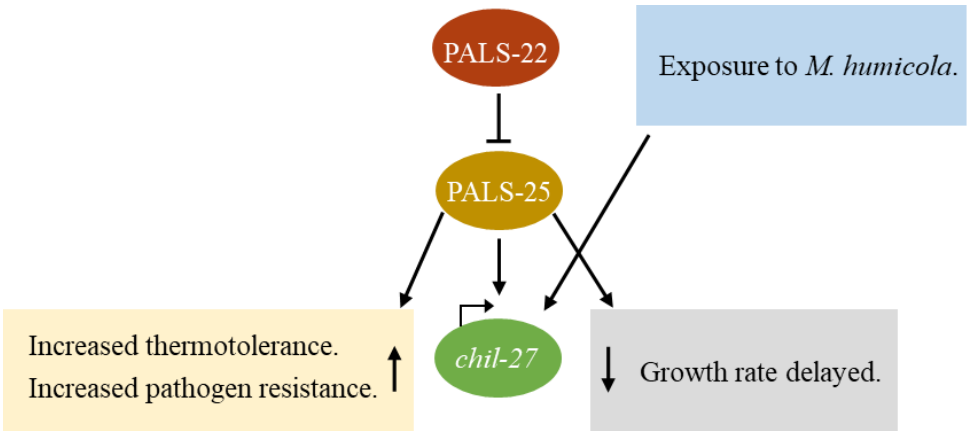

Figure 6.12: A proposed model to explain how *pals-22* and *pals*-25 transcriptionally regulate *chil-27* expression. Under normal conditions, PALS-22 represses the activity of PALS-25, but under stress conditions or as a consequence of no PALS-25 suppression, we observe a broad change in host gene expression. This change ultimately results in the expression of immunity related genes, including *chil-27*, and the retardation of growth. Under standard conditions, only the presence of the oomycete induces the expression of *chil-27*.

Chapter 7. Conclusions and future directions

7.1. Conclusions and future directions.

In this thesis, we have described the establishment of a new animal-oomycete pathosystem. We show that the *M. humicola* infection in *C. elegans* is both reproducible and robust, indicating a viable infection system. Furthermore, our pathosystem does not exhibit the same limitations described for other animal-oomycete model systems, as *C. elegans* is a genetically amenable, well developed model organism, with a wealth of molecular tools available to study gene function. Additionally, we have also developed a range of tools to investigate the oomycete-host interactions, including an infection assay and FISH staining for easy visualisation of the pathogen. Undoubtedly, in the future, these tools, may help us to answer such fundamental questions about the host-pathogen interaction as, what are the main virulence factors utilised by *M. humicola* to infect *C. elegans*? The work herein this thesis, presents detailed insights into a novel infection process with distinct etiology, and contributes to delineating further components of the *C. elegans* immune system.

By profiling the hosts transcriptional response to *M. humicola*, we were able to discover a new class of *C. elegans* resistance genes, the *chitinase-like* (*chil*) genes. Intriguingly, the *chil* genes appear to be induced in response to pathogen detection rather than as a consequence of infection. Through attachment assays, we were able to deduce that the *chil* genes antagonise pathogen attachment. Furthermore, we have shown that CHIL-27 is expressed in a manner reminiscent to structures of the cuticle. Thus, an outstanding question is, how exactly do the *chil* genes antagonise *M. humicola* attachment? Could CHIL proteins bind components of the cuticle to hinder the pathogens ability to attach? To determine the CHIL proteins mode of action, we propose to use the CHIL-27 translation reporter to perform 1) co-localisation studies with markers that target components of the cuticle, such as collagen, in order to resolve CHIL-27 protein site of expression, and 2) GFP immunoprecipitation to discover physical interactors of CHIL-27. Of course, initially, we would verify that the translational reporter accurately

depicts CHIL-27 expression and function, by observing if the reporter could rescue the *chil-27* CRISPR mutants, increased *M. humicola* infection susceptibility phenotype.

During our studies to characterise *chil* gene transcriptional expression, we determined that the p38 MAPK pathway and the GATA transcription factor ELT-3, both previously reported to regulate components of the *C. elegans* inducible immune response, also regulate *chil-27* induction. Accordingly, it would be prudent to examine if other *chil* genes are also controlled by these regulators. To accomplish this goal, we would use qRT-PCR to measure changes in *chil* gene expression in the mutant strains, and compare to wild-type animals post exposure to the oomycete. This method will allow us to circumvent the necessity to produce other *chil* gene transcriptional reporters, as well as the need to generate transgenic animals. Furthermore, by using a strong loss-of-function allele, we have shown that the *daf-6* gene is important for normal *chil-27* expression, and indirectly, we speculated that this indicated the requirement for normal amphid morphology. To confirm or dismiss our suppositions, we would initially perform laser or genetic ablation studies targeting the amphids, these experiments could help us to determine conclusively if the amphid chemosensory neurons are used for the detection of *M. humicola*. Afterwards, depending on our results, we would then determine if a subset of the chemosensory neurons are required, this would be accomplished by the tissue specific expression of *daf-6* in *daf-6*(*e1377*) mutants harbouring the *chil-27* transcriptional reporter.

In addition, by performing multiple mutagenesis screens, we discovered a unique mechanism that regulates immunity and growth involving novel antagonistic paralogs. In this interaction, *pals-22* negatively regulates the expression of immunity related genes, and inversely, *pals-25* acts as a positive regulator. Future experimental objectives based on this work, will aim to characterise the precise nature of the interaction between *pals-22* and *pals-25*. Firstly, we would further validate our conclusions, namely that mutations in *pals-22* and

pals-25 were the causative genes. We would accomplish this goal by either rescuing the mutants with wild-type copies of the respective target genes, or we would utilise CRISPR to introduce the respective mutations into wild-type animals, and examine the resulting phenotypes. Subsequently, we would then study how the *pals-22* and *pals-25* genes ultimately regulate the induction of *chil-27*. We would initially aim to target *pals-22* or *pals-25* in specific tissues e.g. the hypodermis, intestine and neurons, as both *pals-22* and *pals-25* are broadly expressed in most tissue types (Reddy et al., 2017, 2019). To accomplish this goal, we would rescue the mutant animals with constructs comprised of tissue specific promoters fused to wild-type copies of the respective target genes. These experiments will help us to determine if the expression of either gene in a particular subset of tissues is required, or redundant for the induction or repression of *chil-27*. In complement to these experiments aimed at understanding *pals-22* and *pals-25* mode of action, and how they may interact, we would also perform immunoprecipitation experiments using the wild-type copies of the PAL-22 and PALS-25 proteins. These experiments will help us determine if they interact directly or as part of a complex. Considering an early stop mutation introduced 40bp before the native stop codon of the *pals-25* gene, resulted in a gain-of-function phenotype, we propose that PALS-25 most likely interacts with PALS-22 either directly or indirectly by way of its C-terminus domain.

In summary, by exploiting *M. humicola* and *C. elegans* natural interaction, we have established a novel and robust pathosystem to study oomycete infections in whole animals. Using this system, we have discovered novel physiological mechanisms required to confer *C. elegans* resistance against *M. humicola* infection, as well as a new mechanism regulating *C. elegans* immunity and development. The work in this thesis presents a new perspective on the biotic challenges that *C. elegans* encounters in its native habitat, and advocates for the use of natural pathogens with model organisms.

References

Aballay, A., Yorgey, P., and Ausubel, F.M. (2000). *Salmonella typhimurium* proliferates and establishes a persistent infection in the intestine of *Caenorhabditis elegans*. Curr. Biol. *10*, 1539–1542.

Alegado, R.A., and Tan, M.W. (2008). Resistance to antimicrobial peptides contributes to persistence of *Salmonella typhimurium* in the *C. elegans* intestine. Cell. Microbiol. *10*, 1259–1273.

Alper, S., McBride, S.J., Lackford, B., Freedman, J.H., and Schwartz, D.A. (2007). Specificity and complexity of the *Caenorhabditis elegans* innate immune response. Mol. Cell. Biol. *27*, 5544–5553.

Andrusiak, M.G., and Jin, Y. (2016). Context specificity of stress-activated mitogen-activated protein (MAP) kinase signaling: The story as told by *Caenorhabditis elegans*. J. Biol. Chem. *291*, 7796–7804.

Bakowski, M.A., Desjardins, C.A., Smelkinson, M.G., Dunbar, T.A., Lopez-Moyado, I.F., Rifkin, S.A., Cuomo, C.A., and Troemel, E.R. (2014). Ubiquitin-mediated response to microsporidia and virus infection in *C. elegans*. PLoS Pathog. *10*, e1004200.

Bargmann, C.I., and Avery, L. (1995). Laser killing of cells in *Caenorhabditis elegans*. Methods. Cell. Biol. *48*, 225–250.

Bargmann, C.I., Hartwieg, E., and Horvitz, H.R. (1993). Odorant-selective genes and neurons mediate olfaction in *C. elegans*. Cell. *74*, 515–527.

Barrière, A., and Félix, M.A. (2005). High local genetic diversity and low outcrossing rate in *Caenorhabditis elegans* natural populations. Curr. Biol. *5*, 1176–1184.

Barron, G.L. (1987). The gun cell of *Haptoglossa mirabilis*. Mycologia. *79*, 877–883.

Beale, E., Li, G., Tan, M.W., and Rumbaugh, K.P. (2006). *Caenorhabditis elegans* senses bacterial autoinducers. Appl. Environ. Microbiol. *72*, 5135–5137.

Belmonte, R., Wang, T., Duncan, G.J., Skaar, I., Mélida, H., Bulone, V., van West, P., and Secombes, C.J. (2014). Role of pathogen-derived cell wall carbohydrates and prostaglandin E2 in immune response and suppression of fish immunity by the oomycete *Saprolegnia parasitica*. Infect. Immun. *82*, 4518–4529.

Black, W. (1970). The nature and inheritance of field resistance to late blight (*Phytophthora infestans*) in potatoes. Am. Potato J. *47*, 279–288.

Boutros, M., and Ahringer, J. (2008). The art and design of genetic screens: RNA interference. Nat. Rev. Genet. *9*, 554–566.

Bozkurt, T.O., Schornack, S., Banfield, M.J., and Kamoun, S. (2012). Oomycetes, effectors, and all that jazz. Curr. Opin. Plant Biol. *15*, 483–492.

Brenner, S. (1974). The genetics of *Caenorhabditis*. Methods. *77*, 71–94.

Bussink, A.P., Speijer, D., Aerts, J.M.F.G., and Boot, R.G. (2007). Evolution of mammalian chitinase(-like) members of family 18 glycosyl hydrolases. Genetics. *177*, 959–970.

Cavalier-Smith, T., and Chao, E.E.Y. (2006). Phylogeny and megasystematics of phagotrophic heterokonts (kingdom Chromista). J. Mol. Evol. *62*, 388–420.

Chae, E., Tran, D.T.N., and Weigel, D. (2016). Cooperation and conflict in the plant immune system. PLoS Pathog. *12*, e1005452.

Chalfie, M., Tu, Y., Euskirchen, G., Ward, W.W., and Prasher, D.C. (1994). Green fluorescent protein as a marker for gene expression. Science. *263*, 802–805.

Chamy, L. El, Leclerc, V., Caldelari, I., and Reichhart, J.-M. (2008). Danger signal and PAMP sensing define binary signaling pathways upstream of Toll. Nat. Immunol. *9*, 1165–1170.

Chang, N.C.A., Hung, S.I., Hwa, K.Y., Kato, I., Chen, J.E., Liu, C.H., and Chang, A.C. (2001). A macrophage protein, Ym1, transiently expressed during inflammation is a novel mammalian lectin. J. Biol. Chem. *276*, 17497–17506.

Chen, C., Fenk, L.A., and De Bono, M. (2013). Efficient genome editing in *Caenorhabditis elegans* by CRISPR-targeted homologous recombination. Nucleic Acids Res. *41*, e193.

Chen, K., Franz, C.J., Jiang, H., Jiang, Y., and Wang, D. (2017). An evolutionarily conserved transcriptional response to viral infection in *Caenorhabditis* nematodes. BMC Genomics. *18*, doi:10.1186/s12864-017-3689-3.

Chisholm, A.D., and Hsiao, T.I. (2012). The *Caenorhabditis elegans* epidermis as a model skin. I: Development, patterning, and growth. Wiley Interdiscip. Rev. Dev. Biol. *1*, 861–878.

Chou, T.C., Chiu, H.C., Kuo, C.J., Wu, C.M., Syu, W.J., Chiu, W.T., and Chen, C.S. (2013). *Enterohaemorrhagic escherichia* coli O157:H7 Shiga-like toxin 1 is required for full pathogenicity and activation of the p38 mitogen-activated protein kinase pathway in *Caenorhabditis elegans*. Cell. Microbiol. *15*, 82–97.

Corsi, A.K. (2006). A biochemist's guide to *Caenorhabditis elegans*. Anal. Biochem. *359*, 1-17.

Craig, H.L., Wirtz, J., Bamps, S., Dolphin, C.T., and Hope, I.A. (2013). The significance of alternative transcripts for *Caenorhabditis elegans* transcription factor genes, based on expression pattern analysis. BMC Genomics. *14*, 249.

Darby, C., Hsu, J.W., Ghori, N., and Falkow, S. (2002). *Caenorhabditis elegans*: Plague

bacteria biofilm blocks food intake. Nature. *417*, 243–244.

Dick, M.W. (1969). Morphology and taxonomy of the oomycetes, with special reference to *Saprolegniaceae*, *Leptomitaceae* and *Pythiaceae*: I. Sexual reproduction. New Phytol. *68*, 751–775.

Doitsidou, M., Flames, N., Lee, A.C., Boyanov, A., and Hobert, O. (2008). Automated screening for mutants affecting dopaminergic-neuron specification in *C. elegans*. Nat. Methods. *5*, 869–872.

Dolphin, C.T., and Hope, I.A. (2006). *Caenorhabditis elegans* reporter fusion genes generated by seamless modification of large genomic DNA clones. Nucleic Acids Res. *34*, e72.

Dunbar, T.L., Yan, Z., Balla, K.M., Smelkinson, M.G., and Troemel, E.R. (2012). *C. elegans* detects pathogen-induced translational inhibition to activate immune signaling. Cell Host Microbe. *11*, 375–386.

Earle, G., and Hintz, W. (2014). New approaches for controlling *Saprolegnia parasitica*, the causal agent of a devastating fish disease. Trop. Life Sci. Res. *25*, 101–109.

Engelmann, I., Griffon, A., Tichit, L., Montañana-Sanchis, F., Wang, G., Reinke, V., Waterston, R.H., Hillier, L.D.W., and Ewbank, J.J. (2011). A comprehensive analysis of gene expression changes provoked by bacterial and fungal infection in *C. elegans*. PLoS One. *6*, e19055.

Essmann, C.L., Elmi, M., Shaw, M., Anand, G.M., Pawar, V.M., and Srinivasan, M.A. (2017). In-vivo high resolution AFM topographic imaging of *Caenorhabditis elegans* reveals previously unreported surface structures of cuticle mutants. Nanomedicine Nanotechnology, Biol. Med. *13*, 183–189.

Feinbaum, R.L., Urbach, J.M., Liberati, N.T., Djonovic, S., Adonizio, A., Carvunis, A.-R., and Ausubel, F.M. (2012). Genome-wide identification of *Pseudomonas aeruginosa* virulence-related genes using a *Caenorhabditis elegans* infection model. PLoS Pathog. *8*, e1002813.

Félix, M.A., and Braendle, C. (2010). The natural history of *Caenorhabditis elegans*. Curr. Biol. *20*, R965–R969.

Félix, M.A., Ashe, A., Piffaretti, J., Wu, G., Nuez, I., Bélicard, T., Jiang, Y., Zhao, G., Franz, C.J., Goldstein, L.D., et al. (2011). Natural and experimental infection of *Caenorhabditis* nematodes by novel viruses related to nodaviruses. PLoS Biol. *9*, e1000586.

Finn, R.D., Attwood, T.K., Babbitt, P.C., Bateman, A., Bork, P., Bridge, A.J., Chang, H.Y., Dosztanyi, Z., El-Gebali, S., Fraser, M., et al. (2017). InterPro in 2017-beyond protein family and domain annotations. Nucleic Acids Res. *45*, D190–D199.

Fire, A., Harrison, S.W., and Dixon, D. (1990). A modular set of lacZ fusion vectors for studying gene expression in *Caenorhabditis elegans*. Gene. *93*, 189–198.

Fire, A., Xu, S., Montgomery, M.K., Kostas, S.A., Driver, S.E., and Mello, C.C. (1998). Potent and specific genetic interference by double-stranded RNA in *Caenorhabditis elegans*. Nature. *391*, 806–811.

Friedland, A.E., Tzur, Y.B., Esvelt, K.M., Colaiácovo, M.P., Church, G.M., and Calarco, J.A. (2013). Heritable genome editing in *C. elegans* via a CRISPR-Cas9 system. Nat. Methods. *10*, 741–743.

Frøkjær-Jensen, C., Davis, M.W., Ailion, M., and Jorgensen, E.M. (2012). Improved Mos1-mediated transgenesis in *C. elegans*. Nat. Methods. *9*, 117–118.

Fujimoto, D., and Kanaya, S. (1973). Cuticlin: A noncollagen structural protein from *Ascaris*

cuticle. Arch. Biochem. Biophys. *157*, 1–6.

Funkhouser, J.D., and Aronson, N.N. (2007). Chitinase family GH18: Evolutionary insights from the genomic history of a diverse protein family. BMC Evol. Biol. *7*, doi:10.1186/1471-2148-7-96.

Gaastra, W., Lipman, L.J.A., De Cock, A.W.A.M., Exel, T.K., Pegge, R.B.G., Scheurwater, J., Vilela, R., and Mendoza, L. (2010). *Pythium insidiosum*: An overview. Vet. Microbiol. *146*, 1–16.

Garsin, D.A., Sifri, C.D., Mylonakis, E., Qin, X., Singh, K. V., Murray, B.E., Calderwood, S.B., and Ausubel, F.M. (2002). A simple model host for identifying Gram-positive virulence factors. Proc. Natl. Acad. Sci. *98*, 10892–10897.

Gilleard, J.S., Shafi, Y., Barry, J.D., and McGhee, J.D. (1999). ELT-3: A *Caenorhabditis elegans* GATA factor expressed in the embryonic epidermis during morphogenesis. Dev. Biol. *208*, 265–280.

Glockling, S.L., and Beakes, G.W. (2000). A review of the taxonomy, biology and infection strategies of "biflagellate holocarpic" parasites of nematodes. Fungal Divers. *4*, 1–20.

Glockling, S.L., and Beakes, G.W. (2008). An ultrastructural study of development and reproduction in the nematode parasite *Myzocytiopsis vermicola*. Mycologia. *98*, 1–15.

Golden, J.W., and Riddle, D.L. (1982). A pheromone influences larval development in the nematode *Caenorhabditis elegans*. Science. *218*, 578–580.

Gravato-Nobre, M.J., and Hodgkin, J. (2005). *Caenorhabditis elegans* as a model for innate immunity to pathogens. Cell. Microbiol. *7*, 741–751.

Greer, A.W. (2008). Trade-offs and benefits: Implications of promoting a strong immunity to gastrointestinal parasites in sheep. Parasite Immunol. *30*, 123–132.

Hadano, S., Hand, C.K., Osuga, H., Yanagisawa, Y., Otomo, A., Devon, R.S., Miyamoto, N., Showguchi-Miyata, J., Okada, Y., Singaraja, R., et al. (2001). A gene encoding a putative GTPase regulator is mutated in familial amyotrophic lateral sclerosis 2. Nat. Genet. *29*, 166–173.

Hakariya, M., Masuyama, N., and Saikawa, M. (2002). Shooting of sporidium by "gun" cells in *Haptoglossa heterospora* and *H. zoospora* and secondary zoospore formation in *H. zoospora*. Mycoscience. *43*, 119–125.

Halaschek-Wiener, J., Khattra, J.S., McKay, S., Pouzyrev, A., Stott, J.M., Yang, G.S., Holt, R.A., Jones, S.J.M., Marra, M.A., Brooks-Wilson, A.R., et al. (2005). Analysis of long-lived *C. elegans daf-2* mutants using serial analysis of gene expression. Genome Res. *15*, 603–615.

Hengartner, M.O., Ellis, R., and Horvitz, H.R. (1992). *Caenorhabditis elegans* gene *ced-9* protects cells from programmed cell death. Nature. *356*, 494–499.

Hentati, A., Bejaoui, K., Pericak-Vance, M.A., Hentati, F., Speer, M.C., Hung, W.Y., Figlewicz, D.A., Haines, J., Rimmler, J., Hamida, C. Ben, et al. (1994). Linkage of recessive familial amyotrophic lateral sclerosis to chromosome 2q33–q35. Nat. Genet. *7*, 425–428.

Hesp, K., Smant, G., and Kammenga, J.E. (2015). *Caenorhabditis elegans* DAF-16/FOXO transcription factor and its mammalian homologs associate with age-related disease. Exp. Gerontol. *72*, 1–7.

Hobert, O. (2002). PCR fusion-based approach to create reporter gene constructs for expression analysis in transgenic *C. elegans*. Biotechniques. *32*, 728–730.

Hodgkin, J., Kuwabara, P.E., and Corneliussen, B. (2000). A novel bacterial pathogen, *Microbacterium nematophilum*, induces morphological change in the nematode *C. elegans*. Curr. Biol. *10*, 1615–1618.

Hoi-Leitner, M., Romero-Pujante, M., Hoi, H., and Pavlova, A. (2001). Food availability and immune capacity in serin (*Serinus serinus*) nestlings. Behav. Ecol. Sociobiol. *49*, 333–339.

Houston, D.R., Recklies, A.D., Krupa, J.C., and Van Aalten, D.M.F. (2003). Structure and ligand-induced conformational change of the 39-kDa glycoprotein from human articular chondrocytes. J. Biol. Chem. *278*, 30206–30212.

Inoue, H., Hisamoto, N., Jae, H.A., Oliveira, R.P., Nishida, E., Blackwell, T.K., and Matsumoto, K. (2005). The *C. elegans* p38 MAPK pathway regulates nuclear localization of the transcription factor SKN-1 in oxidative stress response. Genes Dev. *19*, 2278–2283.

Irazoqui, J.E., Troemel, E.R., Feinbaum, R.L., Luhachack, L.G., Cezairliyan, B.O., and Ausubel, F.M. (2010a). Distinct pathogenesis and host responses during infection of *C. elegans* by *P. aeruginosa* and *S. aureus*. PLoS Pathog. *6*, 1–24.

Irazoqui, J.E., Urbach, J.M., and Ausubel, F.M. (2010b). Evolution of host innate defence: Insights from *Caenorhabditis elegans* and primitive invertebrates. Nat. Rev. Immunol. *10*, 47–58.

Jansson, H.B. (1994). Adhesion of Conidia of *Drechmeria coniospora* to *Caenorhabditis elegans* wild type and mutants. J. Nematol. *26*, 430–435.

Jeong, P.Y., Jung, M., Yim, Y.H., Kim, H., Park, M., Hong, E., Lee, W., Kim, Y.H., Kim, K., and Paik, Y.K. (2005). Chemical structure and biological activity of the *Caenorhabditis elegans* dauer-inducing pheromone. Nature. *433*, 541–545.

Johnstone, I.L. (1994). The cuticle of the nematode *Caenorhabditis elegans*: A complex collagen structure. BioEssays. *16*, 171–178.

Johnstone, I.L. (2000). Cuticle collagen genes expression in *Caenorhabditis elegans*. Trends Genet. *16*, 21–27.

Johnstone, I.L., and Barry, J.D. (1996). Temporal reiteration of a precise gene expression pattern during nematode development. EMBO J. *15*, 3633–3639.

Kabir, M.A., and Hussain, M.A. (2009). Human fungal pathogen *Candida albicans* in the postgenomic era: An overview. Expert Rev. Anti. Infect. Ther. *7*, 121–134.

Kamoun, S. (2003). Molecular genetics of pathogenic oomycetes. Eukaryot. Cell. *2*, 191–199.

Keoprasom, N., Chularojanamontri, L., Chayakulkeeree, M., Chaiprasert, A., Wanachiwanawin, W., and Ruangsetakit, C. (2013). Vascular pythiosis in a thalassemic patient presenting as bilateral leg ulcers. Med. Mycol. Case Rep. *2*, 25–28.

Kerry, S., TeKippe, M., Gaddis, N.C., and Aballay, A. (2006). GATA transcription factor required for immunity to bacterial and fungal pathogens. PLoS One. *1*, e77.

Kim, D. (2008). Studying host-pathogen interactions and innate immunity in *Caenorhabditis elegans*. DMM Dis. Model. Mech. *1*, 205–208.

Kim, D.H., Feinbaum, R., Alloing, G., Emerson, F.E., Garsin, D.A., Inoue, H., Tanaka-Hino, M., Hisamoto, N., Hatsumoto, K., Tan, M.W., et al. (2002). A conserved p38 MAP kinase pathway in *Caenorhabditis elegans* innate immunity. Science. *297*, 623–626.

Kimura, K.D., Tissenbaum, H.A., Liu, Y., and Ruvkun, G. (1997). *daf-2*, an insulin receptor-like gene that regulates longevity and diapause in *Caenorhabditis elegans*. Science. *277*, 942–946.

Kiontke, K., and Sudhaus, W. (2006). Ecology of *Caenorhabditis* species. Wormbook. 1-14.

Kutscher, L.M., and Shaham, S. (2014). Forward and reverse mutagenesis in *C. elegans*. Wormbook. 1-26.

Kzhyshkowska, J., Gratchev, A., and Goerdt, S. (2007). Human chitinases and chitinase-like proteins as indicators for inflammation and cancer. Biomark. Insights. *2*, 128–146.

L. Barron, G., and G. Percy, J. (2011). Nematophagous fungi: a new *Myzocytium*. Can. J. Bot. *53*, 1306–1309.

Langmead, B., and Salzberg, S.L. (2012). Fast gapped-read alignment with Bowtie 2. Nat. Methods. *9*, 357–359.

Lee, C.G. (2009). Chitin, chitinases and chitinase-like proteins in allergic inflammation and tissue remodeling. Yonsei Med. J. *50*, 22–30.

Lee, C.G., Da Silva, C.A., Dela Cruz, C.S., Ahangari, F., Ma, B., Kang, M.-J., He, C.-H., Takyar, S., and Elias, J.A. (2011). Role of chitin and chitinase/chitinase-like proteins in inflammation, tissue remodeling, and injury. Annu. Rev. Physiol. *73*, 479–501.

Lévesque, C.A., and De Cock, A.W.A.M. (2004). Molecular phylogeny and taxonomy of the genus *Pythium*. Mycol. Res. *108*, 1363–1383.

Leyva-Díaz, E., Stefanakis, N., Carrera, I., Glenwinkel, L., Wang, G., Driscoll, M., and Hobert, O. (2017). Silencing of repetitive DNA is controlled by a member of an unusual *Caenorhabditis elegans* gene family. Genetics. *207*, 529–545.

Liberati, N.T., Fitzgerald, K.A., Kim, D.H., Feinbaum, R., Golenbock, D.T., and Ausubel, F.M. (2004). Requirement for a conserved Toll/interleukin-1 resistance domain protein in the *Caenorhabditis elegans* immune response. Proc. Natl. Acad. Sci. U. S. A. *101*, 6593–6598.

Litman, G.W., Rast, J.P., and Fugmann, S.D. (2010). The origins of vertebrate adaptive immunity. Nat. Rev. Immunol. *10*, 543–553.

Lochmiller, R.L., Vestey, M.R., and Boren, J.C. (1993). Relationship between protein nutritional status and immunocompetence in northern bobwhite chicks. Auk. *110*, 503–510.

Love, M.I., Huber, W., and Anders, S. (2014). Moderated estimation of fold change and dispersion for RNA-seq data with DESeq2. Genome Biol. *15*, 550.

Mallo, G. V., Kurz, C.L., Couillault, C., Pujol, N., Granjeaud, S., Kohara, Y., and Ewbank, J.J. (2002). Inducible antibacterial defense system in *C. elegans*. Curr. Biol. *12*, 1209–1214.

Matsuzawa, A., Saegusa, K., Noguchi, T., Sadamitsu, C., Nishitoh, H., Nagai, S., Koyasu, S., Matsumoto, K., Takeda, K., and Ichijo, H. (2005). ROS-dependent activation of the TRAF6-ASK1-p38 pathway is selectively required for TLR4-mediated innate immunity. Nat. Immunol. *6*, 587–592.

McEwan, D.L., Kirienko, N. V., and Ausubel, F.M. (2012). Host translational inhibition by *Pseudomonas aeruginosa* exotoxin A triggers an immune response in *Caenorhabditis elegans*. Cell Host Microbe. *11*, 364–374.

Meisel, J.D., and Kim, D.H. (2014). Behavioral avoidance of pathogenic bacteria by *Caenorhabditis elegans*. Trends Immunol. *35*, 465–470.

Mendoza, L., and Vilela, R. (2013). The mammalian pathogenic oomycetes. Curr. Fungal Infect. Rep. *7*, 198–208.

Millet, A.C.M., and Ewbank, J.J. (2004). Immunity in *Caenorhabditis elegans*. Curr. Opin. Immunol. *16*, 4–9.

Minevich, G., Park, D.S., Blankenberg, D., Poole, R.J., and Hobert, O. (2012). CloudMap: A cloud-based pipeline for analysis of mutant genome sequences. Genetics. *192*, 1249–1269.

Moerman, D.G., Baillie, D.L., Chaudhry, I., Taylor, J., Neil, S.E., Rogula, A., Zapf, R., Hirst, M., Butterfield, Y., Jones, S.J., et al. (1979). Genetic organization in *Caenorhabditis elegans*: fine-structure analysis of the *unc-22* gene. Genetics. *91*, 95–103.

Moret, Y., and Schmid-Hempel, P. (2000). Survival for immunity: The price of immune

system activation for bumblebee workers. Science. *290*, 1166–1168.

Nicholas, H.R., and Hodgkin, J. (2004). The ERK MAP kinase cascade mediates tail swelling and a protective response to rectal infection in *C. elegans*. Curr. Biol. *14*, 1256–1261.

Nowak, M.A., Boerlijst, M.C., Cooke, J., and Smith, J.M. (1997). Evolution of genetic redundancy. Nature. *388*, 167–170.

O'Rourke, D., Baban, D., Demidova, M., Mott, R., and Hodgkin, J. (2006). Genomic clusters, putative pathogen recognition molecules, and antimicrobial genes are induced by infection of *C. elegans* with *M. nematophilum*. Genome Res. *16*, 1005–1016.

Oikonomou, G., Perens, E.A., Lu, Y., Watanabe, S., Jorgensen, E.M., and Shaham, S. (2011). Opposing activities of LIT-1/NLK and DAF-6/patched-related direct sensory compartment morphogenesis in *C. elegans*. PLoS Biol. *9*, e1001121.

Osman, G.A., et al., (2018). Natural infection of *C. elegans* by an oomycete reveals a new pathogen-specific immune response. Curr. Biol. *28*, 640-648.e5.

Page, A.P., and Winter, A.D. (2003). Enzymes involved in the biogenesis of the nematode cuticle. Adv. Parasitol. *53*, 85–148.

Papp, D., Csermely, P., and Soti, C. (2012). A role for SKN-1/Nrf in pathogen resistance and immunosenescence in *Caenorhabditis elegans*. PLoS Pathog. *8*, e1002673.

Pellegrino, M.W., Nargund, A.M., Kirienko, N. V, Gillis, R., Fiorese, C.J., and Haynes, C.M. (2014). Mitochondrial UPR-regulated innate immunity provides resistance to pathogen infection. Nature. *516*, 414–417.

Perales, R., King, D.M., Aguirre-Chen, C., and Hammell, C.M. (2014). LIN-42, the *Caenorhabditis elegans* PERIOD homolog, negatively regulates microRNA transcription. PLoS Genet. *10*, e1004486.

Pesch, Y.Y., Riedel, D., Patil, K.R., Loch, G., and Behr, M. (2016). Chitinases and imaginal disc growth factors organize the extracellular matrix formation at barrier tissues in insects. Sci. Rep. *6*, doi:10.1038/srep1834.

Phillips, A.J., Anderson, V.L., Robertson, E.J., Secombes, C.J., and van West, P. (2008). New insights into animal pathogenic oomycetes. Trends Microbiol. *16*, 13–19.

Playfair, J.H. (1971). Cell cooperation in the immune response. Clin. Exp. Immunol. *8*, 839–856.

Politz, S.M., Philipp, M., Estevez, M., O'Brien, P.J., and Chin, K.J. (1990). Genes that can be mutated to unmask hidden antigenic determinants in the cuticle of the nematode *Caenorhabditis elegans*. Proc. Natl. Acad. Sci. U. S. A. *87*, 2901–2905.

Pradel, E., Zhang, Y., Pujol, N., Matsuyama, T., Bargmann, C.I., and Ewbank, J.J. (2007). Detection and avoidance of a natural product from the pathogenic bacterium *Serratia marcescens* by *Caenorhabditis elegans*. Proc. Natl. Acad. Sci. U. S. A. *104*, 2295–2300.

Pujol, N., Link, E.M., Liu, L.X., Kurz, C.L., Alloing, G., Tan, M.W., Ray, K.P., Solari, R., Johnson, C.D., and Ewbank, J.J. (2001). A reverse genetic analysis of components of the Toll signaling pathway in *Caenorhabditis elegans*. Curr. Biol. *11*, 809–821.

Pujol, N., Zugasti, O., Wong, D., Couillault, C., Kurz, C.L., Schulenburg, H., and Ewbank, J.J. (2008). Anti-fungal innate immunity in *C. elegans* is enhanced by evolutionary diversification of antimicrobial peptides. PLoS Pathog. *4*, e1000105.

Quinlan, A.R., and Hall, I.M. (2010). BEDTools: A flexible suite of utilities for comparing genomic features. Bioinformatics. *26*, 841–842.

R Development Core Team, R. (2011). R: A language and environment for statistical computing. R foundation for statistical computing. doi:10.1007/978-3-540-74686-7.

Raj, A., van den Bogaard, P., Rifkin, S.A., van Oudenaarden, A., and Tyagi, S. (2008). Imaging individual mRNA molecules using multiple singly labeled probes. Nat. Methods. *5*, 877–879.

Rantala, M.J., and Roff, D.A. (2005). An analysis of trade-offs in immune function, body size and development time in the mediterranean field cricket, *Gryllus bimaculatus*. Funct. Ecol. *19*, 323–330.

Reboul, J., Vaglio, P., Rual, J.F., Lamesch, P., Martinez, M., Armstrong, C.M., Li, S., Jacotot, L., Bertin, N., Janky, R., et al. (2003). *C. elegans* ORFeome version 1.1: Experimental verification of the genome annotation and resource for proteomescale protein expression. Nat. Genet. *34*, 35–41.

Reddy, K.C., Dror, T., Sowa, J.N., Panek, J., Chen, K., Lim, E.S., Wang, D., and Troemel, E.R. (2017). An intracellular pathogen response pathway promotes proteostasis in *C. elegans*. Curr. Biol. *27*, 3544-3553.e5.

Reddy, K.C., Dror, T., Underwood, R.S., Osman, G.A., Elder, C.R., Desjardins, C.A., Cuomo, C.A., Barkoulas, M., and Troemel, E.R. (2019). Antagonistic paralogs control a switch between growth and pathogen resistance in *C. elegans*. PLoS Pathog. *15*, e1007528.

Reece-Hoyes, J.S., Deplancke, B., Shingles, J., Grove, C.A., Hope, I.A., and Walhout, A.J.M. (2005). A compendium of *Caenorhabditis elegans* regulatory transcription factors: A resource for mapping transcription regulatory networks. Genome Biol. *6*, R110.

Renkema, G.H., Boot, R.G., Au, F.L., Donker-Koopman, W.E., Strijland, A., Muijsers, A.O., Hrebicek, M., and Aerts, J.M.F.G. (1998). Chitotriosidase a chitinase, and the 39-kDa human cartilage glycoprotein, a chitin-binding lectin, are homologues of family 18 glycosyl hydrolases secreted by human macrophages. Eur. J. Biochem. *251*, 504–509.

Riddle, D.L., Blumenthal, T., Meyer, B.J., and Priess, J.R. (1997). Genetic and environmental regulation of dauer larva development. In *C. elegans* II, D.L. Riddle, T. Blumenthal, B.J. Meyer, and J.R. Priess, eds. (Cold Spring Harbor (NY): Cold Spring Harbor Laboratory Press). p. 26.

Robb, E.J., and Barron, G.L. (1982). Nature's ballistic missile. Science. *218*, 1221–1222.

Robideau, G.P., De Cock, A.W.A.M., Coffey, M.D., Voglmayr, H., Brouwer, H., Bala, K., Chitty, D.W., Désaulniers, N., Eggertson, Q.A., Gachon, C.M.M., et al. (2011). DNA barcoding of oomycetes with cytochrome c oxidase subunit I and internal transcribed spacer. Mol. Ecol. Resour. *11*, 1002–1011.

Rohlfing, A.K., Miteva, Y., Hannenhalli, S., and Lamitina, T. (2010). Genetic and physiological activation of osmosensitive gene expression mimics transcriptional signatures of pathogen infection in *C. elegans*. PLoS One *5*, e9010.

Sarkies, P., Ashe, A., Le Pen, J., McKie, M.A., and Miska, E.A. (2013). Competition between virus-derived and endogenous small RNAs regulates gene expression in *Caenorhabditis elegans*. Genome Res. *23*, 1258–1270.

Sarowar, M.N., Saraiva, M., Jessop, C.N., Lilje, O., Gleason, F.H., and West, P. van (2014). 10. Infection strategies of pathogenic oomycetes in fish (Berlin, Germany: de Gruyter).

Schulenburg, H., Kurz, C.L., and Ewbank, J.J. (2004). Evolution of the innate immune system: the worm perspective. Immunol. Rev. *198*, 36–58.

Sebastiano, M., Lassandro, F., and Bazzicalupo, P. (1991). *cut-1* a *Caenorhabditis elegans* gene coding for a dauer-specific noncollagenous component of the cuticle. Dev. Biol. *146*, 519–530.

Shapira, M., Hamlin, B.J., Rong, J., Chen, K., Ronen, M., and Tan, M.W. (2006). A

conserved role for a GATA transcription factor in regulating epithelial innate immune responses. Proc. Natl. Acad. Sci. U. S. A. *103*, 14086–14091.

Silva, J.M., Mizuno, H., Brady, A., Lucito, R., and Hannon, G.J. (2004). RNA interference microarrays: High-throughput loss-of-function genetics in mammalian cells. Proc. Natl. Acad. Sci. *101*, 6548–6552.

Spies, C.F.J., Grooters, A.M., Lévesque, C.A., Rintoul, T.L., Redhead, S.A., Glockling, S.L., Chen, C. yu, and de Cock, A.W.A.M. (2016). Molecular phylogeny and taxonomy of *Lagenidium-like* oomycetes pathogenic to mammals. Fungal Biol. *120*, 931–947.

Stiernagle, T. (2006). Maintenance of *C. elegans*. WormBook. 1–11.

Strange, K. (2006). An overview of *C. elegans* biology. Methods Mol. Biol. *351*, 1–11.

Sulston, J.E., and Horvitz, H.R. (1977). Post-embryonic cell lineages of the nematode, *Caenorhabditis elegans*. Dev. Biol. *56*, 110–156.

Sulston, J.E., Schierenberg, E., White, J.G., and Thomson, J.N. (1983). The embryonic cell lineage of the nematode *Caenorhabditis elegans*. Dev. Biol. *100*, 64–119.

Sutherland, T.E., Logan, N., Rückerl, D., Humbles, A.A., Allan, S.M., Papayannopoulos, V., Stockinger, B., Maizels, R.M., and Allen, J.E. (2014). Chitinase-like proteins promote IL-17-mediated neutrophilia in a tradeoff between nematode killing and host damage. Nat. Immunol. *15*, 1116–1125.

Tan, M.-W., Mahajan-Miklos, S., and Ausubel, F.M. (1999). Killing of *Caenorhabditis elegans* by *Pseudomonas aeruginosa* used to model mammalian bacterial pathogenesis. Proc. Natl. Acad. Sci. *96*, 715–720.

Timmons, L., and Fire, A. (1998). Specific interference by ingested dsRNA. Nature. *395*, 854.

Troemel, E.R., Chu, S.W., Reinke, V., Lee, S.S., Ausubel, F.M., and Kim, D.H. (2006). p38 MAPK regulates expression of immune response genes and contributes to longevity in *C. elegans*. PLoS Genet. *2*, 1725–1739.

Troemel, E.R., Félix, M.A., Whiteman, N.K., Barrière, A., and Ausubel, F.M. (2008). Microsporidia are natural intracellular parasites of the nematode *Caenorhabditis elegans*. PLoS Biol. *6*, e309.

Trolezi, R., Azanha, J.M., Paschoal, N.R., Chechi, J.L., Dias Silva, M.J., Fabris, V.E., Vilegas, W., Kaneno, R., Fernandes Junior, A., and Bosco, S. de M.G. (2017). *Stryphnodendron adstringens* and purified tannin on *Pythium insidiosum*: in vitro and in vivo studies. Ann. Clin. Microbiol. Antimicrob. *16*, 7.

Wong, D., Bazopoulou, D., Pujol, N., Tavernarakis, N., and Ewbank, J.J. (2007). Genome-wide investigation reveals pathogen-specific and shared signatures in the response of *Caenorhabditis elegans* to infection. Genome Biol. *8*, R194.

Wood ed., W.B. (1988). The nematode *Caenorhabditis elegans* (Cold Spring Harbor (NY): Cold Spring Harbor Laboratory Press). *107*, 99-107.

Yadav, M.K., Pradhan, P.K., Sood, N., Chaudhary, D.K., Verma, D.K., Chauhan, U.K., Punia, P., and Jena, J.K. (2016). Innate immune response against an oomycete pathogen *Aphanomyces invadans* in common carp (*Cyprinus carpio*), a fish resistant to epizootic ulcerative syndrome. Acta Trop. *155*, 71–76.

Yang, W., Dierking, K., and Schulenburg, H. (2016). WormExp: A web-based application for a *Caenorhabditis elegans*-specific gene expression enrichment analysis. Bioinformatics. *32*, 943–945.

Yoshida, K., Schuenemann, V.J., Cano, L.M., Pais, M., Mishra, B., Sharma, R., Lanz, C.,

Martin, F.N., Kamoun, S., Krause, J., et al. (2013). The rise and fall of the *Phytophthora infestans* lineage that triggered the Irish potato famine. Elife. *2*, e00731.

Zaheer-ul-Haq, Dalal, P., Aronson, N.N., and Madura, J.D. (2007). Family 18 chitolectins: Comparison of MGP40 and HUMGP39. Biochem. Biophys. Res. Commun. *359*, 221–226.

Zanette, R.A., Santurio, J.M., Loreto, É.S., Alves, S.H., and Kontoyiannis, D.P. (2013). Toll-deficient *Drosophila* is susceptible to *Pythium insidiosum* infection. Microbiol. Immunol. *57*, 732–735.

Zentmyer, G.A. (1961a). Attraction of zoospores of *Phytophthora cinnamomi* to avocado roots. Calif. Avocado Soc. *45*, 93–95.

Zentmyer, G.A. (1961b). Chemotaxis of zoospores for root exudates. Science. *133*, 1595–1596.

Zhang, H., and Kato, Y. (2003). Common structural properties specifically found in the CSαβ-type antimicrobial peptides in nematodes and mollusks: Evidence for the same evolutionary origin? Dev. Comp. Immunol. *27*, 499–503.

Zhang, Z., Xu, Y., Song, G., Gao, X., Zhao, Y., Jia, M., Chen, Y., Suo, B., Chen, Q., Wu, D., et al. (2019). *Phytophthora sojae* zoospores differ in chemotaxis to the root and root exudates of host soybean and nonhost common bean. J. Gen. Plant Pathol. *85*, 201–210.

Zugasti, O., and Ewbank, J.J. (2009). Neuroimmune regulation of antimicrobial peptide expression by a noncanonical TGF-β signaling pathway in *Caenorhabditis elegans* epidermis. Nat. Immunol. *10*, 249–256.

Zugasti, O., Bose, N., Squiban, B., Belougne, J., Kurz, C.L., Schroeder, F.C., Pujol, N., and Ewbank, J.J. (2014). Activation of a G protein-coupled receptor by its endogenous ligand triggers the innate immune response of *Caenorhabditis elegans*. Nat. Immunol. *15*, 833–838.

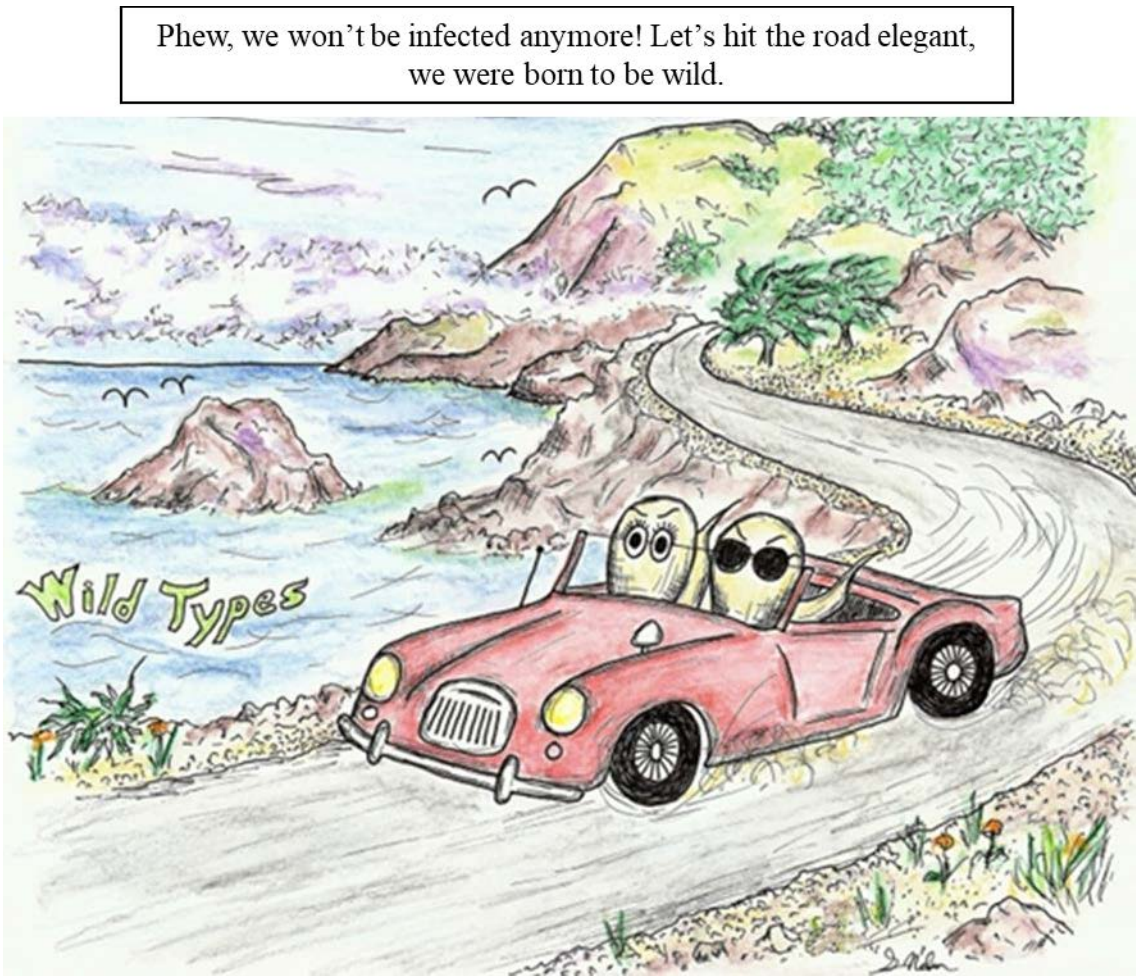

The image is taken from the worm breeder's gazette, Wormbook.